PhD Thesis 2016

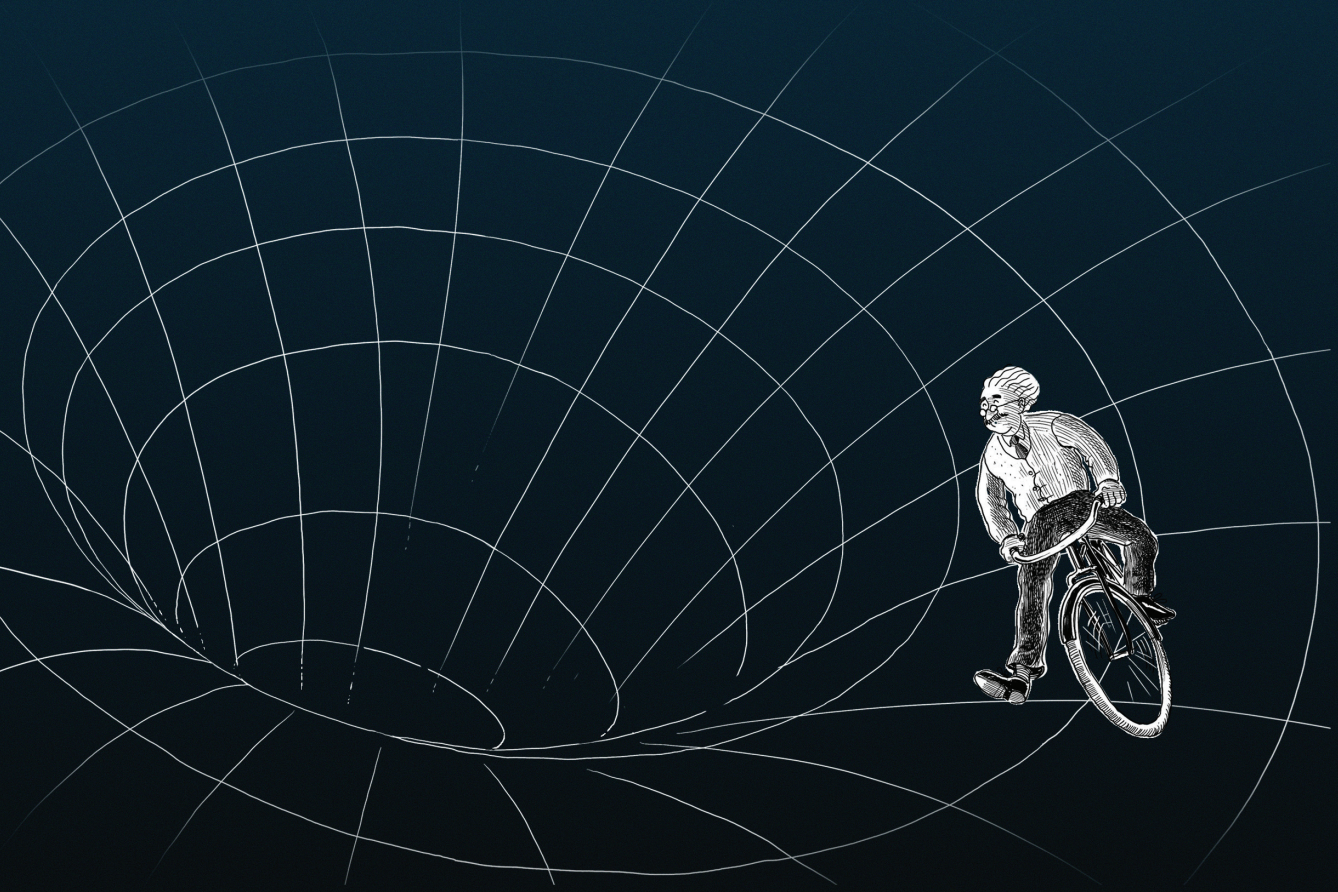

Satish Kumar Saravanan

Spin Dynamics in General Relativity

Lorentz Institute for Theoretical Physics
Leiden University

Spin Dynamics in General Relativity

Proefschrift

ter verkrijging van
de graad van Doctor aan de Universiteit Leiden,
op gezag van Rector Magnificus prof.mr. C.J.J.M. Stolker,
volgens besluit van het College voor Promoties
te verdedigen op donderdag 7 juli 2016
klokke 13.45 uur

door

Satish Kumar Saravanan

geboren te Salem (India)
in 1987

Promotor: Prof.dr J.W. van Holten

Promotiecommissie: Prof.dr R. Kerner (Université Pierre et Marie Curie, Paris, FR)
Prof.dr N. Obers (Niels Bohr Institute, Copenhagen, DK)
Dr. M. Postma (Nikhef)
Prof.dr A. Achúcarro
Prof.dr E.R. Eliel
Prof.dr K.E. Schalm

Casimir PhD series, Delft-Leiden, 2016-20
ISBN 978-90-8593-264-2
An electronic version of this thesis can be found at https://openaccess.leidenuniv.nl

The work presented in this thesis was supported by Leiden Institute of Physics. This work was carried out at Lorentz Institute, Leiden University and NIKHEF, Amsterdam.

Cover: The front side shows the artistic representation of a orbiting particle (here Einstein) deviating from the circular orbit in Schwarzschild space-time. Back side – a spinning particle in the Schwarzschild space-time obeys the plane circular orbital equation. Illustration by *Jeffrey Phillips*.

எப்பொருள் எத்தன்மைத் தாயினும் அப்பொருள்
மெய்ப்பொருள் காண்பது அறிவு.

- திருக்குறள் (355) ~ கி.மு முதல் நூற்றாண்டு

The mark of wisdom is to see the reality
Behind each appearance.

- Thirukkural (355) ~ first century B.C

Contents

List of Figures

Overview

The gravitational two-body problem has been a subject of interest long before the origin of General Relativity. In Newtonian mechanics, an isolated system of two point particles interacting through gravity is readily solvable and the resulting motion is periodic. The energy and angular momentum are represented by two conserved integrals of motion. In General Relativity non-separable centre of mass co-ordinates require taking account of the internal structures of the bodies, and therefore it is extremely complicated. The problem has been investigated since the beginning of General Relativity through the pioneering works of Einstein, Lorentz, Droste and De Sitter. The equations of motion for comparable mass binaries have been computed with the Post-Newtonian expansion. Even after 100 years of General Relativity the analysis is still incomplete. The Post-Newtonian description is sensible only in the weak field regime i.e., in-spiralling stage. When the two compact bodies are too close the gravity is so strong that the objects travel almost at the speed of light: the strong-field dynamical regime.

The dynamics of binaries is nonlinear in General Relativity and therefore the orbits are never periodic: as the system emits gravitational waves it continuously loses energy and angular momentum. Then the radiation back-reaction drives the objects closer and closer, eventually to merge. During the final stages of merger the analytical methods are ineffective and therefore the Numerical Relativistic treatment is used [1]. The reverse is also true; Numerical Relativistic methods are less efficient when the two objects are far apart, or when one of the components is much heavier than the other.

The latter type of system is known as the *Extreme Mass Ratio System*. Since the orbiting object is much smaller than the stable central one, the system can be analysed within the framework of black hole perturbation theory. If we neglect the internal structure and back reaction of the smaller compact object, we can treat it as a point particle moving on a world line, as described by Einstein [2] for test masses. In this limit many quantities which describe the evolution of the binaries can be solved quite precisely. Since all astrophysical objects spin, it is essential to include the internal angular momentum of compact objects. Such a

description of Extreme Mass Ratio binaries is important e.g. for low frequency space-based gravitational-wave detectors such as the evolved Laser Interferometer Space Antenna.

For more than eighty years, mathematical descriptions have aimed at keeping track of the centre of mass with various spin supplementary conditions; with the gravitating objects possessing quasi-rigid rotation along with orbital motion (extended bodies), this defines the framework of the Mathisson-Papapetrou model. But in determining the overall motion of the body by following a detailed microscopic description of a material body is often too complicated and the correct spin supplementary condition is still in debate.

Therefore we have given a alternate complementary formalism to the subject. We construct effective equations of motion for point-like objects, which is an idealization of a compact body, at the price of neglecting details of the internal structure by assigning the point-like object an overall position, momentum and spin. This is also known as the spinning-particle approximation, and is used for the semi-classical description of elementary particles as well. A detailed account on the qualitative connections and differences between the two formalisms have been given in section 4.4.

We have derived equations of motion for compact spinning bodies in curved space-time in an effective world-line formalism. The equations are obtained both from a hamiltonian formulation, without using any supplementary conditions and also from local energy-momentum conservation. The price to pay is that the world-line does not always coincide with that of a centre of mass but rather follows the spin, with the result that there is a mass dipole describing the displacement between the two in the presence of curvature. One of its strong points is that it does not require an a priori choice of hamiltonian. Since the closed set of Poisson-Dirac brackets is model independent, it can be applied to a large variety of models of relativistic spin dynamics. Using a minimal choice of hamiltonian we obtain the equations of motion by computing its bracket with this hamiltonian. The analysis has been extended with gravitational and electric Stern-Gerlach interactions by introducing the non-minimal hamiltonians. Also modified conservation laws emerge reflecting the spin-orbit coupling.

We have applied our formalism to study the dynamics of spinning particles in Schwarzschild space-time and established number of physical results. We obtain the simplest orbit: circular, for the particle in the equatorial plane. Method of geodesic deviation in General Relativity has been generalised to world lines of particles carrying spin. The complete first-order solution for the non-circular planar orbits are found starting from the circular orbit. The spin-influenced perturbations have double periods, and therefore the periastron and apastron behave in a complicated way (non-constant intervals) i.e., not only subject to an angular shift, but the point of closest approach shows radial variations as well. The presence of spin alters

the stability conditions and therefore the location of the Innermost Stable Circular Orbit. We have shown for over a wide range of spin values $-0.5M < \sigma < 0.5M$, the Innermost Stable Circular Orbit is quite close to the orbit of minimal orbital angular momentum and coincides only for spineless particles. We have furthermore extended our analysis for a non-minimal hamiltonian to include Stern-Gerlach force of gravitational origin and determined circular orbits in the case of Schwarzschild. As a further generalisation we investigated non-planar eccentric orbits around a massive stable black hole. We have obtained an analytical formula for the orbital precession frequency.

Chapter 1 introduces gravity in the Newtonian framework, stating its merits and short comings. Then by describing Einstein's general relativistic idea of gravitation, I define gravitational waves and its properties. The indirect evidence of gravitational waves has been explained with binary pulsar PSR B1913+16. The first direct detection of gravitational waves: GW150914, conforms the existence of black holes and binary black holes. With these motivations, I describe my system of research – Extreme Mass Ratio Systems and its scope of experimental detection with the evolved Laser Interferometer Space Antenna.

1

Introduction

1.1 Gravitation

Of the four fundamental forces of nature, gravity is the weakest. For instance, the gravitational force between the proton and electron is 10^{40} times smaller than the electric force that binds these particles together in atoms. However gravity is a universal force. Newton's law of gravitation was the first major physical theory which attempts to describe gravity. According to Newton's theory, two bodies, irrespective of whether they are on the Earth or in the heavens, whether they are in the state of motion or rest, always mutually attract each other with a force directly proportional to the product of their mass and inversely proportional to the square of their mutual distance

$$F = G\,\frac{mM}{d^2}, \tag{1.1.1}$$

where F is the force between the masses; G is the universal gravitational constant, whose value is $6.674 \times 10^{-11} Nm^2/kg^2$; m and M are two masses, and d is the distance between the centers of the masses. This implies, the gravitational force propagates in space at an infinitely great speed. This is the weak point of Newton's theory, because it means that something is simultaneously having an effect somewhere, where it is not present, and this is a physical impossibility. Despite this weakness, it still provides an excellent basis for explaining and calculating the planetary movements.

This absurd idea of "action at a distance" emerging in Newton's theory was not resolved, until Einstein in 1915. Einstein described space and time as different aspects of reality in which matter and energy are ultimately the same. With this he describes gravitation very accurately in this 4-dimensional universe (3 spatial dimension + 1 time dimension) in which we are living in. The presence of large amounts of mass or energy distorts space-time – in essence causing the fabric to "warp" and we observe this as gravity.

Freely falling objects – whether a soccer ball, a satellite, or a beam of starlight – simply follow the shortest space-time path (geodesic) in this curved space-time.

Therefore, the planets are moving in "straight lines" in the curvature produced by the sun and it appears as if they are in circular or elliptical motion around the sun. This is the central idea of general theory of relativity [3].

Thus the Newtonian idea of a gravitational force acting at a distance between bodies was replaced by the idea of a body moving in response to the curvature of space-time. Indeed Newton's theory of gravity is not completely wrong. It is a correct approximation to Einstein's theory when space-time curvature is negligible and the velocities of masses are much smaller than the velocity of light.

Newton's theory forms an excellent basis for describing weak gravitational regimes like in earth or solar system. In this regimes the general relativistic corrections to the Newton's theory are very small. But general relativity also predicts new strong gravitational phenomena like bending of light, black holes, gravitational waves and the big bang.

1.2 Gravitational Waves

Accelerated mass varies space-time and the change propagates as ripples in space-time curvature with the speed of light known as gravitational waves. Gravitational waves are analogous to the electromagnetic waves, the oscillations in the electric and magnetic fields produced by the accelerated charges.

Mass in motion is the source of gravitational waves. In turn, gravitational waves can be detected through the motion of masses produced as the ripple in space-time curvature passes by. When a gravitational wave passes through a ring of particles it changes their relative positions, depending on the wave's polarisation [4]. Here we have shown the particle's motion produced by a wave with "+" polarisation (top line) and " × " polarisation (bottom line).

Fig. 1.1 implies that a single wave cycle of a gravitational wave changes the ring (R being the radius) into an ellipse with semi-major axis $R + dR$ and semi-minor axis $R - dR$, back through a ring into the same ellipse rotated by 90° and finally back to a ring. The strength of a gravitational wave is determined by how rapidly the quadrupole moment of its source is changing:

$$h \simeq \frac{G}{c^4} \frac{d^2Q/dt^2}{D} \tag{1.2.1}$$

where h is the strain, the strength of a gravitational wave, Q is the quadrupole moment of the source and D is the distance from source to observer and c is the speed of light.

In principle any accelerated mass produces gravitational waves, for example a falling apple. But the quantity $\frac{G}{c^4} = 8.26 \times 10^{-45} kg^{-1}(m/s^2)^{-1}$ is very tiny, therefore we need very large masses undergoing extreme accelerations to produce detectable gravitational waves. Thus we look for most energetic phenomena in the universe like big bang, supernovae explosion or compact binary coalescence [5].

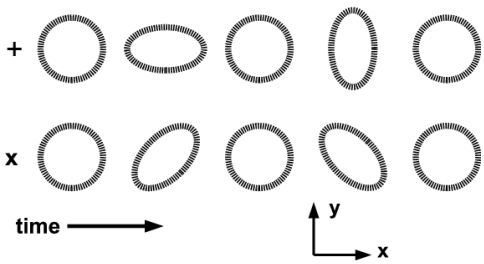

Figure 1.1. The effect of a gravitational wave on a ring of particles. The wave is traveling in the z-direction (perpendicular to the page). The upper and lower parts are the effects of a "+" and " × " polarised wave, respectively.

1.3 PSR B1913+16: Indirect Evidence of Gravitational Waves

Even after several years of general relativistic predictions of gravitational waves, their existence was not universally believed. The very first convincing experimental evidence was given by Russell Hulse and Joseph Taylor in 1974 [6] in connection with the discovery of binary pulsar PSR B1913+16. The observed system must be composed of neutron stars, at least one of which is a pulsar. We observe a pulse of radio waves every time the bright spot sweeps around to face Earth [7]. The pulsar has a rotational period of 59 ms and its frequency varied with a period of 7.75 hours; apparently it is a member of a binary system with high eccentricity [8, 9].

After several years of observation [10, 11], a variety of relativistic effects has been recognized: orbital precession, advance of periastron, gravitational redshift, and the time-dilation and so on. It is found that both the objects in the system were neutron stars (incredibly dense objects the burned-out core often left behind after a supernovae) with masses around 1.4 $M_{\odot}$ (solar mass). But the most exciting prediction was that they found the orbital period was decreasing by about 75 millionths of a second per year. This could not be understood unless the dissipative reaction force associated with gravitational waves produced is included. Thus the two neutron stars gradually fall closer to each other and their orbital speed increases steadily because it emits energy as gravitational waves and this is in excellent agreement with the rate predicted by the general relativity as shown in the Fig. 1.2.

The frequency of the gravitational waves from the Hulse-Taylor binary system are too low for the existing ground based detectors to detect the signal. But the rate of orbital decay as predicted by the general relativity is in perfect agreement with the experimental observation is the very first strong evidence for the existence of gravitational waves [12, 13]. This discovery of Hulse and Taylor has opened a new window to study gravitation and they were awarded Nobel prize in 1993.

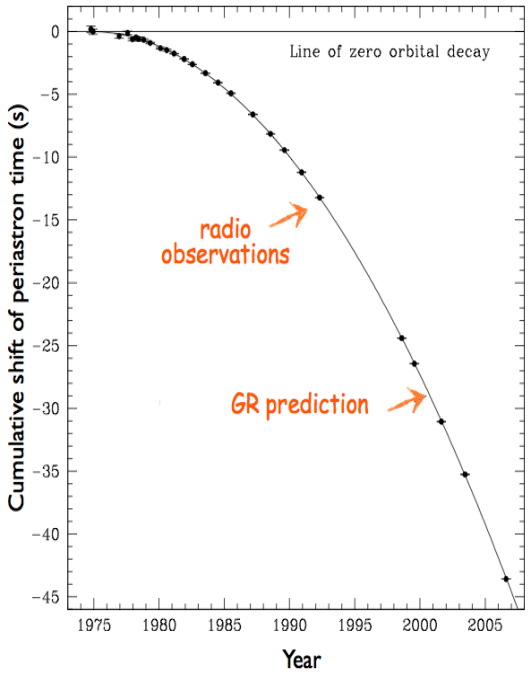

Figure 1.2. The orbital period of binaries PSR B1913+16 decreases because the system loses energy as gravitational waves. Since the system is relativistic, the effect is very strong here. The measure of this decrease in orbital period is due to the steady shift over time of the time of the pulsar's periastron (closest approach to its companion). The points are the observed data points over several decades and the solid line is the general relativity prediction.

1.4 GW150914: The Direct Detection of Gravitational Waves

According to general relativity, whenever a sufficient mass is compressed into a very small volume such that the gravitational pull at the surface is too large, even light cannot escape once it enters into the surface. Such objects are called black holes. Black holes can be identified with minimum number of properties like mass, spin and charge.

Coalescence of black hole binaries are the most promising sources of gravitational radiation [14, 15]. According to general relativity the coalescence happens in three phases: in-spiral, merger and ringdown (Fig. 1.3). During the evolution there is loss in the energy and angular momentum of the system; as they are carried away by the gravitational waves. Therefore the orbit shrinks at the rate predicted by general relativity, and is already confirmed by the observation in the Hulse-Taylor binary system.

"The black holes of nature are the most perfect macroscopic objects there are in the universe: the only elements in their construction are our concepts of space and time. And since the general theory of relativity provides only a single unique family of solutions for their descriptions, they are the simplest objects as well."

– S. Chandrasekhar, The Mathematical Theory of Black Holes [16]

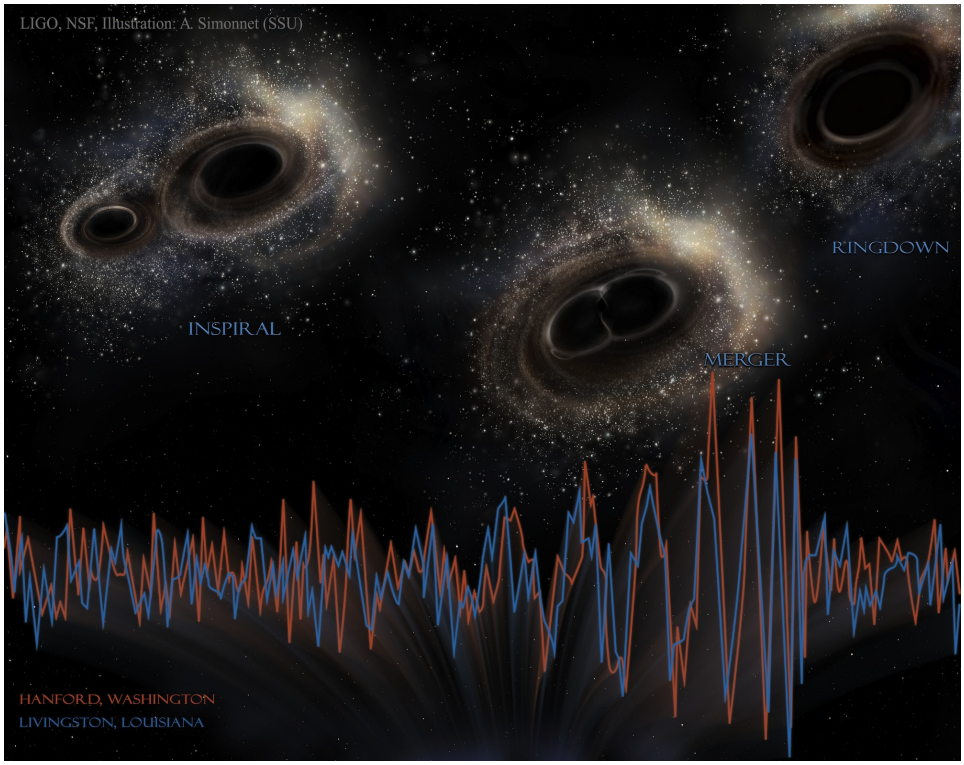

Figure 1.3. The evolution of binaries occur in three stages: in-spiral, merger and ring-down, as shown above. During the merger phase the system emits huge amount of gravitational waves. The orange coloured wave is the gravitational wave pattern observed in LIGO - Hanford and similarly the blue coloured wave is the pattern obeserved in LIGO - Livingston. These observations are named as GW150914 to indicate that the gravitational waves passed the detectors on 2015 September 14 (EST). Credit: LIGO / NSF / A. Simonnet (SSU)

After the completion of field equations in 1915, Einstein predicted the existence of gravitational waves in 1916. Historically searches for gravitational waves were started with the development of "Weber bar" detectors [17] and then Interferometric detectors since 1970 [18, 19].

After five decades of work, advanced Laser Interferometer Gravitational-Wave Observatory (advanced LIGO) is in operation now and made the *first* direct observation of gravitational waves [20, 21]. The event is named as GW150914 to indicate that the gravitational waves passed the detectors on 2015 September 14 (EST). The wave appeared first at Livingston, LIGO detector and then at Hanford, detector, a 7 ms later. This time difference is consistent with the fact that *gravitational wave travels at the speed of light*. The gravitational wave stretched and squeezed space-time with the frequency sweeping from 40 Hz to 260 Hz over 0.2s in the pattern of two black holes merging together (Fig. 1.4). The masses of two black holes are

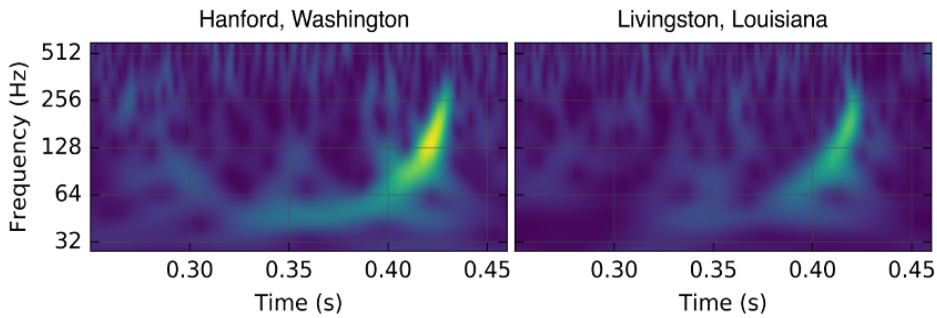

Figure 1.4. Pictures from the paper [20] reporting the GW150914 discovery. The frequency of gravitational wave oscillation plotted vertical, as a function of time plotted horizontally. The colors show the strength of the waves. Green and yellow represents the oscillations of gravitational wave; yellow represents the very strong oscillations during the merger phase. Blue colour due to noise in the detector. At both Hanford and Livingston, the green-yellow oscillations have precisely the form that we expect for gravitational waves produced by binary black holes in-spiralling and colliding.

predicted to be 29 $M_\odot$ and 36 $M_\odot$. They merged to form a single black hole with a mass of 62 $M_\odot$. Thus the remaining 3 $M_\odot$ energy is released as gravitational waves during the inspiral and merger phases of these black holes. Then the remnant black hole has spin at a rate of 100 rotations per second. Thus the discovery implies the following conclusions:

(i). First direct detection of gravitational waves
(ii). First direct evidence of existence of black holes
(iii). First observation of binary black holes.

This discovery give rise to a new branch of astrophysics: gravitational wave astronomy [22, 23]. Through which we can explore the dark side of the universe in the very broad spectrum which were inaccessible to us with electromagnetic astronomy.

Black holes and/or neutron stars, composed of stellar mass binaries are optimistic sources for ground based network of detectors [24–27] like advanced-LIGO, VIRGO, KAGRA, GEO 600 and LIGO-India. The observation of gravitational waves from such binaries will bring various information: event rate, binary parameters and even possible deviations from general relativity [28–30].

1.5 Laser Interferometer Space Antenna (eLISA) and sources

The existing ground based detectors are sensitive around 100 Hz. The universe is rich in strong sources of gravitational waves when we probe below these frequencies. But the seismic noise makes the ground based detectors insensitive for lower frequencies. Therefore we need observations from space. The space based detector eLISA is sensitive for frequencies from 0.1 mHz to 100 mHz [31,32], and it is planned to be launched by European Space Agency (ESA) in 2034. These frequencies corresponds to wide range of gravitational wave sources and its direct detection with eLISA will answer the very fundamental questions; mapping the present universe to all the way shortly after the Big bang. The mission has been named with the science theme *The Gravitational Universe* [33] by the ESA.

The electromagnetic observations clearly show that stars, black holes, and galaxies are ubiquitous components of the universe [34]. eLISA will study these objects in the gravitational wave spectrum. Thus it measures the amplitude of the strain in the space as a function of time. The following are the prospective sources (not limited to) of gravitational waves:

Supermassive Binary Black Holes Almost all bright galaxies (including our own Milky Way) host one or more massive central black holes. Their masses range from $10^4\ M_\odot$ – $10^7\ M_\odot$ and these are called as supermassive black holes. When galaxies coalesce (Fig. 1.5), these black holes will merge eventually [35], releasing huge amount of gravitational radiation during the process. Thus detecting these signals will not only test theories of gravity and black holes, but also reveal information about the evolution and merger history of galaxies [36].

Ultra-Compact Binaries The components of binaries could be compact objects like stellar mass black holes, neutron star or white dwarf. The Milky Way is full of these sources [37], but only a small fraction is observable in the radio and X-ray spectrum. Since the maximum loss of energy from these systems are always through gravitational waves, and it lies in the frequency range of eLISA [38], it should be possible to map all these objects soon.

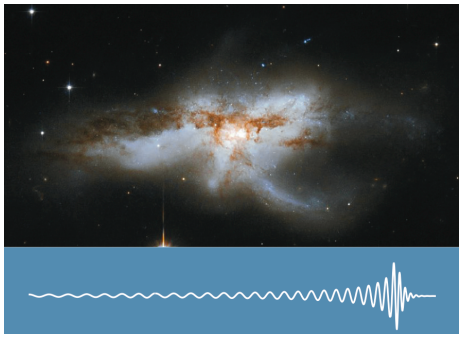

Figure 1.5. Coalescence of two supermassive black holes. The expected gravitational waveform has in-spiral, merger and ringdown phase. Merging galaxy NGC 6240 [35] has two giant black holes as reported by NASA's Chandra X-ray observatory. Credit: NASA / ESA / the Hubble heritage / A. Evans.

Figure 1.6. The fossil gravitational waves are the only way to probe the early Universe all the way immediately after the Big Bang. The expected gravitational waveform is stochastic background (random noise). Credit: NASA / WMAP science team.

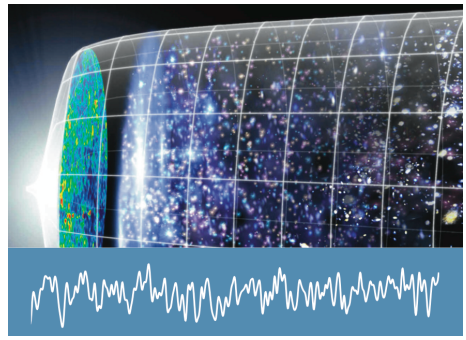

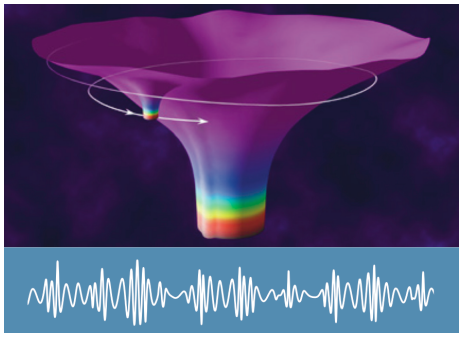

Figure 1.7. An artist impression of EMRS; a small black hole inspiralling around a supermassive black hole. The modelled waveform would have many harmonics as shown. Credit: NASA.

The Big Bang and The Early Universe Since the universe was transparent to gravity moments after the Big Bang and long before light (remember the first light still present, Cosmic Microwave Background was produced only about 300,000 years after the Big Bang), gravitational waves will allow us to observe further back into the history of the universe than ever before. And since gravitational waves are not absorbed or reflected by the matter in the rest of the universe, we will be able to see them in the form in which they were created. Immediately after the Big Bang, when the Universe was very young it underwent a period of very rapid expansion, as a result space-time got distorted which in turn produced gravitational waves between approximately 10^{-43} to 10^{-32} seconds after the Big Bang (Fig. 1.6). These relic gravitational waves from the early evolution of the universe may carry information about the origin and history of the universe.

Extreme Mass Ratio Systems The supermassive black holes in the galactic centres may be accompanied by one or more stellar mass compact objects like black hole, neutron star or white dwarf, of few solar masses are called Extreme Mass Ratio Systems (EMRS) (Fig. 1.7). eLISA will track the complex relativistic orbits of the stellar companion around a central black hole in the mass interval between $10^4\ M_\odot < M < 5 \times 10^6\ M_\odot$ for upto $10^4 - 10^5$ cycles [39, 40]. The waveforms emitted from these systems would inform us about the stellar mass compact object populations, mass spectrum and their spin. It will also describe the properties of space-time geometry around the central black hole [41, 42] and the formation of supermassive black holes at the galactic centers [43].

Infrared astronomy has given the *best empirical evidence* for the existence of a 4 million solar mass black hole in our Milky Way. Observation has not only tracked the 28 stars orbiting a supermassive black hole [44, 45]: Sagittarius A*, but also predicted its mass and distance (27,000 light years away from the solar system). The stellar orbits in the galactic centre show that the central mass concentration of four million solar masses must be a black hole, beyond any reasonable doubt [46].

Though most of the black holes in nature are spinning, we start modelling EMRS as a small spinning black hole or a neutron star orbiting around a static spherically symmetric - supermassive black hole. This is the subject of this thesis. The mass ratio between the smaller compact object and the central black hole is typically $\sim 10^{-5}$. Because of this extreme mass ratio, the curvature produced by the smaller object can be neglected. I introduce the necessary general relativistic tools for modelling EMRS in chapter 2 & 3. After this I discuss EMRS: a test mass orbiting a Schwarzschild black hole in chapter 3. Then I discuss the formalism for a spinning compact object in Schwarzschild space-time in chapter 4, which we have developed recently [47]. In chapter 5, I discuss the applications of our formalism and important aspects of the dynamics of EMRS [48]. The theoretical model I present in the rest of the thesis is esentially the preparation for eLISA observations. The

first direct observation of EMRS and therefore supermassive black holes, through gravitational wave detection is expected immediately after the launch of eLISA mission. The estimated detection rates based on the best available models are 50 events for a 2 year mission [49].

Chapter 2 presents the Equivalence Principle and builds up the necessary differential geometry to describe General Relativity. The geodesic equations of motion are developed starting from the action principle and also from the Hamiltonian dynamics. I conclude by describing the field equation and its significance.

2

Gravity and General Relativity

2.1 The Equivalence Principle

The Equivalence Principle is a corner stone of Einstein's theory of gravity, General Relativity (GR) [50].

In its original form it refers to the equivalence between gravitational and inertial mass, as demonstrated experimentally by various scientists from the late 16th century onward. This was the starting point for Newton's theory of gravity in which the gravitational pull of the earth gives the same acceleration to an apple and to the moon. In GR it holds as the acceleration of objects results from the geometry of space-time, independent of mass or composition. In this context it is usually referred to as the *Weak Equivalence Principle*.

The Equivalence Principle formulated by Einstein, the *Einstein Equivalence Principle* is slightly stronger. It says that a reference system in free fall is a local Lorentz frame, in which the laws of special relativity hold. In such a system non-interacting objects fall at the same rate with no relative acceleration. It is a *local* Lorentz frame as these statements only hold in the limit that distances are small compared to the local scale of space-time curvature, otherwise there would be tidal accelerations.

There also exists a third version of the Equivalence Principle, which states that the equivalence of gravitational and inertial mass includes all possible contributions to the mass including gravitational binding energy (self-energy). This is called the *Strong Equivalence Principle* and is most difficult to test, as usually gravitational binding energy is extremely weak. The only objects in which gravitational contribution to mass is significant are compact bodies like neutron stars and black holes.

2.2 Coordinates, metric and motion

In the absence of gravity, in a local Lorentz frame, free particles move with constant velocities on straight trajectories. When different sections of these trajectories in overlapping Lorentz frames are glued together, one gets trajectories which are still in a generalized sense the "shortest path" between two space-time points: *geodesics* [51].

An invariant measure of distance along a particle's space-time trajectory, or *world line*, is the proper time τ. It is the time measured during any short sections of the worldline by a clock at rest w.r.t. the particle. Let (x) be a coordinates for the patch of space-time where the trajectory is located, and consider two points on the trajectory with coordinates (x^μ) and $(x^\mu + dx^\mu)$. Then the proper time interval $d\tau$ is determined from a quadratic expression in the coordinate intervals dx^μ:

$$-d\tau^2 = g_{\mu\nu}(x) dx^\mu dx^\nu. \tag{2.2.1}$$

The coefficients $g_{\mu\nu}(x)$ define the metric for the coordinate system x^μ at the given point. As it is an invariant, the same quantity measured in terms of a different coordinate system (x') is

$$-d\tau^2 = g'_{\mu\nu}(x') dx'^\mu dx'^\nu. \tag{2.2.2}$$

Now the *diffeomorphism* $x^\mu \to x'^\mu(x)$ if it is smooth allows us to write the last expression also as

$$g'_{\mu\nu}(x') \frac{\partial x'^\mu}{\partial x^\kappa} \frac{\partial x'^\nu}{\partial x^\lambda} dx^\kappa dx^\lambda. \tag{2.2.3}$$

Comparing with expression (2.2.1) gives

$$g_{\kappa\lambda}(x) = g'_{\mu\nu}(x') \frac{\partial x'^\mu}{\partial x^\kappa} \frac{\partial x'^\nu}{\partial x^\lambda}. \tag{2.2.4}$$

This shows how the metric coefficients change between different coordinate systems. The inverse metric is written $g^{\mu\nu}(x)$, such that at the same point in the same coordinate system

$$g^{\mu\lambda} g_{\lambda\nu} = \delta^\mu_\nu.$$

It changes between coordinate systems by the inverse transformation

$$g^{\mu\nu}(x) = g'^{\kappa\lambda}(x') \frac{\partial x^\mu}{\partial x'^\kappa} \frac{\partial x^\nu}{\partial x'^\lambda}.$$

Now the total proper time along a curve $x^\mu(\tau)$ between two space-time points (a, b) with time-like separation is

$$\int_a^b d\tau. \tag{2.2.5}$$

Notice that we can introduce an arbitrary parameter λ labeling the points on the curve, as long as it is monotonic between (a, b). Therefore, the time interval

$$d\tau = \left(-g_{\mu\nu}\frac{dx^\mu}{d\lambda}\frac{dx^\nu}{d\lambda}\right)^{1/2} d\lambda, \tag{2.2.6}$$

where $d\lambda$ is the displacement on space-time. We are varying the paths

$$x^\mu(x) \to x^\mu(x) + \delta x^\mu(x) \tag{2.2.7}$$

keeping the end-points fixed, and will denote the τ-derivatives by $\dot{x}(\tau)$ and $\partial_\lambda \equiv \frac{\partial}{\partial x^\lambda} = ,\lambda$. By the standard variational procedure one then finds

$$\begin{aligned}
\delta S &= \frac{1}{2}\int d\lambda \left(-g_{\mu\nu}\frac{dx^\mu}{d\lambda}\frac{dx^\nu}{d\lambda}\right)^{-1/2}\left[-\delta g_{\mu\nu}\frac{dx^\mu}{d\lambda}\frac{dx^\nu}{d\lambda} - 2g_{\mu\nu}\frac{d\delta x^\mu}{d\lambda}\frac{dx^\nu}{d\lambda}\right] \\
&= \frac{1}{2}\int d\tau \left[-g_{\mu\nu,\lambda}\,\dot{x}^\mu\dot{x}^\nu\delta x^\lambda + 2g_{\mu\nu}\ddot{x}^\nu\delta x^\mu + 2g_{\mu\nu,\lambda}\,\dot{x}^\lambda\dot{x}^\nu\delta x^\mu\right] \\
&= \int d\tau \left[g_{\mu\nu}\ddot{x}^\nu + \frac{1}{2}\left(g_{\mu\nu,\lambda} + g_{\mu\lambda,\nu} - g_{\nu\lambda,\mu}\right)\dot{x}^\nu\dot{x}^\lambda\right]\delta x^\mu
\end{aligned} \tag{2.2.8}$$

Here the factor of 2 in the first equality is a consequence of the symmetry of the metric, the second equality follows from an integration by parts, the third from relabelling the indices in one term and using the symmetry in the indices of $\dot{x}^\lambda\dot{x}^\nu$ in the other.

We set the variation of action to zero, $\delta S = 0$. Further re-naming $\mu \to \kappa$ and multiplying by $g^{\mu\kappa}$, we obtain the equations for a timelike geodesic in an arbitrary gravitational field:

$$\frac{d^2x^\mu}{d\tau^2} + \Gamma^\mu_{\nu\lambda}\frac{dx^\nu}{d\tau}\frac{dx^\lambda}{d\tau} = 0, \tag{2.2.9}$$

where $\Gamma^\mu_{\nu\lambda}$ is the Christoffel connection or Levi-Civita symbol, which is symmetric in the second and third indices:

$$\Gamma^\mu_{\lambda\nu} = \Gamma^\mu_{\nu\lambda} = \frac{1}{2}\,g^{\mu\kappa}\left(g_{\kappa\lambda,\nu} + g_{\kappa\nu,\lambda} - g_{\lambda\nu,\kappa}\right). \tag{2.2.10}$$

2.3 Hamiltonian dynamics

The equation (2.2.9) for geodesic motion was derived from the geometric principle of extremizing the amount of proper time along the curve. However the same equation of motion can also be obtained in a canonical phase-space approach with an appropriate hamiltonian. This approach introduces next to the particle's coordinates $x^\mu(\tau)$ also the canonical momenta $\pi_\mu(\tau)$. The appropriate hamiltonian is

$$H = \frac{1}{2m}\,g^{\mu\nu}(x)\pi_\mu\pi_\nu. \tag{2.3.1}$$

Hamilton's equations then imply the following equations of motion:

$$\begin{aligned}\dot{x}^\mu &= \frac{\partial H}{\partial \pi_\mu} = \frac{1}{m}\, g^{\mu\nu}\pi_\nu, \\ \dot{\pi}_\mu &= -\frac{\partial H}{\partial x^\mu} = \frac{1}{m} g_{\kappa\lambda,\mu} g^{\kappa\rho} g^{\lambda\sigma}\pi_\rho\pi_\sigma = m g_{\kappa\lambda,\mu}\dot{x}^\kappa\dot{x}^\lambda.\end{aligned} \tag{2.3.2}$$

These equations can be rewritten in the form

$$\pi_\mu = m g_{\mu\nu}\dot{x}^\nu, \quad \ddot{x}^\mu + \Gamma^\mu_{\lambda\nu}\dot{x}^\lambda\dot{x}^\nu = 0. \tag{2.3.3}$$

Thus equation (2.2.9) is reobtained. Although less geometric, this method is entirely equivalent and is useful if more interactions than just with the curved background geometry are to be included, like electric charge or spin. This will become clear in the chapters to follow.

2.4 Differential geometry

The quantities that appeared in the previous sections can be introduced in a more general way not only on curves (geodesics) but as fields of geometric objects on the space-time manifold at large [52]. Vector fields $A_\mu(x)$ are sets of functions transforming under a change of coordinates as

$$A_\mu(x) = A'_\nu(x')\frac{\partial x'^{\,\nu}}{\partial x^\mu},$$

and similarly for higher-rank tensors $A_{\mu\nu\ldots}$. Taking the derivative of a vector or tensor is somewhat delicate, as in general it produces an new object which is not a tensor itself. However, one can define a *covariant* derivative using the Christoffel connection introduced before. Indeed one can construct a proper rank-2 tensor from a vector by taking

$$\mathcal{D}_\lambda A_\mu = \partial_\lambda A_\mu - \Gamma^\nu_{\lambda\mu} A_\nu. \tag{2.4.1}$$

Similarly a rank-2 tensor is lifted to a rank-3 tensor by taking

$$\mathcal{D}_\lambda A_{\mu\nu} = \partial_\lambda A_{\mu\nu} - \Gamma^\kappa_{\lambda\mu} A_{\kappa\nu} - \Gamma^\kappa_{\lambda\nu} A_{\mu\kappa},$$

etc. To prove the statement one has to check the transformation properties of the connection coefficients:

$$\Gamma^\mu_{\lambda\nu}(x) = \Gamma'^{\,\kappa}_{\rho\sigma}(x')\frac{\partial x'^{\,\rho}}{\partial x^\lambda}\frac{\partial x'^{\,\sigma}}{\partial x^\nu}\frac{\partial x^\mu}{\partial x'^{\,\kappa}} - \frac{\partial^2 x'^{\,\kappa}}{\partial x^\lambda \partial x^\nu}\frac{\partial x^\mu}{\partial x'^{\,\kappa}}.$$

For proofs we refer to the literature [3, 50].

Clearly in contrast to ordinary partial derivatives, covariant derivatives do not commute. Indeed

$$\begin{aligned}
[\mathcal{D}_\mu, \mathcal{D}_\nu]\, V_\lambda &= \mathcal{D}_\mu \left(\partial_\nu V_\lambda - \Gamma^\rho_{\nu\lambda} V_\rho\right) - (\mu \leftrightarrow \nu) \\
&= \partial_\mu \left(\partial_\nu V_\lambda - \Gamma^\rho_{\nu\lambda} V_\rho\right) - \Gamma^\sigma_{\mu\nu} \left(\partial_\sigma V_\lambda - \Gamma^\rho_{\sigma\lambda} V_\rho\right) - \Gamma^\sigma_{\mu\lambda} \left(\partial_\nu V_\sigma - \Gamma^\rho_{\nu\sigma} V_\rho\right) \\
&\quad - (\mu \leftrightarrow \nu) \\
&= -\partial_\mu \left(\Gamma^\rho_{\nu\lambda} V_\rho\right) - \Gamma^\sigma_{\mu\lambda} \left(\partial_\nu V_\sigma - \Gamma^\rho_{\nu\sigma} V_\rho\right) - (\mu \leftrightarrow \nu) \\
&= -\partial_\mu \Gamma^\rho_{\nu\lambda} V_\rho + \Gamma^\sigma_{\mu\lambda} \Gamma^\rho_{\nu\sigma} V_\rho - (\mu \leftrightarrow \nu) \\
&= R_{\mu\nu\lambda}{}^\rho V_\rho
\end{aligned} \tag{2.4.2}$$

where

$$R_{\mu\nu\lambda}{}^\rho = -\partial_\mu \Gamma^\rho_{\nu\lambda} + \partial_\nu \Gamma^\rho_{\mu\lambda} - \Gamma^\sigma_{\nu\lambda} \Gamma^\rho_{\mu\sigma} + \Gamma^\sigma_{\mu\lambda} \Gamma^\rho_{\nu\sigma}. \tag{2.4.3}$$

Here although each single term in $R_{\mu\nu\lambda}{}^\rho$ is not a tensor, under a diffeomorphsim, we can prove the following transformation properties [3] for the resulting combination

$$R'_{\sigma\alpha\xi}{}^\beta = \frac{\partial x^\mu}{\partial x'^\sigma} \frac{\partial x^\nu}{\partial x'^\alpha} \frac{\partial x^\lambda}{\partial x'^\xi} \frac{\partial x'^\beta}{\partial x^\rho} R_{\mu\nu\lambda}{}^\rho, \tag{2.4.4}$$

and therefore, it is a (1, 3)-tensor; called as the *Riemann tensor*. It includes second-order derivatives of the metric: it does not vanish therefore in a locally inertial frame. It vanishes if and only if a manifold is flat. It is therefore the curvature tensor. In particular, if the Riemann tensor vanishes, we can always construct a coordinate system in which the metric components are constant.

The Riemann tensor (2.4.3) satisfies a number of symmetry properties. It is anti-symmetric in the first two or last two indices and symmetric in the first and last pairs of indices:

$$R^\mu{}_{\nu\rho\sigma} = -R^\mu{}_{\nu\sigma\rho}, \quad R_{\mu\nu\rho\sigma} = -R_{\nu\mu\rho\sigma}, \quad R_{\mu\nu\rho\sigma} = R_{\rho\sigma\mu\nu}, \tag{2.4.5}$$

and sum of cyclic permutation are zero:

$$R^\mu{}_{\nu\rho\sigma} + R^\mu{}_{\rho\sigma\nu} + R^\mu{}_{\sigma\nu\rho} = 0, \tag{2.4.6}$$

where the first index has been lowered using the metric: $R_{\mu\nu\rho\sigma} = g_{\mu\eta} R^\eta{}_{\nu\rho\sigma}$. It can be shown that these constraints reduce the number of independent components of the Riemann tensor in n dimensions from n^4 to $n^2\left(n^2-1\right)/12$, i.e. 20 in 4 dimensions, and only 1 in two dimensions.

Then the invariant parts of the Riemann tensor are defined as the Ricci tensor (a symmetric tensor) $R_{\mu\nu}$ and Ricci or curvature scalar R:

$$R_{\mu\nu} \equiv R^{\alpha}{}_{\mu\alpha\nu}, \qquad R \equiv g^{\mu\nu} R_{\mu\nu}. \tag{2.4.7}$$

In addition to these algebraic identities, the Riemann tensor obeys a differential identity:

$$\nabla_\gamma R^{\mu}{}_{\nu\rho\sigma} + \nabla_\sigma R^{\mu}{}_{\nu\gamma\rho} + \nabla_\rho R^{\mu}{}_{\nu\sigma\gamma} = 0, \tag{2.4.8}$$

also called as Bianchi identity. Further contracting the Bianchi identity gives

$$\nabla^\mu R_{\mu\nu} = \frac{1}{2} \nabla_\nu R. \tag{2.4.9}$$

This allows to define a "conserved" tensor, the *Einstein tensor*:

$$G_{\mu\nu} = R_{\mu\nu} - \frac{1}{2} g_{\mu\nu} R, \tag{2.4.10}$$

i.e., the Bianchi identity implies that the divergence of this tensor vanishes identically,

$$\nabla^\mu G_{\mu\nu} = 0. \tag{2.4.11}$$

This is sometimes called the contracted Bianchi identity.

2.5 Einstein's Field Equation

Einstein field equations [3, 53] describe the physical universe as a 4-dimensional Lorentzian manifold. It is the relation between curvature and energy-momentum content in the universe. This allows us to view the curvature tensor as a physical property of the universe, as a function of mass, momentum and energy.

The curvature of the Lorentzian manifold of space-time is caused by energy-momentum. Since geodesics on this manifold are motions of particles in free fall; that is, only affected by the force of gravity, curvature and gravitation are linked. The source of gravity is energy-momentum, and the source of curvature in this manifold is gravity. The precise equation for this relation is formulated as

$$R_{\mu\nu} - \frac{1}{2} g_{\mu\nu} R = -\frac{8\pi G T_{\mu\nu}}{c^4}, \tag{2.5.1}$$

where the left hand side is the Einstein tensor $G_{\mu\nu}$ as we defined in (2.4.10), $G = 6.674 \times 10^{-11} Nm^2/kg^2$ is the Newton's constant, $c = 3 \times 10^8$ is the speed of light and $T_{\mu\nu}$ is the *Energy-momentum tensor* of all gravitating matter.

Now, number of observations can be made: As a consequence of Bianchi identity, the Einstein's tensor is covariantly conserved as shown in (2.4.11). Then the

consistency of the Einstein's field equation (2.5.1) implies that the Energy momentum tensor $T_{\mu\nu}$ must also be covariantly conserved,

$$\nabla^{\mu} T_{\mu\nu} = 0. \tag{2.5.2}$$

Einstein's field equations constitutes a set of non-linear coupled partial differential equations whose general solution is not known. Usually one makes some assumptions, for instance spherical symmetry. Because the Ricci tensor is symmetric, the Einstein's field equations constitute a set of 10 algebraically independent second order differential equations for $g_{\mu\nu}$. Then the general covariant nature of Einstein equations makes us to expect only 6 independent equations for the metric.

Observe that the Riemann curvature tensor (2.4.3) contains terms, which are of the form a single derivative acting on the Christoffel connection, and terms which are quadratic forms in the connection. The Christoffel connection (2.2.10) is in turn expressed in terms of single derivatives acting on the metric tensor. This then implies that the Einstein's field equation (2.5.1) contains derivatives of the metric tensor up to second order in space-time, and in that sense it resembles the Maxwell equations.

The principal difference between the electrodynamics and the dynamics of gravitational field in GR are the nonlinear terms, contained in the quadratic forms in the Christoffel connection, which makes the theory more complicated. These terms are dynamically very relevant in strong gravitational fields. A second difference is that, in GR the dynamical field is the metric tensor, which is a rank two symmetric tensor field, while in the electrodynamics there are vector fields.

Finally, the coupling constant, $8\pi G/c^4 \sim 2 \times 10^{-43} s^2\, kg^{-1}\, m^{-1}$ is dimensionfull, but extremely small on any other physical scale, such that only in the presence of matter under extreme conditions (large energy densities), the matter effects on space-time can be strong. Such extreme conditions are found in compact objects like black holes and neutron stars.

Thus, GR models the effects of gravity as the curvature of Lorentzian manifold. It of course also generalizes the special relativity by using an in general non-flat metric tensor, and in fact is required to approximate to special relativity locally. Special relativity is a special case of GR, where there is no gravitational force acting on the particle. Further, when the motion is non-relativistic and in the weak gravitational field, we can recover Newton's theory of gravity: $\nabla^2\phi = 4\pi G\rho$ (ϕ is the gravitational potential and ρ is the matter density).

Chapter 3 explores the motion of test particles in curved space-time in the Hamiltonian formalism. I develop the particle's dynamics with the Poisson brackets, the minimal Hamiltonian and the conserved quantities. Then applying the formalism in the Schwarzschild space-time, the circular orbits and the Innermost Stable Circular Orbit are found. By describing the effective potential, the various kinds of orbits: circular, eccentric, scattering and plunging orbits are explained. Further exploring the geodesic deviation method, the fully relativistic first order perturbation theory for eccentric orbits are obtained. From the frequency analysis and stability criterion the method of finding the Innermost Stable Circular Orbit is generalized. The chapter is concluded with the equations of motion obtained from the conservation of the energy-momentum tensor.

3

Motion in Curved Space-time

3.1 Hamiltonian Formalism

The basic machinery of GR has been described in the previous chapter. Now we want to investigate the dynamics of test particles in curved space-time with in the Hamiltonian framework. Hamiltonian formalism includes three sets of ingredients: equations of motion, phase-space and the conserved quantities.

The equations describe test particle dynamics are so-called geodesic equations. We have derived geodesic equations of motion starting from the standard variational procedure and also from the Hamiltonian dynamics. In the following sections it is further shown that, it can be obtained from the principles of energy-momentum conservation.

The phase-space formulation of motion in curved space-time is being constructed with the closed set of covariant Poisson-Dirac brackets, obeying Jacobi identities. It consists of the position co-ordinate x^μ and the covariant momentum π_μ, and therefore its anti-symmetric bracket is:

$$\{x^\mu, \pi_\nu\} = \delta^\mu_\nu, \tag{3.1.1}$$

all other possible brackets vanish. These brackets are independent of the specific Hamiltonian. Therefore, in principle we can use varieties of covariant Hamiltonians with the brackets to obtain the equation of motion. However, here we are interested in studying the geodesic motion of the test particle in curved space-time i.e., the particle's interaction is strictly gravitational. Therefore as described in the previous chapter the appropriate Hamiltonian is

$$H = \frac{1}{2m} g^{\mu\nu}(x)\pi_\mu\pi_\nu. \tag{3.1.2}$$

Then the proper-time evolution equations for phase-space co-ordinates are obviously generated by computing the brackets. It is important to note that this Hamiltonian describes the particle's mass as a universal constant of motion for any space-time:

$$H = -\frac{m}{2} \qquad \Rightarrow \qquad g_{\mu\nu}u^\mu u^\nu = -1. \tag{3.1.3}$$

It is called the Hamiltonian constraint in the literature.

3.2 Symmetries, Killing vectors, and Constants of motion

In addition to the universal constants of motion eq. (3.1.3), there exists conserved quantities as a result of symmetries of space-time. Emmy Noether discovered that physical quantities such as energy, momentum, angular momentum, etc. which remain constant during the evolution of the system are related to symmetries of the dynamics. Thus symmetries lead to conservation laws, and knowing a conserved quantity of a dynamical system allows to reduce the dimension of the phase space in which the system is defined.

From special theory of relativity we know that suitable coordinate transformations on the Minkowski metric leaves the metric invariant, giving rise to the Poincaré group of symmetries. Similarly, the standard metrics on the two- or three-sphere have rotational symmetries because they are invariant under rotations of the sphere. We can describe this in two ways: either as an active transformation, in which we rotate the sphere and nothing changes, or as a passive transformation, in which we do not move the sphere, and we just rotate the coordinate system. These descriptions are equivalent.

In the context of geometry we define *symmetry* as an invariance of the metric under a coordinate transformation. The symmetries of a metric are called *isometries*. Quantitatively, we start with a manifold $\mathcal{M}$, with coordinates x^μ. Let the metric in these coordinates be $g_{\mu\nu}(x)$. Suppose we make an infinitesimal change of coordinates

$$x^\mu \to x'^\mu = x^\mu - \xi^\mu(x) \tag{3.2.1}$$

For detecting continuous symmetries we require the invariance of the line element under infinitesimal transformations. We know that the metric tensor transforms as

$$g'_{\mu\nu}(x') = \frac{\partial x^\alpha}{\partial x'^\mu}\frac{\partial x^\beta}{\partial x'^\nu} g_{\alpha\beta}(x). \tag{3.2.2}$$

Using the invariance of the metric under an isometry we can also write

$$g'_{\mu\nu}(x') = g_{\mu\nu}(x') \simeq g_{\mu\nu}(x) - \xi^\lambda \partial_\lambda g_{\mu\nu}(x). \tag{3.2.3}$$

The infinitesimal coordinate transformation also implies

$$\frac{\partial x^\alpha}{\partial x'^{\,\mu}} \simeq \delta^\alpha_\mu + \partial_\alpha \xi^\mu, \quad \frac{\partial x^\beta}{\partial x'^{\,\nu}} \simeq \delta^\beta_\nu + \partial_\alpha \xi^\nu. \tag{3.2.4}$$

Combining these results the Lie derivative of the metric w.r.t. the displacement vector ξ_μ must vanish:

$$\mathcal{L}_\xi g_{\mu\nu} \equiv \xi^\lambda \partial_\lambda g_{\mu\nu} + \partial_\mu \xi^\lambda g_{\lambda\nu} + \partial_\nu \xi^\lambda g_{\mu\lambda} = 0. \tag{3.2.5}$$

Using the metric postulate

$$\nabla_\lambda g_{\mu\nu} = 0, \tag{3.2.6}$$

this can be rewritten covariantly as

$$\mathcal{L} g_{\mu\nu} = \nabla_\mu \xi_\nu + \nabla_\nu \xi_\mu = 0. \tag{3.2.7}$$

Vector fields satisfying these equations are called the *Killing vectors*. Now we will establish the conserved quantities associated with these Killing vectors.

3.2.1 Constants of motion

In classical mechanics, the angular momentum of a particle moving in a rotationally symmetric gravitational field is conserved. In GR the concept of symmetries of a newtonian gravitational field is replaced by symmetries of the metric, and we therefore expect conserved quantities associated with the presence of Killing vectors.

Let us consider a massive particle moving along a geodesic of a spacetime which admits a Killing vector ξ_α. The geodesic equations written in terms of the particle's four-velocity $u^\alpha = dx^\alpha/d\tau$ read

$$\frac{du^\alpha}{d\tau} + \Gamma^\alpha_{\beta\nu} u^\beta u^\nu = 0, \tag{3.2.8}$$

by contracting the above equation with ξ_α, we find

$$\xi_\alpha \left[\frac{du^\alpha}{d\tau} + \Gamma^\alpha_{\beta\nu} u^\beta u^\nu \right] \equiv \frac{d\left(\xi_\alpha u^\alpha\right)}{d\tau} - u^\alpha \frac{d\xi_\alpha}{d\tau} + \Gamma^\alpha_{\beta\nu} u^\beta u^\nu \xi_\alpha = 0 \tag{3.2.9}$$

Since

$$u^\alpha \frac{d\xi_\alpha}{d\tau} = u^\beta u^\nu \frac{\partial \xi_\beta}{\partial x^\nu} \tag{3.2.10}$$

therefore eq. (3.2.9) becomes,

$$\frac{d(\xi_\alpha u^\alpha)}{d\tau} - u^\beta u^\nu \left[\frac{\partial \xi_\beta}{\partial x^\nu} - \Gamma^\alpha_{\beta\nu} \xi_\alpha \right] \equiv \frac{d(\xi_\alpha u^\alpha)}{d\tau} - u^\beta u^\nu \xi_{\beta;\nu} = 0. \tag{3.2.11}$$

Since $\xi_{\beta;\nu}$ is antisymmetric in β and ν, while $u^\beta u^\nu$ is symmetric, the term $u^\beta u^\nu \xi_{\beta;\nu}$ vanishes, and eq. (3.2.11) finally becomes

$$\frac{d(\xi_\alpha u^\alpha)}{d\tau} = 0 \quad \Rightarrow \quad \xi_\alpha u^\alpha = g_{\alpha\mu} \xi^\mu u^\alpha = const. \tag{3.2.12}$$

Eq. (3.2.12) can re-written as $\xi^\mu \pi_\mu = \text{constant} \equiv J$ (let's say), where $\pi_\mu = m g_{\mu\nu} u^\nu$. It is also straight forward to check the quantity J is a constant of the particle motion, by demanding its brackets to vanish with the Hamiltonian:

$$\{J, H\} = 0 \qquad \Rightarrow \qquad J_i = \xi^\mu_i \pi_\mu \tag{3.2.13}$$

Thus, for every Killing vector there exists an associated conserved quantity.

3.3 Spherical symmetry

The Einstein Field Equations are a complicated set of non-linear equations with 10 unknown functions of space-time. These equations are most easily solved in space-times with a maximal number of symmetries as these give rise to a maximal number of constants of motion. This accessibility makes using spherically symmetric spacetimes all the more attractive as a starting point. Birkhoff's theorem classifies all vacuum spherically symmetric spacetimes.

A spacetime is spherically symmetric if it admits an SO(3) group of isometries. In particular every point will lie on some round sphere, on which the rotation group acts transitively, which means that one can go from any point on the sphere to any other point by means of a rotation. Further a space-time is said to be stationary or static, if it exhibits the property of time-translation symmetry. Static spherically symmetric metrics admit four Killing vectors, one of which is timelike, while the remaining three are spacelike, representing the Lie algebra of the rotation group SO(3).

The most general, static and spherically symmetric metric can be expressed in spherical polar coordinates with the ansatz [16]

$$ds^2 = -f(r)dt^2 + g(r)dr^2 + r^2\left(d\theta^2 + sin^2\theta d\varphi^2\right). \tag{3.3.1}$$

The coefficients $f(r)$ and $g(r)$ are fixed by requiring the asymptotic limit i.e., for $r \to \infty$, the metric should be Minkowskian: $ds^2 = -dt^2+dr^2+r^2\left(d\theta^2 + sin^2\theta d\varphi^2\right)$. Due to isotopy and time independence these coefficients cannot depend on (t, θ, φ) and no linear terms in $d\theta$ and $d\varphi$.
Note that this metric is diagonal. Therefore the metric and its inverse has the following components only

$$\begin{aligned} &g_{tt} = -f(r) \qquad g_{rr} = g(r) \qquad g_{\theta\theta} = r^2 \qquad g_{\varphi\varphi} = r^2 sin^2\theta \\ &g^{tt} = -\frac{1}{f(r)} \qquad g^{rr} = \frac{1}{g(r)} \qquad g^{\theta\theta} = \frac{1}{r^2} \qquad g^{\varphi\varphi} = \frac{1}{r^2 sin^2\theta}. \end{aligned} \tag{3.3.2}$$

The next steps are standard, we first compute the non-vanishing components of affine connections $\Gamma^{\mu}_{\lambda\nu} = \Gamma^{\mu}_{\nu\lambda} = \frac{1}{2}\, g^{\mu\kappa}\left(g_{\kappa\lambda,\nu} + g_{\kappa\nu,\lambda} - g_{\lambda\nu,\kappa}\right)$:

$$\begin{aligned} &\Gamma^t_{tr} = \Gamma^t_{rt} = \frac{1}{2}\frac{f'}{f} \qquad \Gamma^r_{tt} = \frac{1}{2}\frac{f'}{g} \qquad \Gamma^r_{rr} = \frac{1}{2}\frac{g'}{g} \\ &\Gamma^\theta_{r\theta} = \Gamma^\theta_{\theta r} = \frac{1}{r} \qquad \Gamma^r_{\theta\theta} = -\frac{r}{g} \qquad \Gamma^r_{\varphi\varphi} = -\frac{r}{g} sin^2\theta \\ &\Gamma^\varphi_{r\varphi} = \Gamma^\varphi_{\varphi r} = \frac{1}{r} \qquad \Gamma^\varphi_{\theta\varphi} = \Gamma^\varphi_{\varphi\theta} = cot\,\theta \qquad \Gamma^\theta_{\varphi\varphi} = -sin\,\theta\, cos\,\theta. \end{aligned} \tag{3.3.3}$$

where $'$ stands for $\frac{\partial}{\partial r}$. Then the Riemann tensor contracted to get Ricci tensor

$$R_{\mu\nu} = \partial_\nu \Gamma^\rho_{\rho\mu} - \partial_\rho \Gamma^\rho_{\mu\nu} + \Gamma^\sigma_{\rho\mu}\Gamma^\rho_{\nu\sigma} - \Gamma^\sigma_{\mu\nu}\Gamma^\rho_{\rho\sigma}, \tag{3.3.4}$$

and as a result

$$\begin{aligned}
R_{tt} &= \frac{1}{2}\frac{f''}{g} + \frac{1}{4}\frac{f'^2}{fg} - \frac{1}{4}\frac{f'g'}{g^2} + \frac{1}{2r}\frac{f'}{g} \\
R_{rr} &= \frac{1}{2}\frac{f''}{f} + \frac{1}{4}\frac{f'^2}{f^2} - \frac{1}{4}\frac{f'g'}{fg} + \frac{1}{2r}\frac{g'}{g} \\
R_{\theta\theta} &= -1 + \frac{1}{g} + \frac{r}{2g}\left(\frac{f'}{f} - \frac{g'}{g}\right) \\
R_{\varphi\varphi} &= sin^2\theta\, R_{\theta\theta}
\end{aligned} \tag{3.3.5}$$

The non-diagonal components $R_{\mu\nu}$ with $\mu \neq \nu$ vanish. These geometric quantities are more general. Therefore it can be used for any static spherically symmetric space-time like Schwarzschild, Reissner-Nordstrøm etc.

3.3.1 The Schwarzschild solution

We now want to find an exact solution of Einstein's equations in vacuum $R_{\mu\nu} = 0$ (for $\mu \neq \nu$), which is spherically symmetric and static. This will be the relativistic generalization of the newtonian solution for a pointlike mass $\varphi = -M/r$ and it will describe the gravitational field in the exterior of a non-rotating body. The solution will be obviously in the form of eq. (3.3.1), where the coefficients f and g are fixed in the following way:

The linear combination of time and radial equations of Ricci tensor implies

$$\frac{R_{tt}}{f} + \frac{R_{rr}}{g} = \frac{1}{r}\frac{g'}{g^2} + \frac{1}{r}\frac{f'}{gf} = 0, \tag{3.3.6}$$

which reveals a simple relation between f and g:

$$\frac{g'}{g} = -\frac{f'}{f} \quad \Rightarrow \quad log(g) = -log(f) + constant, \quad or \quad g \propto \frac{1}{f}. \tag{3.3.7}$$

Now, we fix the proportionality constant between f and g as follows. Imagine we are extremely far away from the star (for example), then the metric should reduce to the Minkowski metric. So in the limit $r \to \infty$ we have $g = f = 1$. This fixes the proportionality constant to be 1. Therefore $g = 1/f$.

Then we only need to compute one of them from one of the differential equations (3.3.5). Let's consider $R_{\theta\theta}$ component and replace g with $1/f$. We have

$$R_{\theta\theta} = 1 - rf' - f = 0 \qquad \Rightarrow \qquad f(r) = 1 + \frac{C}{r}, \tag{3.3.8}$$

where C is some constant we want to determine. We can fix the constant by resorting to the weak-field limit which should reproduce the Newtonian gravitational potential φ. In the weak-field limit we just have

$$f(r) = 1 + 2\varphi(r), \qquad where \qquad \varphi = -\frac{M}{r}, \tag{3.3.9}$$

so the constant $C = -2M$. Then the complete line element in Droste co-ordinates; with M the mass, r the radius of the object,

$$ds^2 = -\left(1 - \frac{2M}{r}\right) dt^2 + \left(1 - \frac{2M}{r}\right)^{-1} dr^2 + r^2 \left(d\theta^2 + sin^2\theta d\varphi^2\right). \tag{3.3.10}$$

This is the famous *Schwarzschild metric*: a unique, static and spherically symmetric vacuum solution, according to Birkhoff's theorem; obtained by the astronomer Karl Schwarzschild [54] in 1916, the very same year that Einstein published his field equations. It was apparently discovered independently by Johannes Droste [55], a student of Lorentz at Leiden University, around the same time.

The Schwarzschild metric (3.3.10) looks divergent at $r = 2M$, the *Schwarzschild radius*. As can be seen by switching to other co-ordinates this is actually a co-ordinate singularity, not a physical singularity of space-time. But the Schwarzschild radius defines a characteristic gravitational scale for any celestial object, related to the formation of a horizon. For the earth or even for the sun the radius is actually very smaller than the radius of the object itself. To compute the radius we need to insert G and c back to the expression and find

$$R_s = \frac{2GM}{c^2} \tag{3.3.11}$$

which is about $3\,km$ for the sun. So, for most astronomical objects this number is so small that we don't need to consider it. However, objects smaller than their Schwarzschild radius disappear behind the horizon and become black holes.

3.3.2 Geodesic equations of motion and effective potential

We now want to consider the motion of a freely falling particle in the Schwarzschild space-time. The analysis can be simplified by using the constants of motion as implied by the Noether's theorem; because of the spherical symmetry of the Schwarzschild metric, there exists four constants associated with the Killing vectors (3.2.13): $J_i = \xi_i^\mu \pi_\mu$. Then

$$E = \xi^0 \pi_0, \qquad J_j = \xi_j^\alpha \pi_\alpha \tag{3.3.12}$$

where E is the particle's energy; $J_j = (J_1, J_2, J_3)$ is the total angular momentum of the system. Without loss of generality we can choose the coordinate system such that $\theta = \pi/2 \Rightarrow u^\theta = 0$, this way the trajectory lies on the plane perpendicular

to the orbital angular momentum. Here the total angular momentum is strictly orbital, and the direction chosen to be z-axis. Then we write the equations of motion (3.2.8) in the component form [56]:

$$\frac{du^t}{d\tau} = -\frac{2M}{r\,(r-2M)}\,u^r u^t, \tag{3.3.13}$$

$$\frac{du^r}{d\tau} = -\frac{M\,(r-2M)}{r^3}\,u^{t\,2} + \frac{M}{r(r-2M)}\,u^{r\,2} + (r-2M)\,u^{\varphi\,2}, \tag{3.3.14}$$

$$\frac{du^\varphi}{d\tau} = -\frac{2}{r}\,u^r u^\varphi. \tag{3.3.15}$$

With z-axis being the choice of the angular momentum, the constants J_1 and J_2 turns out to be zero i.e., $J_1 = J_2 = 0$. Then we are left with the remaining two constants from (3.3.12); $\varepsilon = E/m$ energy per unit mass and $\ell = J_3/m$ angular momentum per unit mass,

$$\varepsilon = \left(1 - \frac{2M}{r}\right) u^t, \qquad\qquad \ell = r^2 sin^2\theta\, u^\varphi = r^2 u^\varphi. \tag{3.3.16}$$

To establish the particle's orbits, we investigate the equations (3.3.13), (3.3.14) and (3.3.15). Eq. (3.3.13) can be re-written as

$$\frac{d}{d\tau}\left[ln(u^t) + ln\left(1 - \frac{2M}{r}\right)\right] = 0, \tag{3.3.17}$$

which can be integrated as $ln\left[u^t\left(1-\frac{2M}{r}\right)\right]$ = constant or

$$u^t\left(1 - \frac{2M}{r}\right) = constant \tag{3.3.18}$$

Similarly eq. (3.3.15) is re-written as

$$\frac{1}{r^2}\frac{d}{d\tau}\left(r^2 u^\varphi\right) = 0, \qquad \Rightarrow \qquad r^2 u^\varphi = constant. \tag{3.3.19}$$

From the Killing constants (3.3.16), we interpret (3.3.18) and (3.3.19) as ε and ℓ. This implies geodesic equations (3.3.13) and (3.3.15) doesn't give any new result. Thus we are left with the radial geodesic equation (3.3.14) only. Upon using the Killing constants (3.3.16) for u^t and u^φ, it turns out be

$$\frac{du^r}{d\tau} = -\frac{M\varepsilon^2}{r\,(r-2M)} + \frac{M}{r(r-2M)}\,u^{r\,2} + \frac{\ell^2}{r^4}\,(r-2M). \tag{3.3.20}$$

a relation for (ε, ℓ). A second relation between these quantities are given by the Hamiltonian constraint: $g_{\mu\nu}u^\mu u^\nu = -1$, similarly by using the Killing constants (3.3.16) we express

$$\left(1-\frac{2M}{r}\right)u^{t\,2} - \frac{u^{r\,2}}{1-\frac{2M}{r}} - r^2\,u^{\varphi\,2} = 1 \quad \Rightarrow \quad u^{r\,2} + \left(1-\frac{2M}{r}\right)\left(\Delta + \frac{l^2}{r^2}\right) = \varepsilon^2. \tag{3.3.21}$$

or

$$E = \frac{1}{2}u^{r\,2} + \frac{1}{2}\left[\left(1-\frac{2M}{r}\right)\left(\Delta+\frac{l^2}{r^2}\right) - 1\right] \tag{3.3.22}$$

where, $E = (\varepsilon^2 - 1)/2$ is the total energy. Note, Δ is 1 for massive particles and 0 for massless particles. If the particle is massless, the geodesic equation cannot be parametrized with the proper time. In this case the particle worldline has to be parametrized using an affine parameter λ such that the geodesic equation takes the form (3.2.8), and the particle tangent vector is $u^\alpha = dx^\alpha/d\lambda$. The derivation of the constants of motion associated to a spacetime symmetry, i.e. to a Killing vector, is similar as for massive particles, recalling that by a suitable choice of the parameter along the geodesic $J = \{E, J_i\}$. Then since for massless particles $m^2 = 0$, the Killing constants ε and ℓ are identified as energy and angular momentum.

Eq. (3.3.22) has the form of an energy equation with a "kinetic energy" term, $\dot{r}^2$ plus a function of r, "potential energy" equalling a constant. Thus the motion in the radial coordinate is exactly equivalent to a particle moving in an effective potential $V_{eff}(r)$ where

$$V_{eff}(r) = \frac{1}{2}\left[\left(1-\frac{2M}{r}\right)\left(\Delta+\frac{l^2}{r^2}\right) - 1\right]. \tag{3.3.23}$$

Then the simplest orbits one can start with are circular orbits i.e., $r = R$, for which we can differentiate the potential and set it to zero: $\partial_r V_{eff}(r) = 0$, which results:

$$\ell^2(R-3M) = \Delta\, MR^2 \tag{3.3.24}$$

Thus we conclude, the circular geodesics exists only for $R > 3M$, for massive particles ($\Delta = 1$) and $R = 3M$ implies null geodesic which is interpreted as *light ring* for massless particles ($\Delta = 0$). Further evaluating the second derivative of the potential yields

$$\frac{\partial^2 V_{eff}(r)}{\partial r^2} = 2\Delta\frac{M}{R^3}\frac{(R-6M)}{(R-3M)} \tag{3.3.25}$$

we observe the circular orbits for $R \geq 6M$ are stable and positive; $R = 6M$ implies the flex point. Then the circular orbits between the radius $3M \leq R < 6M$ are necessarily unstable.

We show the above results qualitatively in Fig. 3.1 [50]. Massive test particles obey four kinds of orbits in Schwarzschild space-time. The Schwarzschild potential has one maximum and one minimum if $\ell/M > 12$. The following 4 points describes the Fig. 3.1 from the top:

(i). The circular orbits exists at the radii, when the potential has minimum or maximum. The orbit at maximum will be in unstable equilibrium, because a small perturbation will through the particle to infinity or the particle will reach the singularity at $r = 0$.

(ii). For $E < 0$, the particle bounds between two turning points. The cross symbols are the turning points: the closest approach to the centre is the perihelion and the farthest approach is the aphelion.

(iii). When E is positive and less than the maximum of the effective potential, then the orbit is scattering. That is the particle comes from infinity and orbits the centre and then moves out to infinity.

(iv). If E is greater than the maximum, then the particle comes from infinity and plunges into the centre.

Now re-writing eq. (3.3.24) for R results,

$$R = \frac{\ell^2}{2M}\left(1 + \sqrt{1 - \frac{12M^2}{\ell^2}}\right) \tag{3.3.26}$$

which relates the radius of the orbits to angular momentum per unit mass ℓ. Thus the minima of the potential lies at a special value of $\ell = 2\sqrt{3}M$, called as the *Innermost Stable Circular Orbit (ISCO)*. *ISCO* can also be predicted through a more general method: *stability criterion*, obtained by evaluating the geodesic deviations between the neighbouring geodesics. This is presented in the next section.
Then returning to the radial geodesic equation (3.3.20); for circular orbits, it yields

$$\varepsilon^2 = \frac{\ell^2}{MR}\left(1 - \frac{2M}{R}\right)^2 \qquad \Leftrightarrow \qquad \frac{u^\varphi}{u^t} = \sqrt{\frac{M}{R^3}} \tag{3.3.27}$$

which is a well known Kepler's result. Thus the geodesic equation (3.2.8) can be viewed as a generalisation of the Kepler's law. Finally, using the above result (3.3.27) along with the normalisation condition (3.3.21), we uniquely express, for circular orbits the Killing constants (ε, ℓ) in terms of the mass M and the radius R

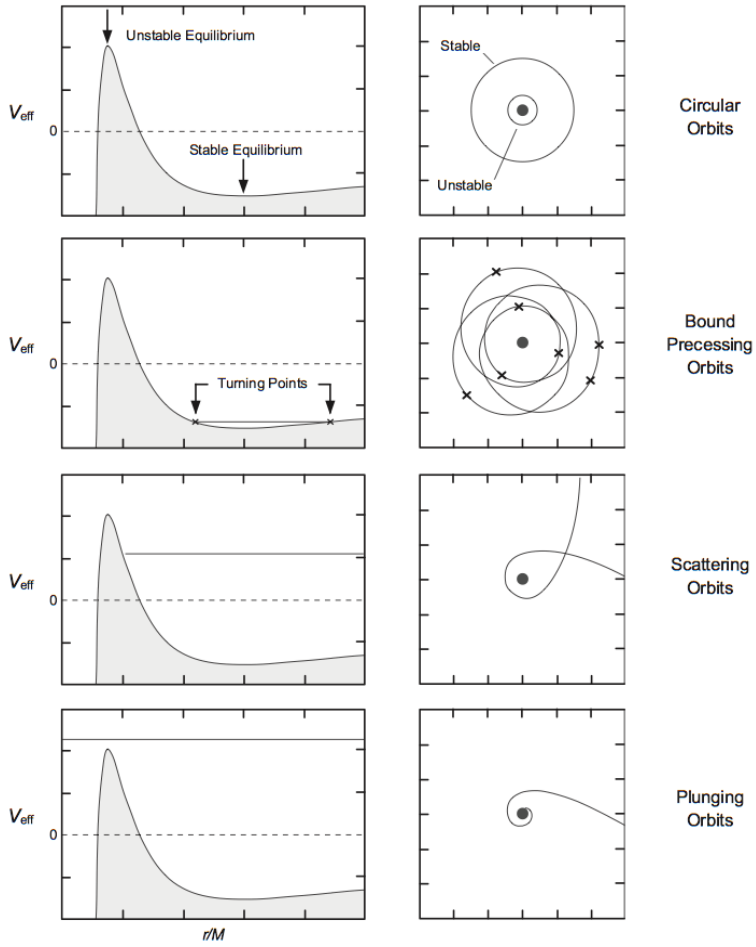

Figure 3.1. The effective potential $V_{eff}(r)$ and its relation to the total energy E is shown in the left, where the vertical axis is $V_{eff}(r)$ and the horizontal axis is r/M. Horizontal lines indicate the vale of E. The shapes of the corresponding orbits are plotted in polar coordinates r and φ, in the plane. The dark region (dot) in each plot is $r < 2M$.

of the black hole

$$\varepsilon_{circ} = \frac{\left(1 - \frac{2M}{R}\right)}{\sqrt{\left(1 - \frac{3M}{R}\right)}}, \qquad \ell_{circ} = \sqrt{\frac{MR}{\left(1 - \frac{3M}{R}.\right)}}. \tag{3.3.28}$$

We conclude this section with re-writing (3.3.16); the angular frequency of the

circular orbits in terms of (M, R) by using (3.3.28)

$$u^{\varphi} \equiv \omega_{circ} = \frac{1}{R^2}\sqrt{\frac{MR}{\left(1-\frac{3M}{R}\right)}}. \tag{3.3.29}$$

3.3.3 Geodesic Deviation: Tidal forces

The equivalance principle is only valid locally, at each point. Two neighbouring mass points which are each in free fall will fall differently. Hence if two such points are physically connected, they will feel a force coming from difference in the way that they free fall. These forces are known as tidal forces.

Thus we are interested in the rate of change of the displacement between the two curves along the geodesic, i.e. the acceleration of the separation [57,58]. Therefore, we consider two geodesic paths traced by the near by test particles, with coordinate vectors, $x^{\lambda}(\tau)$ and $x'^{\lambda}(\tau)$. Then $\delta x^{\lambda}(\tau) = x'^{\lambda}(\tau) - x^{\lambda}(\tau)$ is the difference of two nearby geodesics. If $v^{\nu} = dx^{\nu}/d\tau$ is the tangent vector to a curve $x^{\nu}(\tau)$, then $u^{\lambda} = v^{\nu}\mathcal{D}_{\nu}\delta x^{\lambda}$ is the velocity of the displacement. Thus from the geodesics analysis we have that

$$u^{\lambda} = v^{\nu}\mathcal{D}_{\nu}\delta x^{\lambda} = \frac{d\delta x^{\lambda}}{d\tau} + \Gamma^{\lambda}_{\mu\nu}v^{\nu}\delta x^{\mu}. \tag{3.3.30}$$

This leads to the acceleration,

$$\begin{aligned} a^{\lambda} = v^{\nu}\mathcal{D}_{\nu}(u^{\lambda}) &= \frac{d}{d\tau}\left(\frac{d\delta x^{\lambda}}{d\tau} + \Gamma^{\lambda}_{\mu\nu}v^{\nu}\delta x^{\mu}\right) + \Gamma^{\lambda}_{\mu\nu}u^{\nu}v^{\mu} \\ &= \frac{d^2\delta x^{\lambda}}{d\tau^2} + \partial_{\rho}\Gamma^{\lambda}_{\mu\nu}v^{\nu}v^{\rho}\delta x^{\mu} - \Gamma^{\mu}_{\rho\sigma}\Gamma^{\lambda}_{\mu\nu}\delta x^{\mu}v^{\rho}v^{\sigma} \\ &\quad + \Gamma^{\lambda}_{\mu\nu}v^{\nu}\frac{d\delta x^{\mu}}{d\tau} + \Gamma^{\lambda}_{\mu\nu}\left(\frac{d\delta x^{\nu}}{d\tau} + \Gamma^{\nu}_{\rho\sigma}v^{\rho}\delta x^{\sigma}\right)v^{\mu} \end{aligned} \tag{3.3.31}$$

where we have used the geodesic equation $\frac{dv^{\mu}}{d\tau} = -\Gamma^{\mu}_{\rho\sigma}v^{\rho}v^{\sigma}$ in the third term on the second line. Then expanding the geodesic equations

$$\begin{aligned} \frac{d^2x^{\lambda}}{d\tau^2} + \Gamma^{\lambda}_{\mu\nu}(x)\frac{dx^{\mu}}{d\tau}\frac{dx^{\nu}}{d\tau} &= 0, \\ \frac{d^2x'^{\lambda}}{d\tau^2} + \Gamma^{\lambda}_{\mu\nu}(x')\frac{dx'^{\mu}}{d\tau}\frac{dx'^{\nu}}{d\tau} &= 0, \end{aligned} \tag{3.3.32}$$

to lowest order in $x'^{\nu}(\tau) - x^{\nu}(\tau) = \delta x^{\nu}(\tau)$ to find an equation for $\delta x^{\nu}(\tau)$;

$$\frac{d^2\delta x^{\lambda}}{d\tau^2} + 2\Gamma^{\lambda}_{\nu\rho}v^{\nu}\frac{d\delta x^{\rho}}{d\tau} + \partial_{\rho}\Gamma^{\lambda}_{\nu\sigma}\delta x^{\rho}v^{\nu}v^{\sigma} = 0, \tag{3.3.33}$$

inserting this equation into (3.3.31), we obtain

$$\begin{aligned} a^\lambda &= -\partial_\rho \Gamma^\lambda_{\nu\sigma} \delta x^\rho v^\nu v^\sigma - \Gamma^\mu_{\rho\sigma}\Gamma^\lambda_{\mu\nu}\delta x^\mu v^\rho v^\sigma + \partial_\rho \Gamma^\lambda_{\mu\nu} v^\nu v^\rho \delta x^\mu + \Gamma^\lambda_{\mu\nu}\Gamma^\nu_{\rho\sigma} v^\rho v^\mu \delta x^\sigma \\ &= -R_{\rho\mu\nu}{}^\lambda v^\mu v^\nu \delta x^\rho. \end{aligned} \tag{3.3.34}$$

The *Riemann curvature tensor* $R_{\rho\mu\nu}{}^\lambda$ in the above equation implies that we can measure the curvature by examining the proper acceleration of the separation of two nearby geodesics. With this definition we can re-write the equation of *geodesic deviation* eq. (3.3.33) in the simple form,

$$\mathcal{D}^2_\tau \delta x^\mu - R_{\lambda\kappa}{}^\mu{}_\nu \, v^\kappa v^\nu \delta x^\lambda = 0. \tag{3.3.35}$$

The equation of geodesic deviation controls the congruence of nearby geodesics. In a flat space-time, the curvature tensor vanishes, and hence $\mathcal{D}^2_\tau \delta x^\mu = d^2_\tau \delta x^\mu = 0$. This means that two initially parallel geodesics remain parallel at all times. In curved space-times however, the Riemann tensor is non-vanishing, and as a consequence a freely moving observer sees a relative acceleration of nearby freely moving test particles, which manifests as *tidal effect*. This method can also be used to obtain the eccentric bound orbits of a test mass in the Schwarzschild space-time.

3.3.4 Stability of bound orbits and ISCO

The horizon of a Schwarzschild black hole is located at R = 2M, and the $ISCO$ is found at a larger value of R. By analysing the effective potential we concluded it is at $R = 6M$. Here we start from the above described geodesic deviation method and analyse the $ISCO$ in the Schwarzschild space-time, in a more generalised way.

The circular orbits found in the previous sections can be used as a special reference orbits to solve the geodesic deviation equations (3.3.33) to obtain the stability criterion for bound orbits. Note, it is easy to work with non-covariant variations (3.3.33) rather than the covariant ones (3.3.35). The conservation of angular momentum implies the motion of the particles in the equatorial plane: $\theta = \pi/2$ i.e., $\delta\theta = 0$. Thus the allowed deviations from the circular orbits are parametrized by $\delta x^\mu = (\delta t, \delta r, \delta\varphi)$ only. Then the deviation equations are written in the compact form

$$\begin{pmatrix} \frac{d^2}{d\tau^2} & \alpha\frac{d}{d\tau} & 0 \\ \beta\frac{d}{d\tau} & \frac{d^2}{d\tau^2} - \kappa & -\gamma\frac{d}{d\tau} \\ 0 & \eta\frac{d}{d\tau} & \frac{d^2}{d\tau^2} \end{pmatrix} \begin{pmatrix} \delta t \\ \delta r \\ \delta\varphi \end{pmatrix} = 0 \tag{3.3.36}$$

where the coefficients are evaluated on the circular reference orbit and are given by

$$\alpha = \frac{2M}{R(R-2M)}\sqrt{\frac{R}{R-3M}} \quad \beta = \frac{2M(R-2M)}{R^3}\sqrt{\frac{R}{R-3M}},$$
$$\gamma = \frac{2(R-2M)}{R}\sqrt{\frac{M}{R-3M}}, \quad \eta = \frac{2}{R^2}\sqrt{\frac{M}{R-3M}}, \tag{3.3.37}$$
$$\kappa = \frac{3M}{R^3}\frac{R-2M}{R-3M}.$$

Then solving the operator (3.3.36) for its eigen frequency ω_d of the oscillations; λ being its eigen values and are related through, $\lambda_\pm = \pm i\omega$,

$$\omega_d = \sqrt{\eta\gamma - \alpha\beta - \kappa} = \sqrt{\frac{M}{R^3}\frac{R-6M}{R-3M}}. \tag{3.3.38}$$

The real eigenvalues corresponds to stable circular orbits and the imaginary ones leads to unstable orbits [58]. Then it is straight forward to conclude from eq. (3.3.38), the eigenvalues are real only for $R \geq 6M$. Therefore, we predict $R = 6M$ is the $ISCO$. Thus the value of $ISCO$ obtained from the stability criterion and from minimising the effective potential are the same. Though the machinery to arrive at $ISCO$ through stability criterion is apparently tedious, this method has advantage when we include additional degrees of freedom; spin and/or charge to the test particles [48].

The generic solution for geodesic deviated bound orbits are periodic and the detailed analysis are given in the references [57]. The frequency ω_d of those orbits can be interpreted as the relativistic generalization of an epicycle and it differs from that of circular orbits frequency (3.3.29) ω_{circ}

$$\omega_d \approx \omega_{circ}\left(1 - \frac{3M}{R}\right) \tag{3.3.39}$$

Therefore the point of closest approach – the periastron, shifts during each orbit by a fixed amount $\delta\varphi$,

$$\delta\varphi = 2\pi\left(\frac{\omega_{circ}}{\omega_d} - 1\right) \approx 2\pi\left(\frac{3M}{R}\right) \tag{3.3.40}$$

In the geodesic deviation method, we develop an approximate analytical solution to the equations of motion and study the generic bound orbits close to circular orbits. Then by analysing the frequency of such orbits, we predict the $ISCO$. The difference in the frequency of bound orbits to that of circular orbits results in periastron shift. The periastron shift calculated through this approximation [57] and the one which is obtained directly by integrating the conservation of the absolute 4-velocity (3.3.21) (a standard exercise [50] for the well-known precession of the periastron in general relativity) are exactly the same.

3.4 Energy-momentum conservation: equations of motion

The equations of motion has been derived from the standard variational procedure and from the Hamiltonian formalism. Here we present an independent proof of the equations of motion from an appropriate energy-momentum tensor.

The Einstein's tensor is covariantly conserved as a result of contraction of the Bianchi identity,

$$G_{\mu\nu} = R_{\mu\nu} - \frac{1}{2}g_{\mu\nu}R = -8\pi G T_{\mu\nu}, \qquad \nabla^\mu G_{\mu\nu} = \nabla^\mu R_{\mu\nu} - \frac{1}{2}\nabla_\nu R = 0, \quad (3.4.1)$$

This implies, Einstein field equation is consistent only if the energy-mometum tensor $T_{\mu\nu}$ is also covariantly conserved. Thus,

$$\nabla^\mu T_{\mu\nu} = 0. \quad (3.4.2)$$

the source term $T_{\mu\nu}$ has the same property as $G_{\mu\nu}$. Then the energy-mometum tensor $T_{\mu\nu}$ for a test particle moving on a world-line $X^\mu(\tau)$ is defined by the proper-time integral[1]

$$T_0^{\mu\nu} = \frac{m}{\sqrt{-g}} \int d\tau \, u^\mu u^\nu \delta^4 \left(x - \xi(\tau)\right) \quad (3.4.4)$$

where $\xi(\tau)$ is the position coordinate of the particle in the phase-space. Then the covariant divergence of $T_0^{\mu\nu}$ vanishes for the particle moving on geodesics:

$$\nabla_\mu T_0^{\mu\nu} = \frac{m}{\sqrt{-g}} \int d\tau \, \frac{Du^\nu}{D\tau} \delta^4 \left(x - \xi(\tau)\right) = 0. \quad (3.4.5)$$

Therefore,

$$\frac{Du^\nu}{D\tau} = 0, \qquad \Rightarrow \qquad \ddot{x}^\mu + \Gamma^\mu_{\lambda\nu} \dot{x}^\lambda \dot{x}^\nu = 0. \quad (3.4.6)$$

Thus we have obtained the geodesic equations of motion in another alternate way. This is an obvious result in GR. In the following chapters we prove the similar computation is also possible for non-trivial cases, like including the spin-dependent forces.

[1] The square root is included because we define the delta-function as a scalar density of weight 1/2, such that for scalar functions $f(x)$

$$\int d^4y \, \delta^4(x - y) f(y) = f(x). \quad (3.4.3)$$

Chapter 4 starts with summarizing the traditional method of describing spin in the curved space-time – Mathisson-Papapetrou formalism. In the spinning particle approximation, I explain an alternative complementary formalism for spin dynamics. I derive equations of motion for point-like objects in curved space-time by using the Poisson-Dirac brackets and the minimal Hamiltonian. Then our method is compared with the traditional one in a qualitative way. The conserved quantities are developed in the Schwarzschild space-time. Since the closed set of Poisson-Dirac brackets is model independent, the analysis has been extended with gravitational and electric Stern-Gerlach interactions by introducing non-minimal Hamiltonians. Also modified conservation laws emerge reflecting the spin-orbit coupling. The equations of motions are also obtained from the conservation of the energy-momentum tensor.

4

Spinning Bodies in Curved Space-time

4.1 Spinning particles

In general relativity (GR), given the metric $g_{\mu\nu}$, the motion of test (single-pole) particles is determined by the geodesic equations of motion. Thus the single-pole particle doesn't have any internal structure [2]. The dynamical equations can be obtained from the covariant conservation of the energy-momentum tensor. A spinning particle in GR is a *pole-dipole particle*. Therefore its motion is generalised on a world line rather than geodesics. The evolution equations for spinning particles were derived (similar to test particles) by applying the conservation law for the energy-momentum tensor of matter $T^{\mu\nu}$, together with the Einstein field equations; and famously known as Mathisson-Papapetrou (MP) equations [59]:

$$\frac{\mathcal{D}p^{\mu}}{d\tau} = -\frac{1}{2}\, R^{\mu}{}_{\nu\kappa\lambda} u^{\nu} S^{\kappa\lambda}, \tag{4.1.1}$$

$$\frac{\mathcal{D}S^{\mu\nu}}{d\tau} = p^{\mu}u^{\nu} - u^{\mu}p^{\nu}, \tag{4.1.2}$$

where p^{μ} is the total 4-momentum of the particle, $u^{\mu} = dx^{\mu}/d\tau$ is the time like tangent vector ($u^{\mu}u_{\mu} = -1$) to the world line along which the particle moves i.e., *centre of mass* line used to make the multipole reduction, τ is the proper time along this world line, and $R^{\mu}{}_{\nu\kappa\lambda}$ is the Riemann tensor.

The energy-momentum vector p^{μ} and the intrinsic angular-momentum tensor $S^{\mu\nu}$ can be constructed by computing integrals of components of the energy-momentum tensor and their first moments over the volume of the body, using suitable boundary conditions [60]:

$$S^{\mu\nu} = \int_{x^0=const} \left(T^{\nu 0}\delta x^{\mu} - T^{\mu 0}\delta x^{\nu}\right) \sqrt{-g}\, d^3x \tag{4.1.3}$$

$$p^{\mu} = mu^{\mu} - u_{\nu}\frac{\mathcal{D}S^{\mu\nu}}{d\tau} \tag{4.1.4}$$

The quantity $m \equiv -p_{\sigma}u^{\sigma}$ is the particle's mass in the rest frame and it reduces to ordinary mass when the spin vanishes. The evolution equations (4.1.1) and

(4.1.2) are not a closed set of first order differential equations i.e., the system has 10 equations, but has 13 unknown quantities: $u(3)$, $p(4)$ and $S(6)$. Therefore it needs additional spin supplementary conditions (SSC) to fix a unique world line, and such that, it makes it possible to keep track of aspects of the structure of the body. A SSC fixes a centre of reference e.g. the centre of mass and different SSC defines a different centre of mass world line. Thus the MP equations describe the evolution of p^μ and $S^{\mu\nu}$ along the centre of mass world lines u^μ.

In literature there are many supplementary conditions, but for our discussion we choose to explore with Tulczyjew-Dixon (TD) condition;

$$S^{\mu\nu}p_\nu = 0, \tag{4.1.5}$$

which is claimed to be more physical [61, 62]. For an excellent review on various supplementary conditions and their relation we refer to [63]. The MP equations along with above conditions are called as Mathisson-Papapetrou-Dixon (MPD) model [64]. Further analysis concludes that different supplementary conditions lead to the same physical motion [63].

These highly non-linear (full) equations have been studied through numerical analysis [65–67]. The analytical solutions are very difficult even in highly symmetric space-times. The physical reason is that the particle has non-zero size i.e., a small extended body, whose internal structure is described by its spin (4.1.3). But through linearising the differential equations (4.1.1) and (4.1.2), an analytical description is achieved.

The dynamical equations imply, spin-orbit coupling, i.e., spin couples to the curvature of the background space-time. Therefore the spin force pushes the particle away from the geodesic. Then the deviation from geodesic motion should be very small compared with the curvature tensor of the space-time, which enforces a *limit* on the particle's spin [64]. Under these assumptions, the back reaction of the particle and the gravitational radiation emitted by the particle in its motion are neglected. This leads to consider the linear approximation of the spin; in this limit p^μ and u^μ are parallel: $p^\mu \approx mu^\mu$. Neglecting the higher order terms, equations (4.1.1) and (4.1.2) reduce to

$$\frac{\mathcal{D}(mu^\mu)}{d\tau} = -\frac{1}{2}R^\mu{}_{\nu\kappa\lambda}u^\nu S^{\kappa\lambda} + \mathcal{O}(2), \tag{4.1.6}$$

$$\frac{\mathcal{D}S^{\mu\nu}}{d\tau} = \mathcal{O}(2). \tag{4.1.7}$$

Which implies the mass of the particle remains constant along the motion: $dm/d\tau = 0$ and the *spin tensor is parallel transported along the path.* Then the TD condition reduces to the so-called Pirani condition:

$$S^{\mu\nu}u_\nu = 0. \tag{4.1.8}$$

Equations (4.1.6), (4.1.7) and (4.1.8) constitutes the Mathisson-Papapetrou-Pirani (MPP) model. Note, the Pirani vector (say) $Z^\mu = S^{\mu\nu}u_\nu = 0$, throughout the evolution.

Finally we conclude this section with some additional references for generalisation of this method. A similar analysis has been extended for charged spinning particle (pole-dipole approx.) in a given gravitational as well as electromagnetic field, by Dixon and Souriau [68–71]. The dynamical equations of motion for an extended body in a given gravitational field were deduced by Dixon in *multipole approximation* to any order [61, 62, 72]. The MP model has been extended for *massless particles* i.e., null multipole reduction world line by Mashhoon [73].

4.2 Spinning-particle approximation

In addition to the above well-known method, there is an other complementary approach to the subject [74] . It constructs effective equations of motion for point-like objects, which is an idealization of a compact body, at the price of neglecting details of the internal structure by assigning the point-like object an overall position, momentum and spin. This is also known as the spinning-particle approximation, and is used for the semi-classical description of elementary particles as well. A large variety of models for spinning particles is found in the literature [75–85].

We take the second point of view for the description of spinning test masses in curved space-time, using an *effective hamiltonian formalism* similar to the one introduced in ref. [86]. One of the advantages of this description is that it can be applied to compact bodies with different types of spin dynamics, such as different gravimagnetic ratios. In this way specific aspects of the structure can still be accounted for.

4.3 Covariant Hamiltonian Formalism

Hamiltonian dynamical systems are specified by three sets of ingredients: *the phase space*, identifying the dynamical degrees of freedom, the *Poisson-Dirac brackets* defining a symplectic structure, and the *hamiltonian* generating the evolution of the system with given initial conditions by specifying a curve in the phase space passing through the initial point. The parametrization of phase-space is not unique, as is familiar from the Hamilton-Jacobi theory of dynamical systems. Changes in the parametrization can be compensated by redefining the brackets and the hamiltonian. A convenient starting point for models with gauge-field interactions is the use of covariant, i.e. kinetic, momenta rather than canonical momenta; see [87] and references cited there for a general discussion, and [86] for the application to spinning particles.

The spin degrees of freedom are described by an antisymmetric tensor $\Sigma^{\mu\nu}$, which can be decomposed into two space-like four-vectors by introducing a time-like unit vector u: $u_\mu u^\mu = -1$, and defining

$$S^\mu = \frac{1}{2\sqrt{-g}}\,\varepsilon^{\mu\nu\kappa\lambda}\,u_\nu\Sigma_{\kappa\lambda}, \qquad Z^\mu = \Sigma^{\mu\nu}u_\nu. \tag{4.3.1}$$

By construction both four-vectors S and Z are space-like:

$$S^\mu u_\mu = 0, \qquad Z^\mu u_\mu = 0. \tag{4.3.2}$$

In the following we take u to be the proper four-velocity of the particle. Then S is the Pauli-Lubanski pseudo-vector, from which a magnetic dipole moment can be constructed, whilst the components of Z, which will be referred to as the Pirani vector, can be used to define an electric dipole moment [88, 89]. Observe that we can invert the relations (4.3.1) to write

$$\Sigma^{\mu\nu} = -\frac{1}{\sqrt{-g}}\,\varepsilon^{\mu\nu\kappa\lambda}\,u_\kappa S_\lambda + u^\mu Z^\nu - u^\nu Z^\mu. \tag{4.3.3}$$

Therefore, if the Pirani vector vanishes: $Z = 0$ [90], the full spin tensor can be reconstructed from S. However, in general this is not the case in our formalism. It is also interesting to note that in addition one can define a third space-like vector

$$W^\mu = -\frac{1}{\sqrt{-g}}\,\varepsilon^{\mu\nu\kappa\lambda}u_\nu S_\kappa Z_\lambda = \left(\Sigma^{\mu\nu} - u^\mu Z^\nu\right) Z_\nu, \tag{4.3.4}$$

orthogonal to the other ones:

$$W \cdot u = W \cdot S = W \cdot Z = 0. \tag{4.3.5}$$

Together (u, S, Z, W) form a set of independent vectors, one time-like and three space-like, which can be used to define a frame of basis vectors carried along the particle world-line.

4.3.1 Covariant phase-space structure

The full set of phase-space co-ordinates of a spinning particle thus consists of the position co-ordinate x^μ, the covariant momentum π_μ and the spin tensor $\Sigma^{\mu\nu}$, with anti-symmetric Dirac-Poisson brackets

$$\begin{aligned}
&\{x^\mu, \pi_\nu\} = \delta^\mu_\nu, \qquad \{\pi_\mu, \pi_\nu\} = \frac{1}{2}\,\Sigma^{\kappa\lambda}R_{\kappa\lambda\mu\nu},\\
&\{\Sigma^{\mu\nu}, \pi_\lambda\} = \Gamma_{\lambda\kappa}{}^{\mu}\,\Sigma^{\nu\kappa} - \Gamma_{\lambda\kappa}{}^{\nu}\,\Sigma^{\mu\kappa},\\
&\left\{\Sigma^{\mu\nu}, \Sigma^{\kappa\lambda}\right\} = g^{\mu\kappa}\Sigma^{\nu\lambda} - g^{\mu\lambda}\Sigma^{\nu\kappa} - g^{\nu\kappa}\Sigma^{\mu\lambda} + g^{\nu\lambda}\Sigma^{\mu\kappa}.
\end{aligned} \tag{4.3.6}$$

The brackets imply that π represents the generator of covariant translations, whilst the spin degrees of freedom Σ generate internal rotations and Lorentz transformations. It is straightforward to check that these brackets are closed in the sense that they satisfy the Jacobi identities for triple bracket expressions. Thus they define a consistent symplectic structure on the phase space.

To get a well-defined dynamical system we need to complete the phase-space structure with a hamiltonian generating the proper-time evolution of the system. In principle a large variety of covariant expressions can be constructed; however if we impose the additional condition that the *particle interacts only gravitationally* and that in the limit of vanishing spin the motion reduces to geodesic motion, the variety is reduced to hamiltonians

$$H = H_0 + H_\Sigma, \qquad H_0 = \frac{1}{2m}\, g^{\mu\nu}\pi_\mu\pi_\nu, \tag{4.3.7}$$

where $H_\Sigma = 0$ whenever $\Sigma^{\mu\nu} = 0$. In the following sections we focus first on the dynamics generated by the minimal hamiltonian H_0. However, we also consider extensions with gravitational and electric Stern-Gerlach forces [80]. Thus the choice of hamiltonians can be enlarged further by including spin-spin interaction via space-time curvature and charges coupling the particle to vector fields like the electromagnetic field [86, 88].

Eqs. (4.3.6) and (4.3.7) specify a complete and consistent dynamical scheme for spinning particles. Note that the choice of hamiltonian is fixed by further physical requirements, and can differ for different compact objects. In that sense the hamiltonian is an *effective* hamiltonian, suitable to describe the motion of various types of objects in so far as the role of other internal degrees of freedom can be restricted to their effects on overall position, linear momentum and spin.

4.3.2 Minimal equations of motion

The simplest model for a massive free spinning particle in the absence of Stern-Gerlach forces and external fields is obtained by restricting the hamiltonian to the minimal geodesic term H_0. By itself this hamiltonian generates the following set of proper-time evolution equations:

$$\dot{x}^\mu = \{x^\mu, H_0\} \quad \Rightarrow \quad \pi_\mu = m g_{\mu\nu}\dot{x}^\nu, \tag{4.3.8}$$

stating that the covariant momentum π is a tangent vector to the world line, proportional to the proper four-velocity $u = \dot{x}$. Next

$$\dot{\pi}_\mu = \{\pi_\mu, H_0\} \quad \Rightarrow \quad D_\tau\pi_\mu \equiv \dot{\pi}_\mu - \dot{x}^\lambda \Gamma_{\lambda\mu}{}^\nu \pi_\nu = \frac{1}{2m}\,\Sigma^{\kappa\lambda} R_{\kappa\lambda\mu}{}^\nu\, \pi_\nu, \tag{4.3.9}$$

which specifies how the world line curves in terms of the evolution of its tangent vector. Finally the rate of change of the spin tensor is

$$\dot{\Sigma}^{\mu\nu} = \{\Sigma^{\mu\nu}, H_0\} \quad \Rightarrow \quad D_\tau\Sigma^{\mu\nu} \equiv \dot{\Sigma}^{\mu\nu} + \dot{x}^\lambda \Gamma_{\lambda\kappa}{}^\mu \Sigma^{\kappa\nu} + \dot{x}^\lambda \Gamma_{\lambda\kappa}{}^\nu \Sigma^{\mu\kappa} = 0. \tag{4.3.10}$$

In these equations the overdot denotes an ordinary derivative w.r.t. proper time τ, whereas D_τ denotes the pull-back of the covariant derivative along the world line $x^\mu(\tau)$. By substitution of eq. (4.3.8) into eq. (4.3.9) one finds that

$$D_\tau^2 x^\mu = \ddot{x}^\mu + \Gamma_{\lambda\nu}{}^\mu \dot{x}^\lambda \dot{x}^\nu = \frac{1}{2m} \Sigma^{\kappa\lambda} R_{\kappa\lambda}{}^\mu{}_\nu \, \dot{x}^\nu, \tag{4.3.11}$$

which reduces to the geodesic equation in the limit $\Sigma = 0$. The world line is the solution of the combined equations (4.3.11) and (4.3.10) satisfying some initial conditions. This *world line is a curve in space-time along which the spin tensor is covariantly constant* (Fig. 4.1).

It has been remarked by many authors [86, 91–93], that the spin-dependent force (4.3.9) exerted by the space-time curvature on the particle is similar to the Lorentz force with spin replacing the electric charge and curvature replacing the electromagnetic field strength. In this analogy the covariant conservation of spin along the world line is the natural equivalent of the conservation of charge.

Even though the spin tensor is covariantly constant, this does not hold for the Pauli-Lubanski and Pirani vectors S and Z individually. Indeed, due to the gravitational Lorentz force

$$\begin{aligned} D_\tau S^\mu &= \frac{1}{4m\sqrt{-g}} \varepsilon^{\mu\nu\kappa\lambda} \Sigma_{\kappa\lambda} \Sigma^{\alpha\beta} R_{\alpha\beta\nu\rho} u^\rho, \\ D_\tau Z^\mu &= \frac{1}{2m} \Sigma^{\mu\nu} \Sigma^{\alpha\beta} R_{\alpha\beta\nu\rho} u^\rho, \end{aligned} \tag{4.3.12}$$

where $\Sigma^{\mu\nu}$ is the linear expression in terms of S^μ and Z^μ given in eq. (4.3.3). We observe that the rate of change of both spin vectors is of order $\mathcal{O}[\Sigma^2]$. In particular, as Z is not conserved in non-flat space-times the condition $Z = 0$ cannot be imposed during the complete motion in general. Indeed, the evolution of the system is completely determined by eqs. (4.3.8, 4.3.9, 4.3.10), and leaves *no room for additional constraints*.

We close this section by remarking that the gravitational Lorentz force for unit mass $1/2\,\Sigma^{\kappa\lambda} R_{\kappa\lambda}{}^\mu{}_\nu u^\nu$ can be interpreted geometrically as the change in the unit vector u^μ generated by transporting it around a closed loop with area projection in the x^κ-x^λ-plane equal to $\Sigma^{\kappa\lambda}$.

4.4 *Effective* Hamiltonian and MPD formalism: a comparison

The dynamical equations in the MP formalism are not a closed set of first order differential equations. The system has 10 equations, but has 13 unknown quantities: $u(3)$, $p(4)$ and $S(6)$. Thus one needs spin supplementary conditions to solve them. SSC define world lines traced by differently defined centres of mass. The most commonly used SSC is TD condition (4.1.5). The system is commonly known

as MPD formalism. The full MPD equations are very difficult to solve even in the highly symmetric space-times. Therefore one linearizes MPD formalism which leads to MPP model. Then the coupled equations (4.1.6), (4.1.7) and (4.1.8) constitutes the closed system.

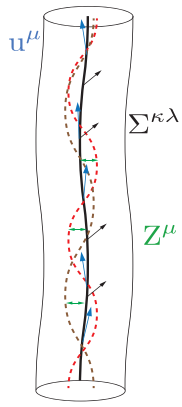

Figure 4.1. Compares the world lines [94] traced by *effective* hamiltonian formalism and MPD model. The thick black line is the world line along which the spin tensor ($\Sigma^{\kappa\lambda}$) is covariantly constant, and u^μ is the tangent vector to this world line. Dotted lines are the world lines followed by some preferred centre of mass in the MPD model. Green double arrows represents the dipole vector Z^μ which quantifies the difference between centre of mass world lines and the world line of spin tensor (thick, black line).

Where as in the hamiltonian dynamics, the system is described by a set of 2N phase-space variables satisfying first-order differential equations in the evolution parameter (proper time). Then by fixing initial conditions the evolution of the system is completely and uniquely determined. For spinning particles the phase-space is 14-dimensional: $x(4)$, $\pi(4)$, $\Sigma(6)$. These are subject to 14 first-order differential equations (4.3.8), (4.3.9) and (4.3.10). Thus the evolution of the system is completely determined by the initial conditions. Therefore we don't need any SSC in our formalism.

The linearized form of MPD formalism precisely coincides with the original equations of motion (4.3.10) and (4.3.11) in our formalism, whose solution is the spin tensor parallelly transported along the world line. Then if we consider the linearized form of our equations of motion, neglecting quadratic or higher order terms in the spin-tensor $\Sigma^{\mu\nu}$, the right-hand side of equations (4.3.12) vanishes, and it is possible to require the Pirani condition $Z^\mu = 0$ at all times. Thus the usual MPP dynamics can be recovered in linearized form from our equations.

In the MPD formalism the equations of motion are constructed in a such a way that, if one fixes an initial condition a constraint on the dipole, such as the Pirani constraint $Z^\mu = 0$; it holds true throughout the evolution. In other words, the

equation of motion for Z^μ has been replaced by an algebraic constraint $Z^\mu = 0$. This is because of the fact that the canonical momentum p^μ in the MPD model is different from the kinetic momentum π^μ in our formalism. Thus the analysis of the evolution equations are complicated in MPD model.

In contrast, in our formulation the momentum is always strictly kinetic: $\pi^\mu = mu^\mu$, but the dipole Z^μ is dynamical and non-vanishing in general. Therefore the mass-dipole constraint has been replaced by a proper equation of motion (4.3.12), which determines how Z^μ evolves even if it vanishes initially.

The two formulations are not necessarily contradicting each other. In the MP case the solution of the dynamical equations is the world line on which the SSC is always true and so it traces the centre of mass (dotted lines in Fig. 4.1). Since it accounts for the internal structure of the particle, the spin dynamics is complicated. In our case the spin-dynamics is simple and straightforward, but the center of mass is not necessarily located on the world-line, as signalled by the non-zero mass dipole. Therefore the solution of our equations of motion is the world line in which the spin tensor is covariantly constant (thick, black line). Thus its a matter of choice.

One of the major advantage in our formalism is that the back reaction of the particle motion on the space-time geometry can be calculated unambiguously. This is accounted by the energy-momentum tensor which exhibits the effect of the mass dipole.

4.5 Conservation laws

The Hamiltonian formalism we have developed is also convenient for deriving constants of motion. There are two classes of constants in the theory. The universal constants which exist for any space-time geometry and the constants of motion emerging as a result of symmetries of the space-time. These constants commute with the hamiltonian in the sense of the brackets.

4.5.1 Universal conserved quantities

For the spinning body in curved space-time, there exist universal constants of motion, irrespective of the specific geometry of the space-time manifold. By construction the time-independent hamiltonian represented by (4.3.7) is a constant of motion. In particular for the minimal geodesic hamiltonian H_0 we have

$$H_0 = -\frac{m}{2}, \tag{4.5.1}$$

defining the particles mass. The above equation is equivalent to normalizing proper time such that $u_\mu u^\mu = -1$. In addition there are two constants of motion for the spin: the total spin I as a result of local Lorentz invariance

$$I = \frac{1}{2}\, g_{\kappa\mu} g_{\lambda\nu} \Sigma^{\kappa\lambda} \Sigma^{\mu\nu} = S_\mu S^\mu + Z_\mu Z^\mu, \tag{4.5.2}$$

and the pseudo-scalar spin-dipole product:

$$D = \frac{1}{8}\sqrt{-g}\,\varepsilon_{\mu\nu\kappa\lambda}\Sigma^{\mu\nu}\Sigma^{\kappa\lambda} = S \cdot Z. \tag{4.5.3}$$

Note, I and D are quadratic expressions in spin. In the Hamiltonian formalism all these three constants obey obviously

$$\{H_0, H_0\} = 0, \qquad \{I, H_0\} = 0, \qquad \{D, H_0\} = 0. \tag{4.5.4}$$

4.5.2 Geometrical conserved quantities

Furthermore, there may exist conserved quantities $J(x, \pi, \Sigma)$ resulting from symmetries of the background geometry, as implied by Noether's theorem [61, 95, 96]. They are solutions of the generic equation

$$\{J, H_0\} = \frac{1}{m}\, g^{\mu\nu}\pi_\nu \left[\frac{\partial J}{\partial x^\mu} + \Gamma_{\mu\lambda}{}^{\kappa}\,\pi_\kappa \frac{\partial J}{\partial \pi_\lambda} + \frac{1}{2}\,\Sigma^{\alpha\beta} R_{\alpha\beta\lambda\mu}\frac{\partial J}{\partial \pi_\lambda} + \Gamma_{\mu\alpha}{}^{\kappa}\,\Sigma^{\lambda\alpha}\frac{\partial J}{\partial \Sigma^{\kappa\lambda}}\right] = 0. \tag{4.5.5}$$

The symmetries of the space-time manifest themselves as Killing vectors. Here due to spin-orbit coupling, the conserved quantities implied by Noether's theorem are linear combinations of momentum [96] and spin components:

$$J = \alpha^\mu \pi_\mu + \frac{1}{2}\,\beta_{\mu\nu}\,\Sigma^{\mu\nu}, \tag{4.5.6}$$

with

$$\nabla_\mu \alpha_\nu + \nabla_\nu \alpha_\mu = 0, \qquad \nabla_\lambda \beta_{\mu\nu} = R_{\mu\nu\lambda}{}^{\kappa}\alpha_\kappa. \tag{4.5.7}$$

These equations imply that α is a Killing vector on the space-time, and β is its anti-symmetrized gradient:

$$\beta_{\mu\nu} = \frac{1}{2}\left(\nabla_\mu \alpha_\nu - \nabla_\nu \alpha_\mu\right). \tag{4.5.8}$$

Similarly constants of motion quadratic in momentum [97] are of the form:

$$J = \frac{1}{2}\,\alpha^{\mu\nu}\pi_\mu\pi_\nu + \frac{1}{2}\beta_{\mu\nu}{}^{\lambda}\,\Sigma^{\mu\nu}\pi_\lambda + \frac{1}{8}\,\gamma_{\mu\nu\kappa\lambda}\Sigma^{\mu\nu}\Sigma^{\kappa\lambda}, \tag{4.5.9}$$

where the coefficients have to satisfy the ordinary partial differential equations

$$\begin{aligned}
&\nabla_\lambda \alpha_{\mu\nu} + \nabla_\mu \alpha_{\nu\lambda} + \nabla_\nu \alpha_{\lambda\mu} = 0,\\
&\nabla_\mu \beta_{\kappa\lambda\nu} + \nabla_\nu \beta_{\kappa\lambda\mu} = R_{\kappa\lambda\mu}{}^{\rho}\alpha_{\nu\rho} + R_{\kappa\lambda\nu}{}^{\rho}\alpha_{\mu\rho},\\
&\nabla_\rho \gamma_{\mu\nu\kappa\lambda} = R_{\mu\nu\rho}{}^{\sigma}\beta_{\kappa\lambda\sigma} + R_{\kappa\lambda\rho}{}^{\sigma}\beta_{\mu\nu\sigma}.
\end{aligned} \tag{4.5.10}$$

Thus α is a symmetric rank-two Killing tensor, and the coefficients (β, γ) satisfy a hierarchy of inhomogeneous Killing-like equations determined by the $\alpha_{\mu\nu}$. In the

case of Grassmann-valued spin tensors $\Sigma^{\mu\nu} = i\psi^\mu\psi^\nu$ the coefficient γ is completely anti-symmetric and the equations are known to have a solution in terms of Killing-Yano tensors [98].

The constants of motion (4.5.6) linear in momentum are special in that they define a Lie algebra: if J and J' are two such constants of motion, then their bracket is a constant of motion of the same type. This follows from the Jacobi identity

$$\{\{J, J'\}, H_0\} = \{\{J, H_0\}, J'\} - \{\{J', H_0\}, J\} = 0. \tag{4.5.11}$$

Thus, if $\{e_i\}_{i=1}^r$ is a complete basis for Killing vectors:

$$\alpha^\mu = \alpha^i e_i^\mu, \qquad e_j^\nu \nabla_\nu e_i^\mu - e_i^\nu \nabla_\nu e_j^\mu = f_{ij}{}^k e_k^\mu,$$

the constants of motion define a representation of the same algebra:

$$J_i = e_i^\mu \pi_\mu + \frac{1}{2} \nabla_\mu e_{i\nu}\, \Sigma^{\mu\nu} \quad \Rightarrow \quad \{J_i, J_j\} = f_{ij}{}^k J_k. \tag{4.5.12}$$

Evidently such constants of motion are helpful in the analysis of spinning particle dynamics [51, 95, 99].

4.6 Non-minimal hamiltonian: gravitational Stern-Gerlach force

So far we have studied the dynamics of compact spinning objects generated by the minimal geodesic hamiltonian H_0. In this section we consider the non-minimal extension including the *spin-spin interaction* via space-time curvature:

$$H = H_0 + H_\Sigma, \qquad H_\Sigma = \frac{\kappa}{4} R_{\mu\nu\kappa\lambda} \Sigma^{\mu\nu} \Sigma^{\kappa\lambda}. \tag{4.6.1}$$

The Dirac-Poisson brackets (4.3.6) remain the same (obviously). It is straightforward to derive the equations of motion:

$$\begin{aligned}
&\dot{x}^\mu = \{x^\mu, H\} \quad \Rightarrow \quad \pi_\mu = m g_{\mu\nu} \dot{x}^\nu, \\
&\dot{\pi}_\mu = \{\pi_\mu, H\} \quad \Rightarrow \quad D_\tau \pi_\mu = \frac{1}{2m} \Sigma^{\kappa\lambda} R_{\kappa\lambda\mu}{}^\nu \pi_\nu - \frac{\kappa}{4} \Sigma^{\kappa\lambda} \Sigma^{\rho\sigma} \nabla_\mu R_{\kappa\lambda\rho\sigma}, \\
&\dot{\Sigma}^{\mu\nu} = \{\Sigma^{\mu\nu}, H\} \Rightarrow \quad D_\tau \Sigma^{\mu\nu} = \kappa \Sigma^{\kappa\lambda} \left(R_{\kappa\lambda}{}^\mu{}_\sigma \Sigma^{\nu\sigma} - R_{\kappa\lambda}{}^\nu{}_\sigma \Sigma^{\mu\sigma} \right).
\end{aligned} \tag{4.6.2}$$

Comparing again with the electro-magnetic force, the middle equation implies that in addition to the gravitational Lorentz force there is a *gravitational Stern-Gerlach force*, coupling spin to the gradient of the curvature. Therefore the coupling parameter κ has been termed the gravimagnetic ratio [81, 100]. Like in the electromagnetic

case [101] the Pauli-Lubanski and Pirani-vectors are affected by this Stern-Gerlach force:

$$D_\tau S^\mu = \frac{1}{4m\sqrt{-g}}\,\varepsilon^{\mu\nu\kappa\lambda}\Sigma_{\kappa\lambda}\Sigma^{\alpha\beta}\left(R_{\alpha\beta\nu\sigma}u^\sigma - \frac{\kappa}{2}\,\Sigma^{\rho\sigma}\nabla_\nu R_{\rho\sigma\alpha\beta}\right),$$

$$D_\tau Z^\mu = -\kappa\Sigma^{\kappa\lambda}R_{\kappa\lambda}{}^{\mu}{}_{\nu}Z^\nu + \left(\kappa + \frac{1}{2m}\right)\Sigma^{\mu\nu}\Sigma^{\kappa\lambda}R_{\kappa\lambda\nu\sigma}u^\sigma - \frac{\kappa}{4m}\,\Sigma^{\mu\nu}\Sigma^{\kappa\lambda}\Sigma^{\rho\sigma}\nabla_\nu R_{\kappa\lambda\rho\sigma}. \tag{4.6.3}$$

The second equation simplifies strongly for the special value

$$\kappa = -\frac{1}{2m}. \tag{4.6.4}$$

In that case an initial condition $Z^\mu = 0$ is conserved up to terms of cubic order in spin.

4.6.1 Extension of conservation laws to non-minimal dynamics

For the extended hamiltonian the conditions for the existence of constants of motion are modified. The total spin I defined in (4.5.2) is still conserved, but the conserved hamiltonian now is of course $H = H_0 + H_\Sigma$. Finally we prove that the constants of motion J of the form (4.5.6) are preserved under this modification of the hamiltonian. To see this, observe that

$$\{J, H_\Sigma\} = -\kappa\Sigma^{\mu\nu}\Sigma^{\rho\sigma}\left(\frac{1}{4}\,\alpha^\lambda\nabla_\lambda R_{\mu\nu\rho\sigma} + \beta_{\mu\lambda}R^\lambda{}_{\nu\rho\sigma}\right). \tag{4.6.5}$$

For the Killing-vector solutions (4.5.7) the right-hand side takes the form

$$\begin{aligned}\Sigma^{\mu\nu}\Sigma^{\rho\sigma}\left(\frac{1}{4}\,\alpha^\lambda\nabla_\lambda R_{\mu\nu\rho\sigma} + \beta_{\mu\lambda}R^\lambda{}_{\nu\rho\sigma}\right) &= \frac{1}{2}\,\Sigma^{\mu\nu}\Sigma^{\rho\sigma}\left(\nabla_\mu\nabla_\rho\nabla_\sigma + \nabla_\rho\nabla_\mu\nabla_\sigma\right)\alpha_\nu \\ &= \frac{1}{2}\,\Sigma^{\mu\nu}\Sigma^{\rho\sigma}\left(\nabla_\mu\nabla_\rho + \nabla_\rho\nabla_\mu\right)\beta_{\sigma\nu} = 0,\end{aligned} \tag{4.6.6}$$

due to the anti-symmetry of the tensor $\beta_{\sigma\nu}$.

4.7 Non-minimal hamiltonian: electric Stern-Gerlach force

In this section we further extend our formalism with the non-minimal hamiltonian generating electric Stern-Gerlach forces. The spinning particle with charge q, in the presence of external fields subject to spin-dependent forces coupling to gradients in the fields like the well-known Stern-Gerlach force [82,86,88,102] in electrodynamics. Such forces can be modeled in our approach by additional spin-dependent terms in the hamiltonian:

$$H = H_0 + H_{SG}, \qquad H_{SG} = \frac{\kappa}{4}\,R_{\mu\nu\kappa\lambda}\Sigma^{\mu\nu}\Sigma^{\kappa\lambda} + \frac{\lambda}{2}\,F_{\mu\nu}\Sigma^{\mu\nu}. \tag{4.7.1}$$

Here the electromagnetic coupling term $\frac{\lambda}{2} F_{\mu\nu}\Sigma^{\mu\nu}$ requires modification of the Poisson-Dirac brackets. Therefore

$$\{\pi_\mu, \pi_\nu\} = \frac{1}{2}\Sigma^{\kappa\lambda}R_{\kappa\lambda\mu\nu} + qF_{\mu\nu}. \tag{4.7.2}$$

The remaining brackets are same as in (4.3.6). Then using this non-minimal hamiltonian in the brackets to construct equations of motion we get

$$\pi_\mu = mg_{\mu\nu}u^\nu,$$

$$mg_{\mu\nu}D_\tau u^\nu = \frac{1}{2}\Sigma^{\kappa\lambda}R_{\kappa\lambda\mu\nu}u^\nu + qF_{\mu\nu}u^\nu - \frac{\kappa}{4}\Sigma^{\rho\sigma}\Sigma^{\kappa\lambda}\nabla_\mu R_{\rho\sigma\kappa\lambda} - \frac{\lambda}{2}\Sigma^{\kappa\lambda}\nabla_\mu F_{\kappa\lambda}, \tag{4.7.3}$$

and

$$D_\tau\Sigma^{\mu\nu} = \left(\kappa\Sigma^{\rho\sigma}R_{\rho\sigma}{}^{\mu}{}_{\lambda} + \lambda F^{\mu}_{\lambda}\right)\Sigma^{\nu\lambda} - \left(\kappa\Sigma^{\rho\sigma}R_{\rho\sigma}{}^{\nu}{}_{\lambda} + \lambda F^{\nu}_{\lambda}\right)\Sigma^{\mu\lambda}. \tag{4.7.4}$$

4.7.1 Extension of conservation laws to non-minimal dynamics

The universal constants of motion (4.5.1), (4.5.2) and (4.5.3), hold true for charged spinning particles as well. But the constants of motion depending on the symmetries of the geometry are altered because of the presence of charge. They are constructed in terms of Killing vectors and tensors. In particular constants of motion J of the form

$$J = \gamma + \alpha^\mu\pi_\mu + \frac{1}{2}\beta_{\mu\nu}\Sigma^{\mu\nu}, \tag{4.7.5}$$

exist if

$$\nabla_\mu\alpha_\nu + \nabla_\nu\alpha_\mu = 0, \quad \nabla_\lambda\beta_{\mu\nu} = R_{\mu\nu\lambda\kappa}\alpha^\kappa, \quad \partial_\mu\gamma = qF_{\mu\nu}\alpha^\nu. \tag{4.7.6}$$

Thus α^μ is a Killing vector and $\beta_{\mu\nu}$ its curl:

$$\beta_{\mu\nu} = \frac{1}{2}\left(\nabla_\mu\alpha_\nu - \nabla_\nu\alpha_\mu\right), \tag{4.7.7}$$

whilst a solution for γ can be found if the Lie-derivative of the vector potential with respect to α vanishes:

$$\alpha^\nu\partial_\nu A_\mu + \partial_\mu\alpha^\nu A_\nu = 0 \quad \Rightarrow \quad \gamma = qA_\mu\alpha^\mu. \tag{4.7.8}$$

This requirement in fact states that the electromagnetic and gravitational fields must both exhibit the same symmetries for an associated constant of motion to exist.

Remarkably, using eqs. (4.7.7, 4.7.8) and the Bianchi identities for $F_{\mu\nu}$ and $R_{\mu\nu\kappa\lambda}$ it is straightforward to generalize the theorem of ref. [47], that any constant

of motion (4.7.5) remains a constant of motion in the presence of Stern-Gerlach forces:

$$\begin{aligned}\{J, H_{SG}\} \;=\; & \kappa\, \Sigma^{\mu\nu}\Sigma^{\rho\sigma}\left(-\frac{1}{4}\,\alpha^{\lambda}\nabla_{\lambda}R_{\rho\sigma\mu\nu} + R_{\rho\sigma\mu}{}^{\lambda}\beta_{\lambda\nu}\right) \\ & +\lambda\,\Sigma^{\mu\nu}\left(-\frac{1}{2}\,\alpha^{\lambda}\nabla_{\lambda}F_{\mu\nu} + F_{\mu}{}^{\lambda}\beta_{\lambda\nu}\right) = 0.\end{aligned} \tag{4.7.9}$$

4.8 Equations of motion from energy-momentum conservation

In the previous sections the equations of motion for a relativistic spinning particle were obtained starting from a closed set of brackets (4.3.6) and the choice of a hamiltonian. The same equations can be derived by energy-momentum conservation using an appropriate energy-momentum tensor [103, 104]. This tensor then also defines the source term in the Einstein equations to compute the back reaction of the particle on the space-time geometry; indeed, the Einstein equations require the energy momentum to be divergence-free

$$G_{\mu\mu} = R_{\mu\nu} - \frac{1}{2}\,g_{\mu\nu}R = -8\pi G T_{\mu\nu} \quad \Rightarrow \quad \nabla^{\mu}G_{\mu\nu} = -8\pi\nabla^{\mu}T_{\mu\nu} = 0. \tag{4.8.1}$$

This identity is to be guaranteed by the equations of motion. For a neutral particle described by the minimal hamiltonian this follows by taking (3.4.3)

$$T_0^{\mu\nu} = m\int d\tau\, u^{\mu}u^{\nu}\,\frac{1}{\sqrt{-g}}\,\delta^4\left(x-X\right) + \frac{1}{2}\,\nabla_{\lambda}\int d\tau\left(u^{\mu}\Sigma^{\nu\lambda} + u^{\nu}\Sigma^{\mu\lambda}\right)\frac{1}{\sqrt{-g}}\,\delta^4\left(x-X\right). \tag{4.8.2}$$

The covariant divergence of $T_0^{\mu\nu}$ is

$$\begin{aligned}\nabla_{\mu}T_0^{\mu\nu} \;=\; & \int d\tau\left(m\frac{Du^{\nu}}{D\tau} - \frac{1}{2}\,\Sigma^{\kappa\lambda}R_{\kappa\lambda}{}^{\nu}{}_{\mu}u^{\mu}\right)\frac{1}{\sqrt{-g}}\,\delta^4\left(x-X\right) \\ & + \frac{1}{2}\,\nabla_{\lambda}\int d\tau\frac{D\Sigma^{\nu\lambda}}{D\tau}\,\frac{1}{\sqrt{-g}}\,\delta^4\left(x-X\right) = 0.\end{aligned} \tag{4.8.3}$$

and vanishes upon applying the equations of motion (4.3.10, 4.3.11) with $q = 0$. Similarly, for a particle subject to the gravitational Stern-Gerlach force with the hamiltonian $H_0 + H_{SG}$ the correct expressions is

$$T^{\mu\nu} = T_0^{\mu\nu} + \kappa\, T_1^{\mu\nu}, \tag{4.8.4}$$

where

$$\begin{aligned}T_1^{\mu\nu} \;=\; & \frac{1}{2}\,\nabla_{\kappa}\nabla_{\lambda}\int d\tau\left(\Sigma^{\mu\lambda}\Sigma^{\kappa\nu} + \Sigma^{\nu\lambda}\Sigma^{\kappa\mu}\right)\frac{1}{\sqrt{-g}}\,\delta^4\left(x-X\right) \\ & + \frac{1}{4}\int d\tau\,\Sigma^{\rho\sigma}\left(R_{\rho\sigma\lambda}{}^{\nu}\Sigma^{\lambda\mu} + R_{\rho\sigma\lambda}{}^{\mu}\Sigma^{\lambda\nu}\right)\frac{1}{\sqrt{-g}}\,\delta^4\left(x-X\right).\end{aligned} \tag{4.8.5}$$

Again performing standard operations from tensor calculus including Ricci- and Bianchi-identities leads to the result

$$\begin{aligned}\nabla_\mu T_1^{\mu\nu} &= \frac{1}{4}\int d\tau\, \nabla^\nu R_{\rho\sigma\kappa\lambda}\, \Sigma^{\rho\sigma}\Sigma^{\kappa\lambda}\frac{1}{\sqrt{-g}}\,\delta^4\left(x-X\right) \\ &\quad + \frac{1}{2}\,\nabla_\lambda \int d\tau\, \Sigma^{\rho\sigma}\left(R_{\rho\sigma\kappa}{}^{\lambda}\Sigma^{\kappa\nu} - R_{\rho\sigma\kappa}{}^{\nu}\Sigma^{\kappa\lambda}\right)\frac{1}{\sqrt{-g}}\,\delta^4\left(x-X\right).\end{aligned} \tag{4.8.6}$$

Combining this with the expression (4.8.3) for $\nabla_\mu T_0^{\mu\nu}$ it follows that the divergence of the full energy-momentum tensor vanishes

$$\nabla_\mu\left(T_0^{\mu\nu} + \kappa T_1^{\mu\nu}\right) = 0, \tag{4.8.7}$$

provided the non-minimal equations of motion (4.6.2) hold. Finally, one can also take into account the electro-magnetic Lorentz- and Stern-Gerlach forces by additional contributions

$$T_{\mu\nu}^{em} = F_\mu{}^\lambda F_{\nu\lambda} - \frac{1}{4}\,g_{\mu\nu}F_{\kappa\lambda}F^{\kappa\lambda} - \frac{\lambda}{2}\,g_{\mu\nu}\int d\tau F_{\kappa\lambda}\,\Sigma^{\kappa\lambda}\frac{1}{\sqrt{-g}}\,\delta^4\left(x-X\right). \tag{4.8.8}$$

Chapter 5 I apply our formalism to study the dynamics of spinning particles in Schwarzschild background, and establish a number of physical results. I obtain the simplest orbit: circular, for the particle in the equatorial plane. The method of geodesic deviation in General Relativity has been generalised to world lines of particles carrying spin. The complete first-order solution for the non-circular planar orbits is found starting from the circular orbit. The spin-influenced perturbations have double periods, and therefore the periastron and apastron behave in a complicated way (non-constant intervals) i.e., not only subject to an angular shift, but the point of closest approach shows radial variations as well. The presence of spin alters the stability conditions and therefore the location of the ISCO. For over a wide range of spin values, $-0.5M < \sigma < 0.5M$, the ISCO is quite close to the orbit of minimal orbital angular momentum and coincides only for spineless particles.

Furthermore our analysis is extended for a non-minimal Hamiltonian to include Stern- Gerlach forces both of electromagnetic and of gravitational origin and determined circular orbits in the case of Schwarzschild. As a further generalisation I investigate non-planar eccentric orbits around a massive stable black hole. I obtain analytical relations between spin precessions and precession of the orbital plane.

5

Spherically Symmetric Space-time

5.1 Schwarzschild space-time

The equations of motion (4.3.10, 4.3.11) and the hamiltonian (4.3.7), constitute a system of coupled linear differential equations for the position variables x^μ, the velocity components u^μ, and the spin tensor $\Sigma^{\mu\nu}$. Equivalently, we can rewrite these in terms of four second-order differential equations for the position and six first-order differential equations of the spin tensor. These equations are most easily solved in space-times with a maximal number of symmetries as these give rise to a maximal number of constants of motion.

The Schwarzschild metric is the unique, static and spherically symmetric vacuum solution, as stated by Birkhoff's theorem and its standard line element in Droste co-ordinates:

$$d\tau^2 = \left(1 - \frac{2M}{r}\right) dt^2 - \frac{dr^2}{1 - \frac{2M}{r}} - r^2 d\theta^2 - r^2 \sin^2\theta \, d\varphi^2. \tag{5.1.1}$$

5.1.1 Conservation laws

The space-time manifold admits four Killing vectors, for time-translations and rotations. As a result of the time-translation symmetry there is a Killing vector field corresponding to the particle energy

$$\begin{aligned} E \;&=\; -\pi_t - \frac{M}{r^2}\,\Sigma^{tr} \\ &=\; m\left(1 - \frac{2M}{r}\right) u^t - \frac{M}{r^2}\,\Sigma^{tr}. \end{aligned} \tag{5.1.2}$$

The spherical symmetry implies three Killing vector fields generating a conserved angular momentum 3-vector:

$$\begin{aligned} J_1 \;=\; &-\sin\varphi\,\pi_\theta - \operatorname{ctg}\theta\cos\varphi\,\pi_\varphi \\ &-r\sin\varphi\,\Sigma^{r\theta} - r\sin\theta\cos\theta\cos\varphi\,\Sigma^{r\varphi} + r^2\sin^2\theta\cos\varphi\,\Sigma^{\theta\varphi}, \end{aligned} \tag{5.1.3}$$

$$J_2 = \cos\varphi\,\pi_\theta - \operatorname{ctg}\theta\sin\varphi\,\pi_\varphi$$
$$+r\cos\varphi\,\Sigma^{r\theta} - r\sin\theta\cos\theta\sin\varphi\,\Sigma^{r\varphi} + r^2\sin^2\theta\sin\varphi\,\Sigma^{\theta\varphi}, \qquad (5.1.4)$$
$$J_3 = \pi_\varphi + r\sin^2\theta\,\Sigma^{r\varphi} + r^2\sin\theta\cos\theta\,\Sigma^{\theta\varphi}.$$

It is straightforward to check that these satisfy the usual algebra of time-translations and spatial rotations:

$$\{E, J_i\} = 0, \qquad \{J_i, J_j\} = \varepsilon_{ijk}J_k. \qquad (5.1.5)$$

The invariance under rotations allows us to choose the direction of total angular momentum to be the z-direction, such that

$$\mathbf{J} = (0,0,J), \qquad J = \sin^2\theta\left(mr^2u^\varphi + r\Sigma^{r\varphi} + r^2\operatorname{ctg}\theta\,\Sigma^{\theta\varphi}\right), \qquad (5.1.6)$$

and

$$\frac{1}{r}\,\pi_\theta = mru^\theta = -\Sigma^{r\theta}, \qquad \frac{1}{r\sin^2\theta}\,\pi_\varphi = mru^\varphi = -\Sigma^{r\varphi} + r\tan\theta\,\Sigma^{\theta\varphi}. \qquad (5.1.7)$$

Therefore we can express four spin-tensor components in terms of co-ordinates and velocities:

$$\Sigma^{tr} = \frac{mr}{M}\left((r-2M)\,u^t - r\varepsilon\right), \quad \Sigma^{r\varphi} = \frac{m}{r}\left(\eta - r^2u^\varphi\right). \qquad (5.1.8)$$

$$\Sigma^{r\theta} = -mru^\theta, \qquad \Sigma^{\theta\varphi} = \frac{m\eta}{r^2}\operatorname{ctg}\theta. \qquad (5.1.9)$$

where $\varepsilon = E/m$ and $\eta = J/m$ are the particle energy and total angular momentum per unit of mass. The other two spin-tensor components $\Sigma^{t\theta}$ and $\Sigma^{t\varphi}$ can be expressed in terms of the constants I and D and the orbital parameters as follows:

$$\begin{aligned} r(r-2M)\left(\Sigma^{t\theta\,2} + \sin^2\theta\,\Sigma^{t\varphi\,2}\right) = &- I - \left[\frac{m^2r^2}{M^2}\left(r-2M\right)^2\right]u^{t\,2} + \left[\frac{m^2r^5}{(r-2M)}\right]u^{\theta\,2} \\ &+ \left[\frac{m^2r^5}{(r-2M)}\sin^2\theta\right]u^{\varphi\,2} \\ &+ \frac{m^2r^3\varepsilon}{M^2}\left(2(r-2M)u^t - r\varepsilon\right) \\ &+ \frac{m^2\eta}{(r-2M)}\left(\left(r-2M\cos^2\theta\right)\eta - 2r^3\sin^2\theta\,u^\varphi\right), \end{aligned} \qquad (5.1.10)$$

by the definition of I, and

$$\left(\eta - r^2\, u^\varphi\right) \Sigma^{t\theta} + r^2 u^\theta\, \Sigma^{t\varphi} = -\frac{D}{mr} \csc^2\theta + \frac{m\eta}{M} \left((r-2M)\, u^t - r\varepsilon\right)\ \mathrm{ctg}\,\theta, \tag{5.1.11}$$

by the definition of D. It then remains to solve for the orbital motion. The relevant equations are supplied by conservation of the hamiltonian, equivalent with the constraint $u^2 = -1$:

$$\left(1 - \frac{2M}{r}\right) u^{t\,2} - \frac{u^{r\,2}}{1 - \frac{2M}{r}} - r^2 u^{\theta\,2} - r^2 \sin^2\theta\, u^{\varphi\,2} = 1; \tag{5.1.12}$$

and in addition the equations of motion.

5.1.2 Equations of motion

In the absence of spin, orbital angular momentum is conserved in a spherically symmetric background. As a result point masses move in a fixed plane. In contrast the conservation of total angular momentum, composed of orbital angular momentum and spin, implies that a variable spin is accompanied by a variable orbital angular momentum, and the generic orbit of a spinning point mass is non-planar. Planar orbits of spinning bodies are possible, but only under special conditions of spin alignment. Before we develop the specific orbits like planar, here we establish the general equations of motion.
For the radial acceleration:

$$\begin{aligned} m D_\tau u^r &= \frac{1}{2} \Sigma^{\kappa\lambda} R_{\kappa\lambda}{}^{r}{}_{\nu} u^\nu \Rightarrow \\ \dot{u}^r &= -\frac{(r-3M)}{r^2} + \frac{2(r-2M)\varepsilon}{r^2} u^t + \frac{M\eta}{r^2}\, u^\varphi \\ &\quad -\frac{(r-2M)}{r^2}\, u^{t\,2} - \frac{(r-4M)}{r(r-2M)}\, u^{r\,2} - M\cos^2\theta\, u^{\varphi\,2}. \end{aligned} \tag{5.1.13}$$

For the angular accelerations:

$$\begin{aligned} D_\tau \Sigma^{r\varphi} = 0 \text{ and } m D_\tau u^\varphi &= \frac{1}{2}\, \Sigma^{\kappa\lambda} R_{\kappa\lambda}{}^{\varphi}{}_{\nu} u^\nu \Rightarrow \\ \frac{M}{mr^3} (r-2M)\, u^t\, \Sigma^{t\varphi} &= r\dot{u}^\varphi + \frac{M\eta}{r^2(r-2M)}\, u^r - \frac{2M\eta}{r^2}\ \mathrm{ctg}\,\theta\, u^\theta \\ &\quad + \frac{(2r-5M)}{(r-2M)}\, u^r u^\varphi + 2r\ \mathrm{ctg}\,\theta\, u^\theta\, u^\varphi; \end{aligned} \tag{5.1.14}$$

and

$$D_\tau \Sigma^{r\theta} = 0 \Rightarrow$$

$$\frac{M}{mr^3}(r-2M)\,u^t\,\Sigma^{t\theta} = r\dot{u}^\theta + \frac{2M\eta}{r^2}\,\sin\theta\cos\theta\,u^\varphi + \frac{(2r-5M)}{(r-2M)}\,u^r u^\theta - r\sin\theta\,\cos\theta\,u^{\varphi\,2}; \tag{5.1.15}$$

$$mD_\tau u^\theta = \frac{1}{2}R^{\theta}{}_{\nu\kappa\lambda}\,\Sigma^{\kappa\lambda}\,u^\nu \Rightarrow$$

$$\frac{M}{mr^3}(r-2M)\,u^t\,\Sigma^{t\theta} = r\dot{u}^\theta + \frac{2M\eta}{r^2}\,\mathrm{ctg}\,\theta\,u^\varphi + \frac{(2r-5M)}{(r-2M)}\,u^r u^\theta - r\sin\theta\,\cos\theta\,u^{\varphi\,2}. \tag{5.1.16}$$

Then the time component:

$$D_\tau \Sigma^{tr} = 0 \Rightarrow$$

$$u^\theta\,\Sigma^{t\theta} + \sin^2\theta\,u^\varphi\,\Sigma^{t\varphi} = \frac{mr}{M}\dot{u}^t - \frac{2mr}{M(r-2M)}\,u^r\varepsilon + \frac{2m(r-M)}{M(r-2M)}\,u^t u^r; \tag{5.1.17}$$

$$mD_\tau u^t = \frac{1}{2}R^{t}{}_{\nu\kappa\lambda}\,\Sigma^{\kappa\lambda}\,u^\nu \Rightarrow$$

$$u^\theta\,\Sigma^{t\theta} + u^\varphi\,\Sigma^{t\varphi} = \frac{mr}{M}\dot{u}^t - \frac{2mr}{M(r-2M)}\,u^r\varepsilon + \frac{2m(r-M)}{M(r-2M)}\,u^t u^r. \tag{5.1.18}$$

And the remaining independent spin-dipole equations are:

$$D_\tau \Sigma^{t\theta} = 0 \Rightarrow$$

$$\dot{\Sigma}^{t\theta} = -\frac{(r-M)}{r(r-2M)}\Sigma^{t\theta}u^r + \frac{mr\varepsilon}{M}u^\theta + \sin\theta\,\cos\theta\,\Sigma^{t\varphi}u^\varphi - \frac{m}{M}\frac{(r-M)(r-3M)}{(r-2M)}u^t u^\theta. \tag{5.1.19}$$

and

$$D_\tau \Sigma^{t\varphi} = 0 \Rightarrow$$

$$\begin{aligned} \dot{\Sigma}^{t\varphi} \;=\; & -\frac{mM\eta}{r^2(r-2M)}u^t - \frac{(r-M)}{r(r-2M)}\Sigma^{t\varphi}u^r - \operatorname{ctg}\theta\,\Sigma^{t\varphi}u^\theta \\ & + \left(\frac{mr\varepsilon}{M} - \operatorname{ctg}\theta\,\Sigma^{t\theta}\right)u^\varphi - \frac{m}{M}\frac{(r-M)(r-3M)}{(r-2M)}u^t u^\varphi. \end{aligned} \tag{5.1.20}$$

Finally the equation for $\Sigma^{\theta\varphi}$ gives an identity.

5.2 Plane circular orbits

To find the simplest orbit: circular, we consider the motion to be in the equatorial plane. As usual, the conservation of total angular momentum and the spherical symmetry of the space-time geometry allow one to take the angular momentum $\mathbf{J}$ as the direction of the z-axis, such that

$$\mathbf{J} = (0, 0, J). \tag{5.2.1}$$

For spinless particles, for which the angular momentum is strictly orbital, this implies that the orbital motion is in a plane perpendicular to the angular momentum 3-vector; with our choice of the z-axis this is the equatorial plane $\theta = \pi/2$.

In the presence of spin the result no longer holds in general, as the precession of spin can be compensated by precession of the orbital angular momentum, resulting in a non-planar orbit [105]. However, one can ask under which conditions planar motion is still possible. As in that case the directions of orbital and spin angular momentum are separately preserved, it means that necessary conditions for motion in the equatorial plane are

$$J_1 = J_2 = 0, \qquad \pi_\theta = 0, \tag{5.2.2}$$

and therefore also

$$\Sigma^{r\theta} = \Sigma^{\theta\varphi} = 0. \tag{5.2.3}$$

Furthermore the absence of acceleration perpendicular to the equatorial plane expressed by $D_\tau \pi_\theta = 0$ implies that

$$\Sigma^{t\theta} = 0. \tag{5.2.4}$$

Thus planar motion requires alignment of the spin with the orbital angular momentum; it is straight forward to show that the reverse statement also holds [48, 64].

In terms of the four-velocity components we are now left with relevant constants of motion: eq. (5.1.8),

$$\varepsilon = \left(1 - \frac{2M}{r}\right) u^t - \frac{M}{mr^2}\,\Sigma^{tr}, \tag{5.2.5}$$

and

$$\eta = r^2 u^\varphi + \frac{r}{m}\Sigma^{r\varphi}, \tag{5.2.6}$$

in addition to the hamiltonian constraint

$$\left(1 - \frac{2M}{r}\right) u^{t\,2} = 1 + \frac{u^{r\,2}}{1 - \frac{2M}{r}} + r^2 u^{\varphi\,2}, \tag{5.2.7}$$

and eq. (5.1.10), the conservation of total spin I reduce to

$$\begin{aligned} r(r-2M)\Sigma^{t\varphi\,2} = &- I - \left[\frac{m^2 r^2}{M^2}\,(r-2M)^2\right] u^{t\,2} + \left[\frac{m^2 r^5}{(r-2M)}\right] u^{\varphi\,2} \\ &+ \frac{m^2 r^3 \varepsilon}{M^2}\left(2(r-2M)u^t - r\varepsilon\right) + \frac{m^2\eta}{(r-2M)}\left(r\eta - 2r^3\,u^\varphi\right), \end{aligned} \tag{5.2.8}$$

and as a final remark, the planar orbits satisfy

$$D = S \cdot Z = 0. \tag{5.2.9}$$

These equations show, that once the orbital velocities are known, all the non-vanishing spin components can be calculated from eqs. (5.2.5), (5.2.6) and (5.2.8).

The simplest type of planar orbit is the circular orbit $r = R =$ constant, $u^r = 0$. In this case the symmetry of the orbit implies that (u^t, u^φ) are constant in time, and that $\Sigma^{t\varphi} = 0$. This can be shown as follows. First, absence of radial acceleration $D_\tau u^r = 0$ gives, upon using the conservation laws for E and J:

$$\left(1 - \frac{2M}{R}\right)\left(2 - \frac{3M}{R}\right) u^{t\,2} - \left(1 - \frac{3M}{R}\right) R^2 u^{\varphi\,2} = 2\varepsilon\left(1 - \frac{2M}{R}\right) u^t + \frac{\eta M}{R}\,u^\varphi, \tag{5.2.10}$$

whilst the hamiltonian constraint (5.2.7) simplifies to

$$\left(1 - \frac{2M}{R}\right) u^{t\,2} = 1 + R^2 u^{\varphi\,2}. \tag{5.2.11}$$

These two equations can be solved for u^t and u^φ in terms of (R, ε, η), implying that they are constant. An immediate consequence is, that Σ^{tr}, $\Sigma^{r\varphi}$ and $\Sigma^{t\varphi}$ are constant as well, and actually $\Sigma^{t\varphi}$ vanishes. This follows directly from the absence of four-acceleration:

$$\frac{du^t}{d\tau} = \frac{M}{mR}\,u^\varphi \Sigma^{t\varphi} = 0, \qquad \frac{du^\varphi}{d\tau} = \frac{M}{mR^3}\left(1 - \frac{2M}{R}\right) u^t \Sigma^{t\varphi} = 0. \tag{5.2.12}$$

Then also the rate of change of $\Sigma^{t\varphi}$ must vanish:

$$-\frac{M}{mR}\left(1-\frac{2M}{R}\right)\frac{d\Sigma^{t\varphi}}{d\tau}$$
$$=\left(1-\frac{M}{R}\right)\left(1-\frac{3M}{R}\right)u^t u^\varphi+\frac{\eta M^2}{R^4}\,u^t-\varepsilon\left(1-\frac{2M}{R}\right)u^\varphi=0. \tag{5.2.13}$$

Now from eqs. (5.2.10) and (5.2.11) it follows that

$$2\varepsilon\left(1-\frac{2M}{R}\right)u^t=\frac{1}{m}\left(2-\frac{3M}{R}\right)+\frac{1}{m}R^2u^{\varphi\,2}-\frac{\eta M}{R}\,u^\varphi. \tag{5.2.14}$$

These equations then allow the elimination of E and u^t, with the result that

$$\frac{\eta M}{R^2}\left(\frac{2M}{R}+R^2u^{\varphi\,2}\right)=Ru^\varphi\left[\frac{M}{R}-\left(1-\frac{6M}{R}+\frac{6M^2}{R^2}\right)R^2u^{\varphi\,2}\right]. \tag{5.2.15}$$

As for the total spin, for circular orbits the expression (5.2.8) can be written as

$$I=-\frac{m^2R^4}{M^2}\left[\left(1-\frac{2M}{R}\right)u^t-\varepsilon\right]^2+\frac{m^2}{\left(1-\frac{2M}{R}\right)^2}\left[\eta-R^2u^\varphi\right]^2. \tag{5.2.16}$$

Thus for circular orbits u^φ and u^t are constants which can be expressed in terms of R and η, in turn fixing ε and I as well.

5.3 World-line deviations

In General Relativity the standard procedure for comparing geodesics is the method of geodesic deviations. It is based on a covariant definition of differences between geometric quantities associated with geodesics, like the unit tangent vectors defining the proper four-velocities of test particles. The procedure can be generalized to world-lines of particles carrying spin as follows.

Consider two solutions $(x^\mu(\tau),u^\mu(\tau),\Sigma^{\mu\nu}(\tau))$ and $(\bar{x}^\mu(\tau),\bar{u}^\mu(\tau),\bar{\Sigma}^{\mu\nu}(\tau))$ of the equations of motion (4.3.9) and (4.3.10). The direct differences between dynamical quantities on each world-line at equal proper time τ are denoted by δ:

$$\delta X(\tau)=\bar{X}(\tau)-X(\tau), \tag{5.3.1}$$

for any $X=(x^\mu,u^\mu,\Sigma^{\mu\nu})$. As the co-ordinates x^μ are space-time scalars, the velocities u^μ space-time vectors and the spin-dipoles $\Sigma^{\mu\nu}$ space-time tensors, we can define their covariant differences by parallel displacement:

$$\begin{aligned}&\Delta x^\mu(\tau)=\delta x^\mu(\tau),\quad \Delta u^\mu=\delta u^\mu(\tau)+\delta x^\lambda\Gamma_{\lambda\nu}{}^\mu u^\nu,\\ &\Delta\Sigma^{\mu\nu}=\delta\Sigma^{\mu\nu}+\delta x^\lambda\Gamma_{\lambda\kappa}{}^\mu\Sigma^{\kappa\nu}+\delta x^\lambda\Gamma_{\lambda\kappa}{}^\nu\Sigma^{\mu\kappa}.\end{aligned} \tag{5.3.2}$$

The equations of motion now imply equations for the proper-time dependence of these covariant variations; to linear order:

$$\begin{aligned}
&\Delta u^\mu = D_\tau \Delta x^\mu, \\
&D_\tau^2 \Delta x^\mu - R_{\lambda\kappa}{}^{\mu}{}_{\nu} u^\kappa u^\nu \Delta x^\lambda = \frac{1}{2m}\,\Sigma^{\rho\sigma} R_{\rho\sigma}{}^{\mu}{}_{\nu}\, D_\tau \Delta x^\nu + \frac{1}{2m}\,\Sigma^{\rho\sigma} \nabla_\lambda R_{\rho\sigma}{}^{\mu}{}_{\nu} u^\nu \Delta x^\lambda \\
&\qquad\qquad + \frac{1}{2m}\,\Delta\Sigma^{\rho\sigma} R_{\rho\sigma}{}^{\mu}{}_{\nu} u^\nu, \\
&D_\tau \Delta\Sigma^{\mu\nu} + \left(R_{\lambda\kappa\sigma}{}^{\mu}\Sigma^{\sigma\nu} - R_{\lambda\kappa\sigma}{}^{\nu}\Sigma^{\sigma\mu}\right) u^\kappa \Delta x^\lambda = 0.
\end{aligned} \tag{5.3.3}$$

The formalism, eventually with higher-order extensions [57,58,106], can be applied to a perturbative construction of world-lines starting from a known solution of the equations of motion. The circular orbits found in the previous section define such a starting point to construct eccentric planar or non-planar bound orbits in Schwarzschild background. However, computationally it is simpler to work with the non-covariant variations (5.3.1) rather than the covariant ones (5.3.2).

5.4 World-line deviations near circular motion

The procedure for computing the world-line equations up to first order in deviations in covariant form is explained in the previous section. It is convenient to rewrite these equations in non-covariant notation to get expressions for $(\delta x^\mu, \delta\Sigma^{\mu\nu})$ in a given co-ordinate system. For the co-ordinate deviations the first equation (5.3.3) becomes

$$\begin{aligned}
&\frac{d^2\delta x^\mu}{d\tau^2} + 2u^\lambda \Gamma_{\lambda\nu}{}^{\mu} \frac{d\delta x^\nu}{d\tau} + u^\kappa u^\lambda \partial_\nu \Gamma_{\kappa\lambda}{}^{\mu} \delta x^\nu \\
&\qquad = \frac{1}{2m}\left[\Sigma^{\rho\sigma} R_{\rho\sigma}{}^{\mu}{}_{\nu} \frac{d\delta x^\nu}{d\tau} + \Sigma^{\rho\sigma} \partial_\nu R_{\rho\sigma}{}^{\mu}{}_{\kappa}\, u^\kappa \delta x^\nu + \delta\Sigma^{\rho\sigma} R_{\rho\sigma}{}^{\mu}{}_{\nu} u^\nu\right],
\end{aligned} \tag{5.4.1}$$

whilst writing out the equation for the spin variation we get

$$\begin{aligned}
&\frac{d\delta\Sigma^{\mu\nu}}{d\tau} + u^\lambda \Gamma_{\lambda\kappa}{}^{\mu}\, \delta\Sigma^{\kappa\nu} + u^\lambda \Gamma_{\lambda\kappa}{}^{\nu}\, \delta\Sigma^{\mu\kappa} \\
&\qquad = \left(\Gamma_{\lambda\kappa}{}^{\mu}\Sigma^{\nu\kappa} - \Gamma_{\lambda\kappa}{}^{\nu}\Sigma^{\mu\kappa}\right) \frac{d\delta x^\lambda}{d\tau} + \left(\partial_\lambda \Gamma_{\rho\kappa}{}^{\mu}\Sigma^{\nu\kappa} - \partial_\lambda \Gamma_{\rho\kappa}{}^{\nu}\Sigma^{\mu\kappa}\right) u^\rho \delta x^\lambda.
\end{aligned} \tag{5.4.2}$$

In spite of their non-covariant appearance, these equations are completely equivalent with the covariant equations shown in the previous section.

In addition to the above deviation equations for orbits (5.4.1) and spin-dipole components (5.4.2), from the conservation laws (5.1.8) and (5.1.9) we obtain the

following variations of the spin-dipole components $\delta\Sigma^{\mu\nu}$ in terms of the orbital parameters :

$$\begin{aligned}
\delta\Sigma^{r\theta} &= -\,(mr)\;\delta u^{\theta} - \left(mu^{\theta}\right)\;\delta r;\\
\delta\Sigma^{\theta\varphi} &= -\left(\frac{m\eta}{r^3}\;\mathrm{ctg}\;\theta\right)\delta r - \left(\frac{m\eta}{r^2}\;\csc^2\;\theta\right)\;\delta\theta + \left(\frac{m}{r^2}\;\mathrm{ctg}\;\theta\right)\;\delta\eta;\\
\delta\Sigma^{tr} &= \left(\frac{mr}{M}(r-2M)\right)\delta u^{t} + \left[\frac{2m}{M}\left((r-M)u^{t} - r\varepsilon\right)\right]\delta r - \left(\frac{mr^2}{M}\right)\delta\varepsilon;\\
\delta\Sigma^{r\varphi} &= -(mr)\,\delta u^{\varphi} - \left(\frac{m}{r^2}\,(\eta + r^2u^{\varphi})\right)\delta r + \left(\frac{m}{r}\right)\;\delta\eta.
\end{aligned} \tag{5.4.3}$$

Then the variation of the pseudo-scalar spin-dipole product D in eq. (5.1.11) gives a new relation for the spin-dipole component $\delta\Sigma^{t\theta}$:

$$\begin{aligned}
\left(\eta - r^2u^{\varphi}\right)\delta\Sigma^{t\theta} = {}& \left[\frac{m\eta}{M}(r-2M)\,\mathrm{ctg}\,\theta\right]\delta u^{t} - \left(r^2\Sigma^{t\varphi}\right)\delta u^{\theta} + \left(r^2\Sigma^{t\theta}\right)\delta u^{\varphi}\\
&+ \left[2ru^{\varphi}\Sigma^{t\theta} - 2ru^{\theta}\Sigma^{t\varphi} + \frac{m\eta}{M}(u^{t}-\varepsilon)\,\mathrm{ctg}\,\theta + \frac{D}{mr^2}\csc^2\theta\right]\delta r\\
&+ \left[\left(\frac{2D}{mr}\,\mathrm{ctg}\,\theta - \frac{m\eta}{M}\left((r-2M)u^{t} - r\varepsilon\right)\right)\csc^2\theta\right]\delta\theta\\
&- \left(r^2u^{\theta}\right)\delta\Sigma^{t\varphi} - \left(\frac{1}{mr}\csc^2\theta\right)\delta D - \left(\frac{m\eta}{M}\,r\,\mathrm{ctg}\,\theta\right)\delta\varepsilon\\
&+ \left[-\Sigma^{t\theta} + \frac{m}{M}\left((r-2M)u^{t} - r\varepsilon\right)\,\mathrm{ctg}\,\theta\right]\delta\eta.
\end{aligned} \tag{5.4.4}$$

Now we develop the deviation equations (5.4.1, 5.4.2) for the most general case i.e., the non-planar motion, of a spinning particle in Schwarzschild space-time and it is given in appendix A. Then the circular orbits (found in section 5.2) can be used as a starting point for the construction of eccentric orbits, which imply all the coefficients in the deviation expressions (appendix A) for δx^{μ} and $\delta\Sigma^{\mu\nu}$ are evaluated at the circular reference orbit, with the necessary conditions:

$$\theta = \frac{\pi}{2} \quad \Rightarrow \quad u^{\theta} = 0, \quad \Sigma^{t\theta} = \Sigma^{r\theta} = \Sigma^{\theta\varphi} = 0, \tag{5.4.5}$$

and

$$r = R, \quad u^{r} = 0, \quad \Sigma^{t\varphi} = 0. \tag{5.4.6}$$

Note that the deviating orbit does not (necessarily) have the same energy and angular momentum as the circular one, so ε and η are the energy and angular

momentum for the circular orbit, and $\varepsilon+\delta\varepsilon$ and $\eta+\delta\eta$ those for the deviated orbit. Of course the variations $\delta\varepsilon$ and $\delta\eta$ are constants, which are input for calculating the new orbit.

By using the circular reference orbit conditions (5.4.5), (5.4.6) and conservation laws (5.1.8), (5.1.9) and its variations (5.4.3), and also the variation of the pseudo-scalar spin-dipole product D (5.4.4), the deviation equations simplify considerably. The orbital deviation equations are then

$$\frac{d\delta u^t}{d\tau} = -\left[\frac{2}{R(R-2M)}\left((R-M)u^t - R\varepsilon\right)\right]\delta u^r + \left[\frac{Mu^\varphi}{mR}\right]\delta\Sigma^{t\varphi}, \tag{5.4.7}$$

$$\begin{aligned}\frac{d\delta u^r}{d\tau} = &\left(\frac{2(R-2M)}{R^2}\varepsilon\right)\delta u^t - \left(2Ru^\varphi - \frac{M\eta}{R^2}\right)\delta u^\varphi \\ &-\left[-\frac{2(R-3M)}{R^3} + u^{\varphi\,2} + \frac{2(R-4M)}{R^3}\varepsilon u^t + \frac{2M\eta}{R^3}u^\varphi\right]\delta r \\ &+\left[\frac{M}{R^2}u^\varphi\right]\delta\eta + \left[\frac{2}{R^2}(R-2M)u^t\right]\delta\varepsilon,\end{aligned} \tag{5.4.8}$$

$$\begin{aligned}\frac{d\delta u^\theta}{d\tau} = &-\left[-\frac{2M\eta}{R^3}u^\varphi + \left[1+\frac{(R-2M)}{R(\eta-R^2u^\varphi)}\eta\right]u^{\varphi\,2} + \frac{\eta(R-2M)\,(1-\varepsilon u^t)}{R^3(\eta-R^2u^\varphi)}\right]\delta\theta, \\ &-\left[\frac{M(R-2M)u^t}{m^2R^5(\eta-R^2u^\varphi)}\right]\delta D.\end{aligned} \tag{5.4.9}$$

$$\frac{d\delta u^\varphi}{d\tau} = -\left[\frac{1}{R(R-2M)}\left((2R-5M)u^\varphi + \frac{M\eta}{R^2}\right)\right]\delta u^r + \left[\frac{M}{mR^4}(R-2M)u^t\right]\delta\Sigma^{t\varphi}, \tag{5.4.10}$$

Similarly the spin-dipole equations reduce to

$$\begin{aligned}\frac{d\delta\Sigma^{t\varphi}}{d\tau} = &-\left[\frac{(R-M)(R-3M)}{M(R-2M)}mu^\varphi + \frac{Mm\eta}{R^2(R-2M)}\right]\delta u^t + \left[\frac{mR}{M}u^\varphi\right]\delta\varepsilon \\ &-\left[\frac{(R-M)(R-3M)}{M(R-2M)}mu^t - \frac{Rm\varepsilon}{M}\right]\delta u^\varphi - \left[\frac{mM}{R^2(R-2M)}u^t\right]\delta\eta \\ &-\left[\frac{R^2-4MR+5M^2}{M(R-2M)^2}mu^tu^\varphi - \frac{M(3R-4M)}{R^3(R-2M)^2}\eta mu^t - \frac{\varepsilon}{M}mu^\varphi\right]\delta r\end{aligned} \tag{5.4.11}$$

$$\frac{d\delta\Sigma^{t\theta}}{d\tau} = \left[\frac{mMu^t}{(R-2M)} - \frac{m}{M}\left((R-2M)u^t - R\varepsilon\right)\right]\delta u^\theta, \tag{5.4.12}$$

The spin deviation equations in the appendix A for variations of $(\delta\Sigma^{tr}, \delta\Sigma^{r\varphi}, \delta\Sigma^{r\theta}, \delta\Sigma^{\theta\varphi})$ do not provide any new information as they become identities under the above mentioned conditions, and along with the orbital deviations equations (5.4.7), (5.4.9) and (5.4.10) for δu^t, δu^θ and δu^φ.

Further, by evaluating the variation of the pseudo-scalar spin-dipole product D from eq. (5.4.4) at the circular reference orbit, we obtain the relation for $\delta\Sigma^{t\theta}$,

$$\left(\eta - R^2u^\varphi\right)\delta\Sigma^{t\theta} = -\left[\frac{m\eta}{M}\left((R-2M)\,u^t - R\varepsilon\right)\right]\delta\theta - \left(\frac{1}{mR}\right)\delta D, \tag{5.4.13}$$

then by using (5.4.13) in the deviation equation (5.4.12) for $\delta\Sigma^{t\theta}$, and using (5.1.8) we end up with a constraint,

$$Mu^t\Sigma^{r\varphi} + (R-2M)u^\varphi\Sigma^{tr} = 0. \tag{5.4.14}$$

Eq. (5.4.14) is completely identical with eq. (5.1.20), the spin equation of motion for $\Sigma^{t\varphi}$ evaluated at the circular reference orbit, and (ε, η) are expressed equivalently in terms of the spin components $(\Sigma^{tr}, \Sigma^{r\varphi})$ by using conservation laws (5.1.8). Therefore the spin deviation equation (5.4.12) for $\delta\Sigma^{t\theta}$ does not provide any new result. Then the system (appendix A) of 10 differential equations reduce to 5 equations (5.4.7 - 5.4.11).

5.5 Motion of the particle

The solutions of the equations (5.4.7 – 5.4.11) constitute the description of the motions of a spinning particle in Schwarzschild space-time, and are obtained in two parts:

(i). As the variation equations for $(\delta t, \delta r, \delta\varphi, \delta\Sigma^{t\varphi})$ are independent of the precessional orbital motion $\theta(\tau)$, equations (5.4.7), (5.4.8), (5.4.10) and (5.4.11) form a coupled system and its solution describes the particle's motion in a non-circular planar orbit, which also includes the spin-dipole components $(\delta\Sigma^{tr}, \delta\Sigma^{r\varphi})$ computed then by using conservations laws (5.4.3).

(ii). Further, by solving the orbital deviation equation (5.4.9) for $\delta\theta$, the precessional orbital motion due to spin-orbit coupling is obtained and therefore $(\delta\Sigma^{r\theta}, \delta\Sigma^{\theta\varphi})$ and $(\delta\Sigma^{t\theta})$ by using conservation laws (5.4.3) and the variation (5.4.13) of pseudo-scalar spin-dipole product D.

5.5.1 Planar orbits: double periodic, precession of periastron

In a condensed notation the relevant linearised deviation equations for planar non-circular orbits takes the form

$$\begin{pmatrix} \frac{d^2}{d\tau^2} & 0 & \alpha\frac{d}{d\tau} & \beta \\ 0 & \frac{d^2}{d\tau^2} & \gamma\frac{d}{d\tau} & \zeta \\ \kappa\frac{d}{d\tau} & \lambda\frac{d}{d\tau} & \frac{d^2}{d\tau^2}+\mu & 0 \\ \nu\frac{d}{d\tau} & \sigma\frac{d}{d\tau} & \chi & \frac{d}{d\tau} \end{pmatrix} \begin{pmatrix} \delta t \\ \delta\varphi \\ \delta r \\ \delta\Sigma^{t\varphi} \end{pmatrix} = \begin{pmatrix} 0 \\ 0 \\ a\delta\eta + b\delta\varepsilon \\ c\delta\eta + d\delta\varepsilon \end{pmatrix} \tag{5.5.1}$$

where the coefficients are defined on the circular reference orbit and are given by

$$\begin{aligned} a &= \frac{Mu^\varphi}{R^2}, & b &= \frac{2(R-2M)}{R^2}\,u^t, \\ c &= -\frac{Mmu^t}{R^2(R-2M)}, & d &= \frac{Rm}{M}\,u^\varphi, \end{aligned} \tag{5.5.2}$$

and furthermore

$$\begin{aligned} \alpha &= \frac{2}{R(R-2M)}\left[(R-M)u^t - R\varepsilon\right], & \beta &= -\frac{Mu^\varphi}{mR}, \\ \gamma &= \frac{1}{R(R-2M)}\left[(2R-5M)u^\varphi + \frac{M\eta}{R^2}\right], & \zeta &= -\frac{M(R-2M)}{mR^4}\,u^t, \\ \kappa &= -\frac{2(R-2M)}{R^2}\,\varepsilon, & \lambda &= 2Ru^\varphi - \frac{M\eta}{R^2}, \end{aligned} \tag{5.5.3}$$

and

$$\begin{aligned} \mu &= -\frac{2(R-3M)}{R^3} + u^{\varphi\,2} + \frac{2M\eta}{R^3}\,u^\varphi + \frac{2(R-4M)}{R^3}\varepsilon u^t, \\ \nu &= \frac{(R-M)(R-3M)}{M(R-2M)}\,mu^\varphi + \frac{Mm\eta}{R^2(R-2M)}, \\ \sigma &= \frac{(R-M)(R-3M)}{M(R-2M)}\,mu^t - \frac{Rm\varepsilon}{M}, \\ \chi &= \frac{R^2-4MR+5M^2}{M(R-2M)^2}\,mu^tu^\varphi - \frac{M(3R-4M)}{R^3(R-2M)^2}\,\eta mu^t - \frac{\varepsilon}{M}\,mu^\varphi. \end{aligned} \tag{5.5.4}$$

The general solution of the inhomogenous linear equations (5.5.1) can be decomposed in a specific solution plus a solution of the homogeneous equation; but it is easy to find a special specific solution: a constant shift δr such that the new circular orbit has the same energy $\varepsilon' = \varepsilon + \delta\varepsilon$ and total angular momentum $\eta' = \eta + \delta\eta$ as the non-circular planar orbit we wish to construct. Hence by taking this special circular orbit as the reference orbit we fix $\delta\varepsilon = \delta\eta = 0$, and we only have to solve the homogeneous equation (5.5.1).

Now the characteristic equation for the periodic eigenfunctions of the operator (5.5.1) reads

$$\omega^3 \left(\omega^4 - A\omega^2 + B\right) = 0, \tag{5.5.5}$$

where

$$\begin{aligned} A &= \mu - \alpha\kappa - \beta\nu - \gamma\lambda - \zeta\sigma, \\ B &= \beta\left(\kappa\chi - \mu\nu + \gamma(\lambda\nu - \kappa\sigma)\right) + \zeta\left(\lambda\chi - \mu\sigma - \alpha(\lambda\nu - \kappa\sigma)\right). \end{aligned} \tag{5.5.6}$$

Therefore there are three 0-modes, and two pairs of non-trivial periodic solutions with angular frequencies

$$\omega_\pm^2 = \frac{1}{2}\left(A \pm \sqrt{A^2 - 4B}\right). \tag{5.5.7}$$

These periodic solutions can be brought to the simple form

$$\begin{aligned} \delta t &= n_+^t \sin\omega_+(\tau - \tau_+) + n_-^t \sin\omega_-(\tau - \tau_-), \\ \delta\varphi &= n_+^\varphi \sin\omega_+(\tau - \tau_+) + n_-^\varphi \sin\omega_-(\tau - \tau_-), \\ \delta r &= n_+^r \cos\omega_+(\tau - \tau_+) + n_-^r \cos\omega_-(\tau - \tau_-), \\ \delta\Sigma^{t\varphi} &= n_+^\sigma \sin\omega_+(\tau - \tau_+) + n_-^\sigma \sin\omega_-(\tau - \tau_-), \end{aligned} \tag{5.5.8}$$

where $\tau_\pm$ are constants of integration determining the relative phases of the oscillations, and up to some common normalization constants $C_\pm$ the amplitudes are

$$\begin{aligned} n_\pm^t &= C_\pm\left[\lambda\left(\beta\gamma - \alpha\zeta\right) + \beta\left(\omega_\pm^2 - \mu\right)\right], \\ n_\pm^\varphi &= C_\pm\left[-\kappa\left(\beta\gamma - \alpha\zeta\right) + \zeta\left(\omega_\pm^2 - \mu\right)\right], \\ n_\pm^r &= C_\pm\,\omega_\pm\left(\beta\kappa + \zeta\lambda\right), \\ n_\pm^\sigma &= C_\pm\,\omega_\pm^2\left(\omega_\pm^2 - \mu + \alpha\kappa + \gamma\lambda\right). \end{aligned} \tag{5.5.9}$$

The null solutions of eq. (5.5.5) suggest that in addition to the periodic solutions (5.5.8) there might also be secular solutions for the orbital degrees of freedom.

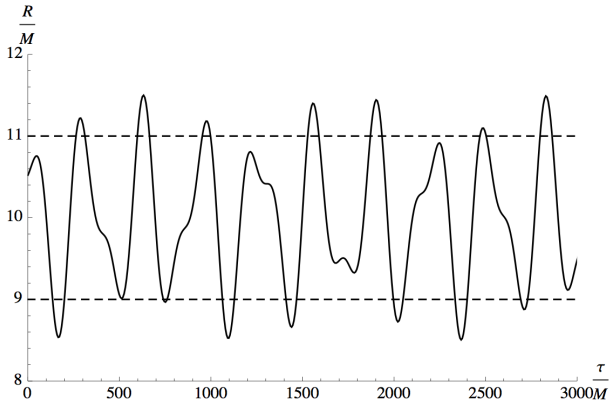

Figure 5.1. Radial deviation from circular orbit with $R = 10M$ and $\ell = 4M$ as a function of proper time in Schwarzschild space-time for deviation parameters as in eq. (5.5.11).

However, as we have chosen the energy and total angular momentum of the orbit to be the same as that of the circular reference orbit no such freedom is left in this case. Therefore the complete first-order solution for the non-circular planar orbits is

$$\begin{aligned} t(\tau) &= u^t\tau + n^t_+ \sin\omega_+(\tau-\tau_+) + n^t_- \sin\omega_-(\tau-\tau_-),\\ \varphi(\tau) &= u^\varphi\tau + n^\varphi_+ \sin\omega_+(\tau-\tau_+) + n^\varphi_- \sin\omega_-(\tau-\tau_-),\\ r(\tau) &= R + n^r_+ \cos\omega_+(\tau-\tau_+) + n^r_- \cos\omega_-(\tau-\tau_-),\\ \Sigma^{t\varphi}(\tau) &= n^\sigma_+ \sin\omega_+(\tau-\tau_+) + n^\sigma_- \sin\omega_-(\tau-\tau_-). \end{aligned} \tag{5.5.10}$$

The perturbations, in particular those in the radial direction, have double periods. Hence the periastron and apastron will behave in a complicated way, as the body reaches different minimal or maximal radial distances at non-constant intervals. However, in the limit $B \ll A^2$ the dominant frequency will be $\omega_+ \simeq \sqrt{A}$, and the variations in the periastron and apastron will be relatively slow. An example for the case of Schwarzschild geometry is given in Fig. 5.1, where we have plotted the radial variation as a function of proper time for a circular reference orbit $R = 10M$ with orbital angular momentum $\ell = 4M$ and for deviation parameters

$$n^r_+ = 0.1R, \quad n^r_- = 0.05R, \quad \tau_+ - \tau_- = 100M. \tag{5.5.11}$$

As we have obtained the non-circular orbits (5.5.8) under the conditions that the specific energy and total angular momentum are the same as those of the circular reference orbits, the conservation laws (5.1.8) for the spin-dipole components link

the variations $\delta\Sigma^{\mu\nu}$ of these quantities to those of the orbital parameters (5.1.9),

$$\begin{aligned}\frac{R}{m}\,\delta\Sigma^{r\varphi} &= -R^2\delta u^{\varphi} - \left(\eta + R^2 u^{\varphi}\right)\frac{\delta r}{R},\\ \frac{M}{mR^2}\,\delta\Sigma^{tr} &= \left(1-\frac{2M}{R}\right)\delta u^t + 2\left[\left(1-\frac{M}{R}\right)u^t - \varepsilon\right]\frac{\delta r}{R}.\end{aligned} \tag{5.5.12}$$

As a result

$$\begin{aligned}\delta\Sigma^{r\varphi} &= N_+^{r\varphi}\cos\omega_+(\tau-\tau_+) + N_-^{r\varphi}\cos\omega_-(\tau-\tau_-),\\ \delta\Sigma^{tr} &= N_+^{tr}\cos\omega_+(\tau-\tau_+) + N_-^{tr}\cos\omega_-(\tau-\tau_-),\end{aligned} \tag{5.5.13}$$

where

$$\begin{aligned}N_\pm^{r\varphi} &= -\frac{m}{R}\left[R^2\omega_\pm n_\pm^{\varphi} + \left(\eta + R^2 u^{\varphi}\right)\frac{n_\pm^r}{R}\right],\\ N_\pm^{tr} &= \frac{mR^2}{M}\left[\left(1-\frac{2M}{R}\right)\omega_\pm n_\pm^t + 2\left(\left(1-\frac{M}{R}\right)u^t - \varepsilon\right)\frac{n_\pm^r}{R}\right].\end{aligned} \tag{5.5.14}$$

Thus we obtain a large class of non-circular planar orbits (to first order in the deviations), parametrised by the constants $C_\pm$ and the radial co-ordinate R of the circular orbit with the same specific energy and total angular momentum.

5.5.2 Planar orbits: stability of circular orbits and the ISCO

In black-hole space-times there is an innermost stable circular orbit (ISCO) at a specific distance from the horizon. For simple point masses in Schwarzschild space-time this orbit is located at $R = 6M$. Here the effective potential has a flex point where the orbital angular momentum reaches a minimum of $\ell^2 = 12M^2$. Circular orbits at values $R < 6M$ are possible in principle but not in practice, as they correspond to maxima of the effective potential rather than minima; thus they are unstable under small perturbations.

The presence of spin alters the stability conditions and therefore the location of the ISCO. The stability conditions for circular orbits can be derived directly from the analysis in the previous section. Indeed, circular orbits are stable as long as the planar deviations display oscillatory behaviour. In contrast, whenever the frequency ω of these deviations develops an imaginary part the radial motion displays exponential behaviour and the orbit becomes unstable [107]. Now the frequencies of the deviations are solutions of the eigenvalue equation (5.5.7). Thus we must ask what is the parameter domain in which the eigenvalues are real, and especially where the boundary between stability and instability is located. The first condition is obviously for $\omega_\pm^2$ to be real; this requires

$$A^2 - 4B \geq 0. \tag{5.5.15}$$

In addition, for the frequencies $\omega_\pm$ themselves to be real as well we must demand that $\omega_\pm^2 \geq 0$, which happens if

$$A \geq 0, \qquad B \geq 0. \tag{5.5.16}$$

Fig. 5.2 shows the solutions of these inequalities for the case of Schwarzschild space-time in terms of the allowed values of the dimensionless radial co-ordinate R/M and of the orbital angular momentum per unit of mass

$$\ell = R^2 u^\varphi. \tag{5.5.17}$$

The shaded area corresponds to stable circular orbits. As we have established in sect. 5.2 that any circular orbit is determined for a given background geometry by the parameters R and J —which fix u^φ, u^t and E— the allowed orbits for fixed R/M and various ℓ/M in Fig. 5.2 differ in the values of $\eta = J/m$. Equivalently they differ in the value of the spin per unit of mass parametrized by the dimensionless variable

$$\frac{\sigma}{M} = \frac{R\Sigma^{r\varphi}}{mM}. \tag{5.5.18}$$

We have also indicated in Fig. 5.2 several curves of constant spin. The curves *g, f, h* represent iso-spin lines for spin $\sigma = 0$, for retrograde spin $\sigma = -0.5M$ and for prograde spin $\sigma = 0.5M$, respectively. In each case the ISCO is defined by the value of R/M where the curve crosses the line $B = 0$. For vanishing spin this is at the well-known value $R = 6M$, for prograde spin it is at a lower value of R and for retrograde spin at a higher value of R. There actually is a smallest ISCO $R \simeq 4.3M$ for $\sigma \simeq 0.55M$, where the curve $B = 0$ reaches a minimum value of orbital angular momentum.

For higher spin values the ISCO is reached at the point where the iso-spin curves cross the line $A^2 - 4B = 0$; an example is the curve labeled p corresponding to $\sigma = 0.7M$. In general such high values of σ/M are possible only if the masses m and M of the test particle and the black hole creating the background become comparable. Of course the back reaction of the test mass can then no longer be ignored and our estimates of the ISCO become unreliable.

By calculating the values of the spin parameter σ/M on the lines separating regions of stable and unstable orbits we have extracted the values of R for the ISCO as a function of σ/M in Schwarzschild space-time. The result is represented by the continuous curve labeled R_{isco} in Fig. 5.3. The two branches correspond to lower-spin ISCOs on the curve $B = 0$ and higher-spin ISCOs on the curve $A^2 - 4B = 0$, respectively. These results agree qualitatively with other studies in the literature based on the conventional Mathisson-Papapetrou-Dixon approach [107, 108].

The iso-spin curves in Fig. 5.2 for lower-spin values, corresponding to the left-hand branch in Fig. 5.3, also suggest that the circular orbits become unstable when

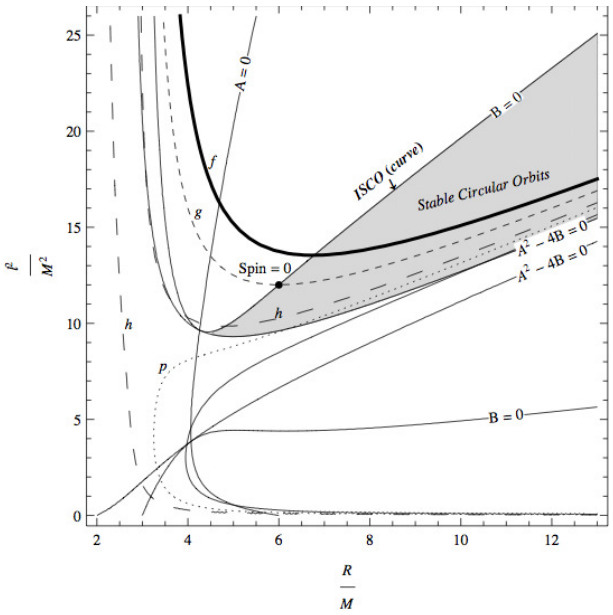

Figure 5.2. Allowed domains of radius R/M and orbital angular momentum ℓ/M for plane circular orbits in Schwarzschild space-time. Included are four curves labeled *f, g, h, p* defining orbits of fixed spin per unit of mass σ for retrograde, vanishing and prograde spin $\sigma/M = (-0.5, 0, 0.5, 0.7)$.

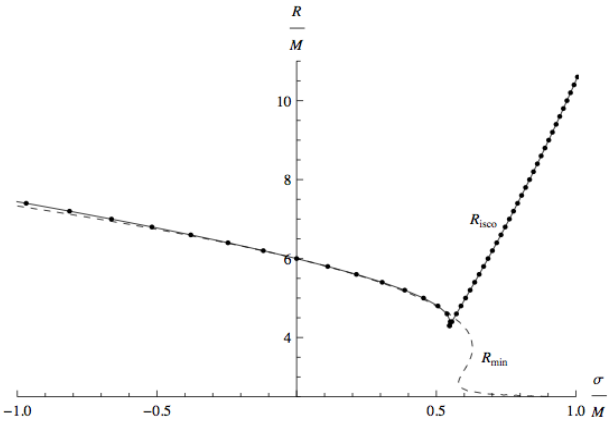

Figure 5.3. Radius of the ISCO: R_{isco}/M, as a function of spin σ/M for Schwarzschild space-time (continuous curve) compared with the radius of minimal orbital angular momentum $R_{\rm min}/M$ at fixed spin (dashed curve).

the orbital angular momentum reaches its minimum as a function of radial distance for contant σ. This issue can be analysed more precisely by returning to eq. (5.2.15)

and rewriting it in the form

$$\frac{\sigma R}{M^2}\left(\frac{2R}{M}+\frac{\ell^2}{M^2}\right)=\frac{\ell}{M}\left(\frac{R}{M}-2\right)\left[\frac{R^2}{M^2}-\frac{\ell^2}{M^2}\left(\frac{R}{M}-3\right)\right]. \tag{5.5.19}$$

From this equation one can derive the minimum of ℓ/M as a function of R/M for fixed spin σ. The result is plotted as the dashed curve labeled R_{min} in Fig. 5.3. Over the range of predominant physical interest $-0.5<\sigma/M<0.5$ the curve nearly coincides with that for R_{isco}. However there are small differences for larger absolute spin values, reminiscent of those found in higher-order Post-newtonian corrections for compact binaries [107]. Note that the parts of the dashed curve for large retrograde spin actually enter the region of instability, hence do not correspond to stable circular orbits.

5.5.3 Non-planar orbits: Geodetic precession

A spinning particle orbiting around a massive Schwarzschild black hole will follow a precessional orbital motion $\theta(\tau)$, due to spin-orbit coupling and it is obtained by solving the simple harmonic oscillator equation (5.4.9) for $\delta\theta$, with the shift proportional to δD

$$\begin{aligned}\theta(\tau) &= \frac{\pi}{2}+\delta\theta(\tau),\\ &= \frac{\pi}{2}+\frac{1}{\Omega_p^2}\left[x_0\cos\Omega_p\tau+\frac{v_0}{\Omega_p}\sin\Omega_p\tau\right]-\left(\frac{M}{m^2R^5\,\Omega_p^2}\frac{(R-2M)u^t}{(\eta-R^2u^\varphi)}\right)\delta D.\end{aligned} \tag{5.5.20}$$

where, x_0 and v_0 are the initial position and velocity of the particle, and Ω_p is the frequency of the precessing orbital plane and it is extracted straight forwardly from eq. (5.4.9),

$$\Omega_p=\sqrt{-\frac{2M\eta}{R^3}u^\varphi+\left[1+\frac{(R-2M)}{R(\eta-R^2u^\varphi)}\eta\right]u^{\varphi\,2}+\frac{\eta(R-2M)\,(1-\varepsilon u^t)}{R^3(\eta-R^2u^\varphi)}}. \tag{5.5.21}$$

Here Ω_p is expressed in terms of constants (M,R). Then the relations between the precession of the orbital plane and the components of spin precessions are obtained as follows: the conservation laws (5.1.8) for the spin-dipole components $(\Sigma^{r\theta},\Sigma^{\theta\varphi})$ link the variations of these quantities to Ω_p (5.4.3):

$$\begin{aligned}\Sigma^{r\theta}(\tau)=\delta\Sigma^{r\theta}(\tau) &= -mR\,\delta u^\theta,\\ &= \frac{mR}{\Omega_p}\left[x_0\sin\Omega_p\tau-\frac{v_0}{\Omega_p}\cos\Omega_p\tau\right].\end{aligned} \tag{5.5.22}$$

$$\begin{aligned}\Sigma^{\theta\varphi}(\tau) = \delta\Sigma^{\theta\varphi}(\tau) \;&=\; -\frac{m\eta}{r^2}\,\delta\theta,\\ &= -\frac{m\eta}{R^2\,\Omega_p^2}\left[x_0\cos\Omega_p\tau + \frac{v_0}{\Omega_p}\sin\Omega_p\tau\right]\\ &\quad +\left(\frac{M\eta}{mR^7\,\Omega_p^2}\frac{(R-2M)u^t}{(\eta - R^2u^\varphi)}\right)\delta D.\end{aligned} \tag{5.5.23}$$

Finally, the variation of the pseudo-scalar spin-dipole product D, links the spin variation $\delta\Sigma^{t\theta}$ to Ω_p (5.4.13):

$$\begin{aligned}\Sigma^{t\theta}(\tau) \;&=\; \delta\Sigma^{t\theta}(\tau)\\ &= -\left(\frac{m\eta}{M\,(\eta - R^2u^\varphi)}\left((R-2M)\,u^t - R\varepsilon\right)\right)\delta\theta\\ &\quad -\left(\frac{1}{mR\,(\eta - R^2u^\varphi)}\right)\delta D,\\ &= -\frac{m\eta}{M\Omega_p^2}\frac{((R-2M)u^t - R\varepsilon)}{(\eta - R^2u^\varphi)}\left[x_0\cos\Omega_p\tau + \frac{v_0}{\Omega_p}\sin\Omega_p\tau\right]\\ &\quad -\frac{1}{mR\,(\eta - R^2u^\varphi)}\left(1 - \frac{\eta}{mR^4\,\Omega_p^2}\frac{(R-2M)\left(1 - \varepsilon u^t + R^2u^{\varphi\,2}\right)}{(\eta - R^2u^\varphi)}\right)\delta D.\end{aligned}$$

Thus eq. (5.5.22), (5.5.23), and (5.5.24) links the precession of the spin and precession of the orbital plane. Therefore for the given radius we can calculate the spin precessions from these relations.

5.6 Circular motion: non-minimal gravitational Stern-Gerlach force

So far we have established the orbital dynamics of spinning particles generated by the minimal hamiltonian H_0. Here we extend our analysis for the particles subject to gravitational Stern-Gerlach force. Such forces can be modelled in our approach by additional spin-dependent terms in the hamiltonian:

$$H = H_0 + H_\Sigma, \qquad H_\Sigma = \frac{\kappa}{4}\,R_{\mu\nu\kappa\lambda}\Sigma^{\mu\nu}\Sigma^{\kappa\lambda}. \tag{5.6.1}$$

The existence of the constants of motion enable us to perform a similar analysis of orbits as in the case of the minimal hamiltonian. As an example we solve for plane circular orbits in a Schwarzschild background similar to those discussed in section 5.2 for the minimal case. Again we take the plane of the orbit to be the

equatorial plane $\theta = \pi/2$ with $u^\theta = u^r = 0$ and $\Sigma^{\theta\nu} = 0$ for all values of ν. Then the conservation laws reduce to the same form as in eqs. (5.1.8):

$$E = m\left(1 - \frac{2M}{R}\right)u^t - \frac{M}{R^2}\,\Sigma^{tr}, \quad J = mR^2u^\varphi + R\Sigma^{r\varphi}.$$

The hamiltonian constraint now reads

$$H = H_0 + H_\Sigma = -\frac{m}{2}, \tag{5.6.2}$$

which becomes

$$-\left(1 - \frac{2M}{R}\right)u^{t\,2} + R^2u^{\varphi\,2} + 1 = -\frac{2\kappa M}{m}\left[\frac{2}{R^3}\,\Sigma^{tr\,2} + \frac{\Sigma^{r\varphi\,2}}{R - 2M} - \frac{1}{R}\left(1 - \frac{2M}{R}\right)\Sigma^{t\varphi\,2}\right]. \tag{5.6.3}$$

Next the total spin is

$$I = -\Sigma^{tr\,2} - R^2\left(1 - \frac{2M}{R}\right)\Sigma^{t\varphi\,2} + \frac{R^2\Sigma^{r\varphi\,2}}{1 - \frac{2M}{R}}, \tag{5.6.4}$$

a constant. These constraints plus the vanishing of the radial acceleration: $\dot{u}^r = 0$ imply that the angular velocity and the time-dilation factor are constant, causing in fact $\Sigma^{t\varphi}$ to vanish:

$$\dot{u}^t = \dot{u}^\varphi = \Sigma^{t\varphi} = 0. \tag{5.6.5}$$

Then one finds a quartic equation for the angular velocity in terms of the radius R and the angular momentum $J = m\eta$, which generalizes eq. (5.2.15):

$$\left(1 - \frac{2M}{R}\right)^2 Ru^\varphi\left[\frac{2M^2\eta}{R^3} - Mu^\varphi + M\eta u^{\varphi\,2} + \left(R^2 - 6MR + 6M^2\right)Ru^{\varphi\,3}\right]$$

$$= \kappa mA + \kappa^2m^2B + \kappa^3m^3C, \tag{5.6.6}$$

The explicit expressions for the quantities A, B and C, which are quartic polynomials in the angular velocity u^φ for given values of radius R and angular momentum per unit of mass η, are:

$$\begin{aligned}
A = \frac{M(\eta - R^2u^\varphi)}{R^2}\Bigg\{&\frac{6M^2\eta}{R^3}\left(1 - \frac{2M}{R}\right)\left(2 - \frac{m}{M}\right)\\
&- 4Mu^\varphi\left[3\left(1 - \frac{2M}{R}\right)\left(1 - \frac{M}{R} - \frac{m}{2R}\right) + \frac{M\eta^2}{R^3}\left(1 - \frac{3M}{R}\right)\right]\\
&+ \eta Ru^{\varphi\,2}\left[\frac{2M}{R}\left(7 - \frac{16M}{R}\right) - \frac{3m}{M}\left(1 - \frac{2M}{R}\right)\left(1 - \frac{4M}{R} + \frac{6M^2}{R^2}\right)\right]\\
&+ 12R^3u^{\varphi\,3}\left[1 - \frac{49M}{6R} + \frac{19M^2}{R^2} - \frac{13M^3}{R^3} + \frac{m}{4M}\left(1 - \frac{6M}{R} + \frac{14M^2}{R^2} - \frac{12M^3}{R^3}\right)\right]\Bigg\},
\end{aligned}$$

$$
\begin{aligned}
B = \frac{12M(\eta - R^2 u^\varphi)^2}{R^3} \Bigg\{ & \frac{3M^2}{R^2}\left(1 - \frac{2M}{R}\right) + \frac{2M^3\eta^2}{R^5} \\
& - \frac{M\eta}{R}\, u^\varphi \left[\frac{M}{R}\left(5 - \frac{6M}{R}\right) - \frac{3m}{M}\left(1 - \frac{2M}{R}\right)^2 \right] \\
& - MR u^{\varphi\,2} \left[3 - \frac{20M}{R} + \frac{26M^2}{R^2} + \frac{3m}{M}\left(1 - \frac{2M}{R}\right)^2 \right] \Bigg\}, \\
C = \frac{72M^3(\eta - R^2 u^\varphi)^4}{R^7} & \left[\frac{M}{R} - \frac{3m}{2M}\left(1 - \frac{2M}{R}\right) \right].
\end{aligned}
\tag{5.6.7}
$$

After solving this equation for u^φ also the energy $E = m\varepsilon$ and the values of u^t, Σ^{tr} and $\Sigma^{r\varphi}$ can be determined.

Thus we have obtained the equation for circular orbits for spinning test particles in the presence of gravitational Stern-Gerlach interactions.

Chapter 6 concludes my theoretical research in connection with the possible experiments. It provides the list of possible problems and directions, as an extension for the future exploration.

6

Conclusion

With our new formalism much physics remains to be explored. The following applications and generalizations are to be made:

- First of all it would be interesting to consider the effect of spin on the emission of gravitational waves from the above established orbits like circular and bound planar-orbits. We have also found these orbits in the Reissner-Nordstrom geometery [48]. Computing gravitational waves for particle in these orbits should be straightforward.

- There exist other types of orbits in spherically symmetric backgrounds. When the spinning particle comes from infinity - orbits the centre and moves to infinity it performs *scattering orbits*. When it comes from infinity and plunges directly into the centre this is known as *plunging orbits*. These orbits and the gravitational waves from the particle obeying these orbits are yet to be computed.

- As we have established the circular orbits for a non-minimal hamiltonian including gravitational Stern-Gerlach force, one can obtain the ISCO for a specific gravimagnetic ratio κ (depends on the object) and other possible orbits like bound non-circular, scattering and plunging orbits and their gravitational waves.

- The supermassive black holes in the galactic centres are of Kerr nature and there are many stars/compact objects orbiting them. Therefore extending our formalism to the Kerr metric is very essential (though it is very difficult analytically) to understand the practical dynamics of such systems. The first step would be calculating the circular orbits in the equatorial plane.

- The gravitational self-force can be incorporated within our formalism. The approach goes beyond the test particle approximation by including the self-field effects which modify the leading-order geodetic motion of a small mass moving in the vicinity of the background geometry [109].

- Finally our approach is based on the point particle approximation. Refining our methods to finite size bodies by including higher order mass multipoles would be helpful in understanding the comparable mass systems studied with ground based detectors.

All the above items are important and left for future investigation. It is desirable to develop a complete theoretical framework along these lines for Extreme Mass Ratio Binaries to be compared with the observations, such as those planned by the eLISA mission scheduled for 2034. Its advantage is that in contrast to the PN methods our scheme is fully relativistic; in fact it can work even in the plunge regime beyond the ISCO, as shown for example by the work in ref. [110].

A

Deviation Equations in Schwarzschild space-time

The deviation equations for the most general case i.e., the non-planar motion, of spinning particles in Schwarzschild space-time is given here.

A.1 The Orbital deviations:

$$
\begin{aligned}
\frac{d\delta u^t}{d\tau} = &- \frac{2M}{r(r-2M)}\,\delta\left(u^t u^r\right) - \frac{2M}{mr^2(r-2M)}\,\delta\left(u^r \Sigma^{tr}\right) \\
&+ \frac{M}{mr}\,\delta\left(u^\theta \Sigma^{t\theta} + u^\varphi \Sigma^{t\varphi}\right) \\
&+ \left[\frac{4M(r-M)}{r^2(r-2M)^2}\,u^t u^r + \frac{2M(3r-4M)}{mr^3(r-2M)^2}\,u^r \Sigma^{tr}\right. \\
&\quad \left. - \frac{M}{mr^2}\left(u^\theta \Sigma^{t\theta} + u^\varphi \Sigma^{t\varphi}\right)\right]\delta r, \\
\frac{d\delta u^r}{d\tau} = &- \frac{M(r-2M)}{r^3}\,\delta\left(u^{t\,2}\right) - \frac{2M(r-2M)}{mr^4}\,\delta\left(u^t \Sigma^{tr}\right) + \frac{2Mu^r}{r(r-2M)}\,\delta u^r \\
&+ (r-2M)\,\delta(u^{\theta\,2}) + \frac{M}{mr}\left[\delta\left(u^\theta \Sigma^{r\theta}\right) + \delta\left(u^\varphi \Sigma^{r\varphi}\right)\right] \\
&+ (r-2M)\,\sin^2\theta\,\delta(u^{\varphi\,2}) + \left((r-2M)u^{\varphi\,2}\,\sin 2\theta\right)\,\delta\theta \\
&+ \left[\frac{2M}{r^4}(r-3M)\,u^{t\,2} - \frac{2M(r-M)u^{r\,2}}{r^2(r-2M)^2} + u^{\theta\,2} + \sin^2\theta\,u^{\varphi\,2}\right. \\
&\quad \left. + \frac{2M}{mr^5}(3r-8M)u^t \Sigma^{tr} - \frac{M}{mr^2}\left(u^\theta \Sigma^{r\theta} + u^\varphi \Sigma^{r\varphi}\right)\right]\delta r,
\end{aligned}
$$

$$\begin{aligned}\frac{d\delta u^\theta}{d\tau} = & \frac{M(r-2M)}{mr^4}\,\delta(u^t\Sigma^{t\theta}) + \frac{M}{mr^2(r-2M)}\delta(u^r\Sigma^{r\theta}) - \frac{2M}{mr}\,\delta(u^\varphi\Sigma^{\theta\varphi}) \\ & - \frac{2}{r}\,\delta(u^r u^\theta) + \sin\theta\,\cos\theta\,\delta(u^{\varphi\,2}) + \left(\cos 2\theta\, u^{\varphi\,2}\right)\,\delta\theta \\ & + \left[\frac{2}{r^2}u^r u^\theta - \frac{M}{mr^5}(3r-8M)u^t\Sigma^{t\theta} + \frac{M(3r-4M)}{mr^3(r-2M)^2}u^r\Sigma^{r\theta}\right. \\ & \left. + \frac{2M}{mr^2}u^\varphi\Sigma^{\theta\varphi}\right]\delta r.\end{aligned}$$

$$\begin{aligned}\frac{d\delta u^\varphi}{d\tau} = & \frac{M(r-2M)}{mr^4}\,\delta(u^t\Sigma^{t\varphi}) - \frac{M}{mr^2(r-2M)}\,\delta(u^r\Sigma^{r\varphi}) + \frac{2M}{mr}\,\delta(u^\theta\Sigma^{\theta\varphi}) \\ & - \frac{2}{r}\,\delta(u^r u^\varphi) - (2\cot\theta\, u^\varphi)\,\delta u^\theta - \left(2\cot\theta\, u^\theta\right)\delta u^\varphi + \left(2\csc^2\theta\, u^\theta u^\varphi\right)\,\delta\theta \\ & + \left[\frac{2}{r^2}u^r u^\varphi - \frac{M}{mr^5}(3r-8M)u^t\Sigma^{t\varphi} + \frac{M(3r-4M)}{mr^3(r-2M)^2}u^r\Sigma^{r\varphi}\right. \\ & \left. - \frac{2M}{mr^2}u^\theta\Sigma^{\theta\varphi}\right]\delta r,\end{aligned}$$

A.2 The spin-dipole deviations:

$$\begin{aligned}\frac{d\delta\Sigma^{t\varphi}}{d\tau} = & -\frac{M}{r(r-2M)}\delta(u^t\Sigma^{r\varphi}) - \frac{(r-M)}{r(r-2M)}\delta(u^r\Sigma^{t\varphi}) \\ & - \operatorname{ctg}\varphi\,\delta(u^\theta\Sigma^{t\varphi}) - \frac{1}{r}\delta(u^\varphi\Sigma^{tr}) + \operatorname{ctg}\theta\,\delta(u^\varphi\Sigma^{t\theta}) \\ & - \left[\frac{1}{r^2}u^\varphi\,\Sigma^{tr} + \frac{2M(r-M)}{r^2(r-2M)^2}u^t\Sigma^{r\varphi} + \frac{1}{r^2}\left(1+\frac{2M(r-M)}{(r-2M)^2}\right)u^r\Sigma^{t\varphi}\right]\delta r,\end{aligned}$$

$$\begin{aligned}\frac{d\delta\Sigma^{tr}}{d\tau} = & (r-2M)\,\delta(u^\theta\Sigma^{t\theta}) + (r-2M)\,\sin^2\theta\,\delta(u^\varphi\Sigma^{t\varphi}) \\ & + \left(u^\theta\Sigma^{t\theta} + \sin^2\theta\,u^\varphi\Sigma^{t\varphi}\right)\delta r + \left((r-2M)\,\sin 2\theta\,u^\varphi\Sigma^{t\varphi}\right)\delta\theta,\end{aligned}$$

$$\begin{aligned}
\frac{d\delta\Sigma^{t\theta}}{d\tau} = & -\frac{M}{r(r-2M)}\,\delta(u^t\Sigma^{r\theta}) - \frac{(r-M)}{r(r-2M)}\,\delta(u^r\Sigma^{t\theta}) - \frac{1}{r}\,\delta(u^\theta\Sigma^{tr}) \\
& + \sin\theta\cos\theta\,\delta(u^\varphi\Sigma^{t\varphi}) + \left(\cos 2\theta\, u^\varphi\Sigma^{t\varphi}\right)\delta\theta \\
& + \left[\frac{2M(r-M)}{r^2(r-2M)^2}u^t\Sigma^{r\theta} + \frac{1}{r^2}\left(1+\frac{2M(r-M)}{(r-2M)^2}\right)u^r\Sigma^{t\theta} + \frac{1}{r^2}u^\theta\,\Sigma^{tr}\right]\delta r,
\end{aligned}$$

$$\begin{aligned}
\frac{d\delta\Sigma^{r\varphi}}{d\tau} = & -\frac{M(r-2M)}{r^3}\,\delta(u^t\Sigma^{t\varphi}) - \frac{(r-3M)}{r(r-2M)}\,\delta(u^r\Sigma^{r\varphi}) - \operatorname{ctg}\theta\,\delta(u^\theta\Sigma^{r\varphi}) \\
& + (r-2M)\,\delta(u^\theta\Sigma^{\theta\varphi}) - \cot\theta\,\delta(u^\varphi\Sigma^{r\theta}) \\
& + \left[\frac{2M}{r^4}(r-3M)\,u^t\,\Sigma^{t\varphi} - \frac{1}{r^2}\left(1-\frac{2M(r-M)}{(r-2M)^2}\right)u^r\Sigma^{r\varphi} + u^\theta\,\Sigma^{\theta\varphi}\right]\delta r \\
& + \left(\csc^2\theta\,u^\theta\,\Sigma^{r\varphi} + \csc^2\theta\,u^\varphi\,\Sigma^{r\theta}\right)\delta\theta,
\end{aligned}$$

$$\begin{aligned}
\frac{d\delta\Sigma^{r\theta}}{d\tau} = & -\frac{M(r-2M)}{r^3}\,\delta(u^t\Sigma^{t\theta}) - \frac{(r-3M)}{r(r-2M)}\,\delta(u^r\Sigma^{r\theta}) \\
& + \sin\theta\,\cos\theta\,\delta(u^\varphi\Sigma^{r\varphi}) - (r-2M)\,\sin^2\theta\,\delta(u^\varphi\Sigma^{\theta\varphi}) \\
& + \left(\cos 2\theta\,u^\varphi\,\Sigma^{r\varphi} - (r-2M)\,\sin 2\theta\,u^\varphi\,\Sigma^{\theta\varphi}\right)\delta\theta \\
& + \left[\frac{2M}{r^4}(r-3M)\,u^t\,\Sigma^{t\theta} + \frac{1}{r^2}\left(1-\frac{2M(r-M)}{(r-2M)^2}\right)u^r\Sigma^{r\theta}\right. \\
& \qquad \left. - \sin^2\theta\,u^\varphi\,\Sigma^{\theta\varphi}\right]\delta r,
\end{aligned}$$

$$\begin{aligned}
\frac{d\delta\Sigma^{\theta\varphi}}{d\tau} = & -\frac{2}{r}\,\delta(u^r\Sigma^{\theta\varphi}) - \frac{1}{r}\,\delta(u^\theta\Sigma^{r\varphi}) + \frac{1}{r}\delta(u^\varphi\Sigma^{r\theta}) + \cot\theta\,\delta(u^\theta\Sigma^{\theta\varphi}) \\
& + \frac{1}{r^2}\left(-u^\varphi\,\Sigma^{r\theta} + u^\theta\,\Sigma^{r\varphi} + 2u^r\,\Sigma^{\theta\varphi}\right)\delta r + \left(\csc^2\theta\,u^\theta\,\Sigma^{\theta\varphi}\right)\delta\theta.
\end{aligned}$$

Of course, any special case like planar orbits can be deduced from these equations, by using the respective conditions.

Bibliography

[1] F. Pretorius, "Binary Black Hole Coalescence," arXiv:0710.1338 [gr-qc].

[2] A. Einstein, "Die Grundlagen der Allgemeinen Relativitätstheorie. (German) [The foundations of the Theory of General Relativity]," *Annalen der Physik* **354** no. 7, (1916) 769–822.

[3] C. W. Misner, K. S. Thorne, and J. A. Wheeler, *Gravitation*. 1973.

[4] M. Maggiore, *Gravitational waves. Volume 1: theory and experiments*. Oxford Univ. Press, Oxford, 2008.

[5] B. Sathyaprakash and B. Schutz, "Physics, Astrophysics and Cosmology with Gravitational Waves," *Living Rev.Rel.* **12** (2009) 2, arXiv:0903.0338 [gr-qc].

[6] R. A. Hulse and J. H. Taylor, "Discovery of a pulsar in a binary system," *The Astrophysical Journal Letters* **195** (1975) L51–L53.

[7] H. M. Van Horn, S. Sofia, M. P. Savedoff, J. G. Duthie, and R. A. Berg, "Binary pulsar psr 1913 + 16: Model for its origin," *Science* **188** no. 4191, (1975) 930–933. http://science.sciencemag.org/content/188/4191/930.

[8] T. Damour, "1974: the discovery of the first binary pulsar," *Class. Quant. Grav.* **32** no. 12, (2015) 124009, arXiv:1411.3930 [gr-qc].

[9] R. N. Manchester, "Pulsars and Gravity," *Int. J. Mod. Phys.* **D24** no. 06, (2015) 1530018, arXiv:1502.05474 [gr-qc].

[10] J. M. Weisberg and J. H. Taylor, "Relativistic binary pulsar B1913+16: Thirty years of observations and analysis," *ASP Conf. Ser.* **328** (2005) 25, arXiv:astro-ph/0407149 [astro-ph].

[11] J. M. Weisberg, D. J. Nice, and J. H. Taylor, "Timing measurements of the relativistic binary pulsar psr b1913+16," *The Astrophysical Journal* **722** no. 2, (2010) 1030. http://stacks.iop.org/0004-637X/722/i=2/a=1030.

[12] J. M. Weisberg, J. H. Taylor, and L. A. Fowler, "Gravitational waves from an orbiting pulsar," *Scientific American* **245** (Oct., 1981) 74–82.

[13] C. Sivaram, "The Hulse-Taylor binary pulsar PSR 1913+16.," *Bulletin of the Astronomical Society of India* **23** (Mar., 1995) 77–83.

[14] L. Blanchet, "Gravitational Radiation from Post-Newtonian Sources and Inspiralling Compact Binaries," *Living Rev. Relativity* **17** (2014) . http://www.livingreviews.org/lrr-2014-2.

[15] B. P. Abbott, L. S. Collaboration, and V. Collaboration, "Prospects for observing and localizing gravitational-wave transients with advanced ligo and advanced virgo," *Living Reviews in Relativity* **19** no. 1, (2016) . http://www.livingreviews.org/lrr-2016-1.

[16] S. Chandrasekhar, *The mathematical theory of black holes*. Oxford classic texts in the physical sciences. Oxford Univ. Press, Oxford, 2002.

[17] J. Weber, "Detection and generation of gravitational waves," *Phys. Rev.* **117** (Jan, 1960) 306–313. http://link.aps.org/doi/10.1103/PhysRev.117.306.

[18] M. Pitkin, S. Reid, S. Rowan, and J. Hough, "Gravitational wave detection by interferometry (ground and space)," *Living Reviews in Relativity* **14** no. 5, (2011) . http://www.livingreviews.org/lrr-2011-5.

[19] A. Freise and K. A. Strain, "Interferometer techniques for gravitational-wave detection," *Living Reviews in Relativity* **13** no. 1, (2010) . http://www.livingreviews.org/lrr-2010-1.

[20] B. Abbott *et al.*, "Observation of Gravitational Waves from a Binary Black Hole Merger," *Phys. Rev. Lett.* **116** (Feb, 2016) 061102. http://link.aps.org/doi/10.1103/PhysRevLett.116.061102.

[21] **Virgo, LIGO Scientific** Collaboration, B. P. Abbott *et al.*, "Tests of general relativity with GW150914," arXiv:1602.03841 [gr-qc].

[22] S. A. Hughes, "Listening to the universe with gravitational-wave astronomy," *Annals of Physics* **303** (Jan., 2003) 142–178, astro-ph/0210481.

[23] B. P. Abbott *et al.*, "Astrophysical implications of the binary black hole merger gw150914," *The Astrophysical Journal Letters* **818** no. 2, (2016) L22.

[24] K. Riles, "Gravitational Waves: Sources, Detectors and Searches," *Prog.Part.Nucl.Phys.* **68** (2013) 1–54, arXiv:1209.0667 [hep-ex].

[25] **LIGO Scientific** Collaboration, B. P. Abbott *et al.*, "LIGO: The Laser interferometer gravitational-wave observatory," *Rept. Prog. Phys.* **72** (2009) 076901, arXiv:0711.3041 [gr-qc].

[26] K. Belczynski, S. Repetto, D. Holz, R. O'Shaughnessy, T. Bulik, E. Berti, C. Fryer, and M. Dominik, "Comparison of LIGO/Virgo upper limits with predicted compact binary merger rates," arXiv:1510.04615 [astro-ph.HE].

[27] K. Barkett, M. A. Scheel, R. Haas, C. D. Ott, S. Bernuzzi, D. A. Brown, B. Szilágyi, J. D. Kaplan, J. Lippuner, C. D. Muhlberger, F. Foucart, and M. D. Duez, "Gravitational waveforms for neutron star binaries from binary black hole simulations," *Phys. Rev. D* **93** (Feb, 2016) 044064. http://link.aps.org/doi/10.1103/PhysRevD.93.044064.

[28] E. Berti, A. Buonanno, and C. M. Will, "Estimating spinning binary parameters and testing alternative theories of gravity with LISA," *Phys.Rev.* **D71** (2005) 084025, arXiv:gr-qc/0411129 [gr-qc].

[29] E. Berti *et al.*, "Testing General Relativity with Present and Future Astrophysical Observations," *Class. Quant. Grav.* **32** (2015) 243001, arXiv:1501.07274 [gr-qc].

[30] C. F. Sopuerta and N. Yunes, "Extreme and Intermediate-Mass Ratio Inspirals in Dynamical Chern-Simons Modified Gravity," *Phys.Rev.* **D80** (2009) 064006, arXiv:0904.4501 [gr-qc].

[31] S. Babak, J. R. Gair, and R. H. Cole, "Extreme mass ratio inspirals: perspectives for their detection," arXiv:1411.5253 [gr-qc].

[32] J. R. Gair, M. Vallisneri, S. L. Larson, and J. G. Baker, "Testing general relativity with low-frequency, space-based gravitational-wave detectors," *Living Reviews in Relativity* **16** no. 7, (2013) . http://www.livingreviews.org/lrr-2013-7.

[33] **eLISA** Collaboration, P. A. Seoane *et al.*, "The Gravitational Universe," arXiv:1305.5720 [astro-ph.CO].

[34] R. Barkana and A. Loeb, "In the beginning: The First sources of light and the reionization of the Universe," *Phys. Rept.* **349** (2001) 125–238, arXiv:astro-ph/0010468 [astro-ph].

[35] S. Komossa, V. Burwitz, G. Hasinger, P. Predehl, J. S. Kaastra, and Y. Ikebe, "Discovery of a binary active galactic nucleus in the ultraluminous infrared galaxy ngc 6240 using chandra," *The Astrophysical Journal Letters* **582** no. 1, (2003) L15. http://stacks.iop.org/1538-4357/582/i=1/a=L15.

[36] C. Cutler and E. E. Flanagan, "Gravitational waves from merging compact binaries: How accurately can one extract the binary's parameters from the inspiral wave form?," *Phys. Rev.* **D49** (1994) 2658–2697, arXiv:gr-qc/9402014 [gr-qc].

[37] G. Nelemans, S. F. Portegies Zwart, F. Verbunt, and L. R. Yungelson, "Population synthesis for double white dwarfs. 2. Semi-detached systems: am cvn stars," *Astron. Astrophys.* **368** (2001) 939–949, arXiv:astro-ph/0101123 [astro-ph].

[38] A. J. Farmer and E. S. Phinney, "The gravitational wave background from cosmological compact binaries," *Mon. Not. Roy. Astron. Soc.* **346** (2003) 1197, arXiv:astro-ph/0304393 [astro-ph].

[39] P. Amaro-Seoane, "Stellar dynamics and extreme-mass ratio inspirals," arXiv:1205.5240 [astro-ph.CO].

[40] P. Amaro-Seoane, J. R. Gair, A. Pound, S. A. Hughes, and C. F. Sopuerta, "Research Update on Extreme-Mass-Ratio Inspirals," arXiv:1410.0958 [astro-ph.CO].

[41] R. Genzel, C. Pichon, A. Eckart, O. E. Gerhard, and T. Ott, "Stellar dynamics in the Galactic centre: Proper motions and anisotropy," *Mon. Not. Roy. Astron. Soc.* **317** (2000) 348, arXiv:astro-ph/0001428 [astro-ph].

[42] R. Genzel, F. Eisenhauer, and S. Gillessen, "The Galactic Center Massive Black Hole and Nuclear Star Cluster," *Rev. Mod. Phys.* **82** (2010) 3121–3195, arXiv:1006.0064 [astro-ph.GA].

[43] M. Freitag, P. Amaro-Seoane, and V. Kalogera, "Stellar remnants in galactic nuclei: mass segregation," *Astrophys. J.* **649** (2006) 91–117, arXiv:astro-ph/0603280 [astro-ph].

[44] L. Ferrarese and H. Ford, "Supermassive black holes in galactic nuclei: Past, present and future research," *Space Sci.Rev.* **116** (2005) 523–624, arXiv:astro-ph/0411247 [astro-ph].

[45] S. Gillessen, F. Eisenhauer, S. Trippe, T. Alexander, R. Genzel, F. Martins, and T. Ott, "Monitoring stellar orbits around the Massive Black Hole in the

Galactic Center," *Astrophys. J.* **692** (2009) 1075–1109, arXiv:0810.4674 [astro-ph].

[46] R. Genzel, "Massive Black Holes: Evidence, Demographics and Cosmic Evolution," in *26th Solvay Conference on Physics: Astrophysics and Cosmology Brussels, Belgium, October 9-11, 2014*. 2014. arXiv:1410.8717 [astro-ph.GA]. https://inspirehep.net/record/1325598/files/arXiv:1410.8717.pdf.

[47] G. d'Ambrosi, S. Satish Kumar, and J. W. van Holten, "Covariant hamiltonian spin dynamics in curved spacetime," *Phys. Lett.* **B743** (2015) 478–483, arXiv:1501.04879 [gr-qc].

[48] G. d'Ambrosi, S. Satish Kumar, J. van de Vis, and J. W. van Holten, "Spinning bodies in curved spacetime," *Phys. Rev.* **D93** no. 4, (2016) 044051, arXiv:1511.05454 [gr-qc].

[49] J. R. Gair, "Probing black holes at low redshift using LISA EMRI observations," *Class. Quant. Grav.* **26** (2009) 094034, arXiv:0811.0188 [gr-qc].

[50] J. B. Hartle, *Gravity: An Introduction to Einstein's General Relativity*. Benjamin Cummings, illustrate ed., Jan., 2003.

[51] J. W. Van Holten, "Gravitational waves and black holes: An introduction to general relativity," *Fortsch.Phys.* **45** (1997) 439–516, arXiv:gr-qc/9704043 [gr-qc].

[52] S. Weinberg, *Gravitation and Cosmology: Principles and Applications of the General Theory of Relativity*. Wiley New York, New York, 1972.

[53] A. Einstein, "Die Feldgleichungen der Gravitation. (German) [The field equations of gravitation]," *Sitzungsberichte der Preussischen Akademie der Wissenschaften zu Berlin* (1915) 844–847.

[54] K. Schwarzschild, "Über das Gravitationsfeld eines Massenpunktes nach der Einsteinschen Theorie," *Sitzungsberichte der Königlichen Prussischen Akademie der Wissenschaften* **7** (1916) 189–196.

[55] J. Droste, "Phd thesis," *Leiden University* (1916) .

[56] G. Koekoek, *The Geodesic Deviation Method and Extreme Mass-Ratio Systems. Theoretical methods and application to the calculation of gravitational waves*. PhD thesis, Vrije U., Amsterdam, 2011. https://inspirehep.net/record/1081429/files/Thesis-2011-Koekoek.pdf.

[57] R. Kerner, J. van Holten, and J. Colistete, R., "Relativistic epicycles: Another approach to geodesic deviations," *Class.Quant.Grav.* **18** (2001) 4725–4742, arXiv:gr-qc/0102099 [gr-qc].

[58] G. Koekoek and J. van Holten, "Epicycles and Poincaré Resonances in General Relativity," *Phys.Rev.* **D83** (2011) 064041, arXiv:1011.3973 [gr-qc].

[59] A. Papapetrou, "Spinning test particles in general relativity. 1.," *Proc.Roy.Soc.Lond.* **A209** (1951) 248–258.

[60] K. Kyrian and O. Semerak, "Spinning test particles in a Kerr field. II.," *Mon.Not.Roy.Astron.Soc.* **382** (2007) 1922–1932.

[61] W. Dixon, "Dynamics of extended bodies in general relativity. I. Momentum and angular momentum," *Proc.Roy.Soc.Lond.* **A314** (1970) 499–527.

[62] W. G. Dixon, "Dynamics of extended bodies in general relativity. ii. moments of the charge-current vector," *Proceedings of the Royal Society of London A: Mathematical, Physical and Engineering Sciences* **319** no. 1539, (1970) 509–547. http://rspa.royalsocietypublishing.org/content/319/1539/509.

[63] L. F. Costa and J. Natário, "Center of mass, spin supplementary conditions, and the momentum of spinning particles," arXiv:1410.6443 [gr-qc].

[64] D. Bini, A. Geralico, and R. T. Jantzen, "Spin-geodesic deviations in the Schwarzschild spacetime," *Gen.Rel.Grav.* **43** (2011) 959, arXiv:1408.4946 [gr-qc].

[65] S. Suzuki and K.-i. Maeda, "Chaos in Schwarzschild space-time: The motion of a spinning particle," *Phys. Rev.* **D55** (1997) 4848–4859, arXiv:gr-qc/9604020 [gr-qc].

[66] M. D. Hartl, "Dynamics of spinning test particles in kerr spacetime," *Phys. Rev. D* **67** (Jan, 2003) 024005. http://link.aps.org/doi/10.1103/PhysRevD.67.024005.

[67] M. D. Hartl, "Survey of spinning test particle orbits in kerr spacetime," *Phys. Rev. D* **67** (May, 2003) 104023. http://link.aps.org/doi/10.1103/PhysRevD.67.104023.

[68] J. Souriau *C. R. Acad. Sc. Paris* **271** (1970) 751.

[69] J. Souriau *C. R. Acad. Sc. Paris* **271** (1970) 1086.

[70] J. Souriau *C. R. Acad. Sc. Paris* **274** (1972) 1082.

[71] J. Souriau *Ann. Inst. H. Poincare'* **20** (1974) 22.

[72] W. G. Dixon, "The definition of multipole moments for extended bodies," *General Relativity and Gravitation* **4** no. 3, 199–209. http://dx.doi.org/10.1007/BF02412488.

[73] B. Mashhoon, "Massless spinning test particles in a gravitational field," *Annals of Physics* **89** no. 1, (1975) 254 – 257. http://www.sciencedirect.com/science/article/pii/0003491675903048.

[74] I. Bailey and W. Israel, "Lagrangian Dynamics of Spinning Particles and Polarized Media in General Relativity," *Commun.Math.Phys.* **42** (1975) 65–82.

[75] J. Frenkel, "Die Elektrodynamik des rotierenden Elektrons," *Z.Phys.* **37** (1926) 243–262.

[76] A. O. Barut, *Electrodynamics and classical theory of fields and particles.* Mac Millan, New York, 1964.

[77] C. Duval, H. H. Fliche, and J. M. Souriau, "Un modèle de particule à spin dans le champ gravitationnel et électromagnétique," *C. R. Acad. Sci. Paris.* **274** (1972) 1082.

[78] L. Brink, P. Di Vecchia, and P. S. Howe, "A Lagrangian Formulation of the Classical and Quantum Dynamics of Spinning Particles," *Nucl.Phys.* **B118** (1977) 76.

[79] A. O. Barut and N. Zanghi, "Classical model of the Dirac electron," *Phys. Rev. Lett.*. **52** (1984) .

[80] I. Khriplovich and A. Pomeransky, "Gravitational interaction of spinning bodies, center-of-mass coordinate and radiation of compact binary systems," *Phys.Lett.* **A216** (1996) 7, arXiv:gr-qc/9602004 [gr-qc].

[81] I. Khriplovich and A. Pomeransky, "Equations of motion of spinning relativistic particle in external fields," *Surveys High Energ.Phys.* **14** (1999) 145–173, arXiv:gr-qc/9809069 [gr-qc].

[82] A. Barducci, R. Casalbuoni, and L. Lusanna, "Supersymmetries and the Pseudoclassical Relativistic electron," *Nuovo Cim.* **A35** (1976) 377.

[83] F. Berezin and M. Marinov, "Particle Spin Dynamics as the Grassmann Variant of Classical Mechanics," *Annals Phys.* **104** (1977) 336.

[84] P. Salomonson, "Supersymmetric Actions for Spinning Particles," *Phys.Rev.* **D18** (1978) 1868–1880.

[85] R. Rietdijk and J. van Holten, "Spinning particles in Schwarzschild space-time," *Class.Quant.Grav.* **10** (1993) 575–594.

[86] I. Khriplovich, "Particle with internal angular momentum in a gravitational field," *Sov.Phys.JETP* **69** (1989) 217–219.

[87] J. W. van Holten, "Covariant Hamiltonian dynamics," *Phys.Rev.* **D75** (2007) 025027, arXiv:hep-th/0612216 [hep-th].

[88] J. W. van Holten, "On the electrodynamics of spinning particles," *Nucl.Phys.* **B356** (1991) 3–26.

[89] L. F. O. Costa, C. A. Herdeiro, J. Natario, and M. Zilhao, "Mathisson's helical motions for a spinning particle: Are they unphysical?," *Phys.Rev.* **D85** (2012) 024001, arXiv:1109.1019 [gr-qc].

[90] F. Pirani, "On the Physical significance of the Riemann tensor," *Acta Phys.Polon.* **15** (1956) 389–405.

[91] L. F. O. Costa, J. Natário, and M. Zilhao, "Spacetime dynamics of spinning particles - exact gravito-electromagnetic analogies," arXiv:1207.0470 [gr-qc].

[92] I. Khriplovich, "Spinning Relativistic Particles in External Fields," arXiv:0801.1881 [gr-qc].

[93] J. W. van Holten, "Relativistic dynamics of spin in strong external fields," arXiv:hep-th/9303124 [hep-th].

[94] S. Satish Kumar, "Motion of a spinning particle in curved space-time," 2015. arXiv:1512.07152 [gr-qc]. http://inspirehep.net/record/1411068/files/arXiv:1512.07152.pdf.

[95] O. Semerak, "Spinning test particles in a Kerr field. I.," *Mon.Not.Roy.Astron.Soc.* **308** (1999) 863–875.

[96] Rüdiger, R., "Conserved quantities of spinning test particles in General Relativity I," *Proc.Roy.Soc. Series A* **375** no. 1761, (1981) 185–193.

[97] Rüdiger R., "Conserved quantities of spinning test particles in General Relativity II," *Proc.Roy.Soc. Series A* **385** no. 1788, (1983) 229–239.

[98] G. Gibbons, R. Rietdijk, and J. van Holten, "SUSY in the sky," *Nucl.Phys.* **B404** (1993) 42–64, arXiv:hep-th/9303112 [hep-th].

[99] R. Plyatsko, O. Stefanyshyn, and M. Fenyk, "Mathisson-Papapetrou-Dixon equations in the Schwarzschild and Kerr backgrounds," *Class.Quant.Grav.* **28** (2011) 195025, arXiv:1110.1967 [gr-qc].

[100] I. Khriplovich and A. Pomeransky, "Equations of motion of spinning relativistic particle in external fields," *J.Exp.Theor.Phys.* **86** (1998) 839–849, arXiv:gr-qc/9710098 [gr-qc].

[101] K. Heinemann, "On Stern-Gerlach forces allowed by special relativity and the special case of the classical spinning particle of Derbenev-Kondratenko," arXiv:physics/9611001 [physics].

[102] J. W. van Holten, *Theory of a charged spinning particle in a gravitational and electro-magnetic field.* in: Proc. Seminar on Math. Structures in Field Theory 1986-87, CWI-syllabus vol. 26, eds. E.A. de Kerf and H.G.J. Pijls (CWI, Amsterdam), 1990.

[103] J. Steinhoff and D. Puetzfeld, "Multipolar equations of motion for extended test bodies in General Relativity," *Phys. Rev.* **D81** (2010) 044019, arXiv:0909.3756 [gr-qc].

[104] J. W. van Holten, "Spinning bodies in General Relativity," in *Workshop on Variational Principles and Conservation Laws in General Relativity: In memory of Prof. Mauro Francaviglia Turin, Italy, June 25-26, 2015.* 2015. arXiv:1504.04290 [gr-qc]. http://inspirehep.net/record/1360263/files/arXiv:1504.04290.pdf.

[105] D. Bini, F. de Felice, A. Geralico, and R. T. Jantzen, "Spin precession in the Schwarzschild spacetime: Circular orbits," *Class.Quant.Grav.* **22** (2005) 2947–2970, arXiv:gr-qc/0506017 [gr-qc].

[106] G. Koekoek and J. van Holten, "Geodesic deviations: modeling extreme mass-ratio systems and their gravitational waves," *Class.Quant.Grav.* **28** (2011) 225022, arXiv:1103.5612 [gr-qc].

[107] L. Blanchet and B. R. Iyer, "Third postNewtonian dynamics of compact binaries: Equations of motion in the center-of-mass frame," *Class. Quant. Grav.* **20** (2003) 755, arXiv:gr-qc/0209089 [gr-qc].

[108] S. Suzuki and K.-i. Maeda, "Innermost stable circular orbit of a spinning particle in Kerr space-time," *Phys. Rev.* **D58** (1998) 023005, arXiv:gr-qc/9712095 [gr-qc].

[109] E. Poisson, A. Pound, and I. Vega, "The motion of point particles in curved spacetime," *Living Reviews in Relativity* **14** no. 7, (2011) . http://www.livingreviews.org/lrr-2011-7.

[110] G. d'Ambrosi and J. van Holten, "Ballistic orbits in Schwarzschild space-time and gravitational waves from EMR binary mergers," *Class.Quant.Grav.* **32** no. 1, (2015) 015012, arXiv:1406.4282 [gr-qc].

Summary

Mankind always had a clue that nature can be understood and described with a limited number of concepts. Modern science explains nature in a more quantitative way: Biology taught us that the cell is the fundamental unit of life; in Chemistry molecules or atoms are the basic building blocks of materials; for Physicists, space and time are the only fundamental entities and everything else in the Universe must be understood from it.

Space, Time and Gravity

For centuries, space and time are considered as two separate things. Space was where events took place and time was a measure of change. Eventually, Einstein with his general theory of relativity revolutionised the way we think about the Universe. His elegant equations state that space and time are intimately connected and melt into one another to form space-time. Thus, the presence of large amounts of mass or energy distorts space-time – in essence causing the space-time fabric to "warp" and we observe this as gravity. For instance, the planets are moving in straight lines in the curvature produced by the sun and it appears as if they are in circular or elliptical motion around the sun. This is the central idea of General Relativity.

General Relativity is the most successful theory of gravity, describing accurately all the gravitational phenomena we know. In addition, it predicts new strong gravitational phenomena like black holes, neutron stars, compact binaries – composed of black holes and/or neutron stars, gravitational waves, and the Big Bang.

Extreme Mass Ratio System

In this thesis, I have presented the scientific work done along with my collaborators on the theoretical modelling and understanding of compact binaries. Specifically, when one of the objects in the binary system is very very small compared to the other, i.e., an Extreme Mass Ratio System. Extreme Mass Ratio Systems consist of

a huge central black hole of mass million times heavier than the sun and a smaller companion with a mass of a few times that of the sun . The smaller companion can be a white dwarf, black hole or a neutron star and the central object is called a supermassive black hole.

Usually these kinds of systems are found in the centre of the galaxies. Almost all the bright galaxies accommodate one or more supermassive black holes in their centres. For example, our own galaxy Milky Way has a supermassive black hole four million times heavier than the sun, named as *Sagittarius A** and there are 28 stars orbiting it closely. Therefore by following the companions of the supermassive black holes and modelling Extreme Mass Ratio Systems will eventually help us to understand the geometry of the supermassive black hole and hence the galactic dynamics.

Black holes are objects in which a huge amount of mass is compressed into a very small volume. As a result, the space-time around them is extremely curved, such that even light can't escape once it enters into the event horizon (the point of no return) and even the tick rate of the clock reduces due to the gravitational pull. Black holes are described with three properties: mass, spin (rotation), and charge.

Technically black holes are solutions of Einstein's field equation - the master equation in the general theory of relativity. The black hole which has only mass and is spherically symmetric is known as Schwarzschild black hole. A massive compact object can also possess angular momentum, that is, rotation about its own axis. Then it is described with the Kerr metric and called a Kerr black hole. If these two kinds of black holes have charge as an additional property, then they are known as Reissner-Nordstrøm black holes and Kerr-Newman black holes. These are the four known, exact, black hole solutions to the Einstein's field equations in General Relativity.

Dynamics of an Extreme Mass Ratio System

The analytical description of systems like *Sagittarius A** is extremely complicated, as the central object is also spinning about its own axis, and many companions orbiting it. Therefore researchers have attempted to understand them in steps: describing the dynamics of a single companion around the supermassive black hole known as Extreme Mass Ratio System. Traditionally the description of spin in Extreme Mass Ratio Systems has been based on the Mathisson-Papapetrou formalism.

Mathisson and Papapetrou described the dynamics of spinning compact objects in curved space-time. But the complication in the formalism is that one has to keep track of the internal structure of the orbiting companion. Further, a fully relativistic calculation has never been done. Usually one does something called Post-Newtonian scheme in which it is assumed that the gravitational field far away from the central

black hole is weak, hence Newton's Law of gravitation is used and the effects of space-time curvature are then added subsequently.

Therefore, my collaborators and I proposed an alternate complementary description for the subject. Since the mass ratio is extreme we have neglected the internal structure of the smaller companion and treated it as a point object. Thus we have generalised the Einstein's description of spinless bodies. Also near black holes the gravitational field curvature, is strong. So, we have developed completely relativistic orbits for spinning bodies by generalising the well known geodesic deviation method in General Relativity.

We then applied our new formalism to *a stellar mass spinning compact object in the curvature of a non-rotating supermassive black hole (Schwarzschild)*. We analytically established three kinds of possible orbits in the relativistic limit:

Circular orbits and Innermost Stable Circular Orbits

When a stellar object is captured by the gravity of the supermassive black hole, then the body may undergo circular orbits in a fixed plane; as shown in the Fig. 6.1. This has been demonstrated with an analytic equation in our theory and the radius of the circular orbits depends on the parameters of the system: the masses of the objects and the spin of the smaller object.

The spin and orbital motion of the body are quantified by the vector quantities called spin angular momentum and orbital angular momentum. The sum of these two are denoted by **J**, the total angular momentum (shown with arrows). *For a stellar object in the planar orbit, the direction of these quantities must remain fixed as implied by our theorem.*

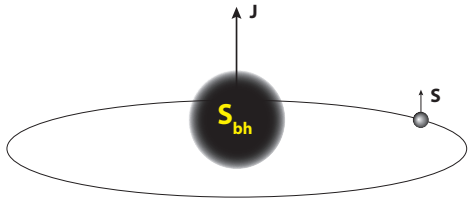

Figure 6.1. A stellar mass spinning black hole or a neutron star is orbiting a supermassive black hole in circular orbits.

The smallest circular orbit in which the stellar companion is stably orbiting the massive object is called *Innermost Stable Circular Orbit (ISCO)*. For a stellar companion which is not spinning, the ISCO is found at three times the Schwarzschild

radius (the radius of the event horizon surrounding a non-rotating black hole) and it is a standard result in General Relativity. Because our orbiting object is spinning, the spin influences the ISCO. We found that, *when the magnitude of the spin increases, the radius of the ISCO increases or decreases, depending on the orientation*. Therefore, for a spinning object the ISCO can be found at more or less than three times the Schwarzschild radius.

Plane non-circular orbits and periastron shift

The orbiting body does not moves on well defined orbits like circular ones. In case the orbit is a little bit perturbed, it is still possible to have orbits in the plane. But, because of the non-constant spin the body possesses two periods. Hence the point of closest approach (periastron) and the point of farthest approach (apastron) behave in a complicated way, as the body reaches different minimum and maximum at non-constant intervals (Fig. 6.2). In addition, after each orbit the body ends ahead of the starting point. This shift in the angle of the orbit due to the warped space-time is known as *periastron shift*.

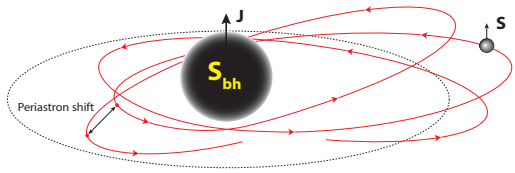

Figure 6.2. The perturbed orbit possesses a periastron shift in the plane. The spinning body reaches different periastra or apastra at non-constant intervals.

This is a well known effect in General Relativity as described by Einstein for the perihelion shift of Mercury. But *the irregular behaviour of the body with two periods is something very new which emerged out of our theory*!

Geodetic precession/de Sitter precession

For a perturbed precessing spinning object the spin precession must be compensated by the orbital angular momentum. Hence the total angular momentum **J** remains constant. Then the body goes in a periodic motion above and below the plane orbiting the massive object. In other words, the whole orbit precesses about its

plane. Therefore the orbital angular momentum **L** sweeps out a cone. This effect is called *Geodetic precession or de Sitter precession* named after Willem de Sitter.

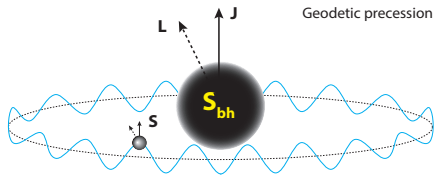

Figure 6.3. The spin precession must be compensated by the precession of the orbital angular momentum **L**. Therefore **L** sweeps out a cone.

The geodetic effect was first predicted by de Sitter in 1916, and he has provided relativistic corrections to the motion of the Earth-Moon system. Later on this effect has been found in many other systems. Here we have discovered this effect in our Extreme Mass Ratio Binaries.

Conclusion

We have described the dynamics of spinning compact objects in a completely new frame work and established three kinds of orbits and its properties. But the orbiting body can behave in more complicated ways, which is left for further investigation. For instance, when the body is orbiting at relativistic speeds it emits gravitational radiation: waves representing ripples in the fabric of space-time.

The European space agency is already working to set up a gravitational laboratory – eLISA, that will orbit the sun along with earth whilst detecting the ripples in space-time and send us the information. A study of this information can unveil the geometry around the central black hole and the stellar object populations, mass spectrum and spin. Almost all bright galaxies hosts one or more massive central black holes. When galaxies coalesce these supermassive black holes will merge eventually, releasing huge amount of gravitational radiation during the process. Thus detecting these signals will not only test theories of gravity and black holes, but also reveal information about the evolution and merger history of galaxies.

Interestingly, Einstein who discovered the gravitational waves in his theory of relativity, didn't think that its detection will ever be possible. But we can now be proud enough to live in an era, where his doubt has been proved wrong with the latest discovery of gravitational waves at LIGO observatories – the event named GW150914.

Samenvatting

De mensheid heeft altijd vermoed dat de natuur begrepen en beschreven kan worden met een beperkt aantal concepten. De moderne natuurwetenschap beschrijft de natuur voornamelijk op een kwantitatieve manier: de biologie leert ons dat de cel de fundamentele eenheid van het leven is, in de scheikunde vormen moleculen en atomen de bouwstenen van materialen; voor natuurkundigen zijn ruimte en tijd de enige fundamentele entiteiten, waar al het andere in het universum vanuit begrepen moet worden.

Ruimte, tijd en zwaartekracht

Eeuwenlang werden ruimte en tijd beschouwd als twee verschillende dingen. De ruimte was waar gebeurtenissen in plaatsvinden en de tijd is een maat voor verandering. Uiteindelijk heeft Einstein met zijn Algemene Relativiteitstheorie de manier waarop we over ons universum denken revolutionair veranderd. Zijn elegante vergelijkingen stellen dat ruimte en tijd nauw met elkaar verbonden zijn en met elkaar versmelten tot de ruimtetijd. De aanwezigheid van grote hoeveelheden massa of energie verstoort de ruimtetijd - het weefsel van de ruimtetijd wordt verbogen - en dit nemen we waar als zwaartekracht. De planeten bewegen bijvoorbeeld in rechte lijnen in de kromming veroorzaakt door de zon en het lijkt alsof ze zich in circulaire of elliptische banen om de zon bevinden. Dat is het centrale idee van de Algemene Relativiteit.

Algemene Relativiteit is de meest succesvolle theorie van de zwaartekracht, ze geeft een nauwkeurige beschrijving van alle zwaartekrachtsverschijnselen die we kennen. Bovendien voorspelt ze nieuwe sterke zwaartekrachtsverschijnselen, zoals zwarte gaten, neutronensterren, compacte dubbelsystemen (bestaande uit zwarte gaten en/of neutronensterren), zwaartekrachtsgolven en de Big Bang.

Systemen met een extreme massaverhouding

In dit proefschrift beschrijf ik het onderzoek dat ik heb gedaan met mijn collega's om dubbelsystemen van compacte objecten theoretisch te modelleren en te begrijpen. We bestuderen het specifieke geval waarin één van de objecten in het dubbelsysteem veel kleiner is dan het andere, ofwel een systeem met een extreme massaverhouding. Systemen met een extreme massaverhouding bestaan uit een enorm zwart gat met een massa van een miljoen zonsmassa's in het midden en een kleiner object van een aantal zonsmassa's. Het kleinere object kan een witte dwerg, een zwart gat of een neutronenster zijn en het centrale object is een zogenaamd superzwaar zwart gat.

Dit soort systemen komt normaal gesproken voor in het centrum van sterrenstelsels. Bijna alle heldere sterrenstelsels hebben één of meerdere superzware zwarte gaten in hun centrum. Ons eigen sterrenstelsel, de Melkweg, heeft bijvoorbeeld een superzwaar zwart gat dat vier miljoen maal zo zwaar is als de zon, genaamd Sagittarius A*, waar 28 sterren dicht omheen draaien. Het bestuderen van de kleinere objecten die om zwarte gaten heen bewegen en het maken van modellen van systemen met een extreme massaverhouding zal ons uiteindelijk helpen om de geometrie van het zwarte gat te begrijpen en daarmee de galactische dynamica.

Zwarte gaten zijn objecten waarin een enorme hoeveelheid massa samengedrukt is in een zeer klein volume. Hierdoor is de omringende ruimtetijd zeer sterk gekromd, waardoor zelfs licht niet kan ontsnappen wanneer het de waarnemingshorizon voorbij gaat. Zelfs het tikken van een klok wordt vertraagd door de zwaartekracht. Zwarte gaten worden beschreven door drie eigenschappen: massa, spin (draaiing) en lading.

Technisch gesproken zijn zwarte gaten oplossingen van de Einsteinvergelijking, de belangrijkste vergelijking in de Algemene Relativiteitstheorie. Een bolsymmetrisch zwart gat dat alleen massa heeft, staat bekend als een Schwarzschild zwart gat. Een massief compact object kan ook impulsmoment hebben, ofwel rotatie om zijn eigen as. In dat geval wordt het zwarte gat beschreven door de Kerr metriek en wordt het een Kerr zwart gat genoemd. Als deze soorten zwarte gaten bovendien lading hebben, staan ze bekend als Reissner-Nordstrøm en Kerr-Newman zwarte gaten. Dit zijn de vier bekende exacte oplossingen van Einsteins veldvergelijkingen in de Algemene Relativiteit.

Dynamica van systemen met een extreme massaverhouding

Een analytische beschrijving van systemen zoals Sagittarius A* is zeer ingewikkeld, aangezien het centrale object ook om zijn eigen as spint en omdat er veel objecten omheen bewegen. Daarom proberen onderzoekers deze systemen stap voor stap te begrijpen: door de dynamica van een enkel object dat beweegt rond een superzwaar zwart gat te beschrijven als een systeem met een extreme massaverhouding. Van

oudsher wordt spin in systemen met een extreme massaverhouding beschreven door middel van het Mattisson-Papapetrou-formalisme.

Mathisson en Papapetrou beschreven de dynamica van spinnende compacte objecten in gekromde ruimtetijd. Een complicatie van hun formalisme is, dat het noodzakelijk is om de interne structuur van het kleinere object bij te houden. Bovendien is een volledig relativistische berekening nog nooit uitgevoerd. Doorgaans gebruikt men een post-Newtoniaanse benadering, waarin wordt aangenomen dat het zwaartekrachtsveld ver weg van het centrale zwarte gat zwak is, zodat de zwaartekrachtswet van Newton gebruikt kan worden. Vervolgens worden de effecten van kromming in de ruimtetijd toegevoegd.

Mijn collega's en ik stellen daarom een alternatieve, complementaire beschrijving voor. Omdat de verhouding tussen de massa's extreem is, verwaarlozen we de interne structuur van het kleinere object en beschouwen we het als een puntdeeltje. We generaliseren hiermee Einsteins beschrijving van lichamen zonder spin. Bovendien is het gravitatieveld rondom een zwart gat sterk, en dus is de ruimtetijd sterk gekromd. Daarom ontwikkelen we geheel relativistische banen voor spinnende objecten door de bekende methode van geodetische afwijking te generaliseren.

We hebben ons nieuwe formalisme toegepast op een systeem van een compact object met spin met een stellaire massa en een superzwaar zwart gat zonder spin (Schwarzschild). In de relativistische limiet vonden we drie soorten banen:

Circulaire banen en binnenste stabiele circulaire banen

Wanneer een stellair object gegrepen wordt door de zwaartekracht van een superzwaar zwart gat, kan het object circulaire banen gaan beschrijven in een constant vlak, zoals geïllustreerd in Fig. 6.4. Dit gedrag wordt gedemonstreerd met een analytische vergelijking in onze theorie. De straal van de circulaire baan wordt bepaald door de parameters van het systeem, zoals de massa's van de objecten en de spin van het kleinere object.

De spin en het baanimpulsmoment van het lichaam worden beschreven door de spin-impulsmoment- en baanimpulsmomentvector. De som van deze vectoren wordt genoteerd als **J**, het totale impulsmoment (aangeduid met pijlen). Volgens ons theorema blijft de richting van deze grootheden behouden, voor een stellair object in een vlakke baan.

De kleinste circulaire baan waarin het stellaire object stabiel rondom het zware object beweegt wordt de binnenste stabiele circulaire baan genoemd. Voor een object zonder spin bevindt de binnenste stabiele circulaire baan zich op een afstand van drie maal de Schwarzschildstraal (de straal waarop de waarnemingshorizon zich bevindt) van het centrum van het zwarte gat; dit is een standaard resultaat in de Algemene Relativiteit. De spin van het object dat om het zwarte gat draait beïnvloedt de binnenste stabiele circulaire baan. We vinden dat, wanneer de grootte van de spin toeneemt, de straal van de binnenste stabiele circulaire baan toeneemt

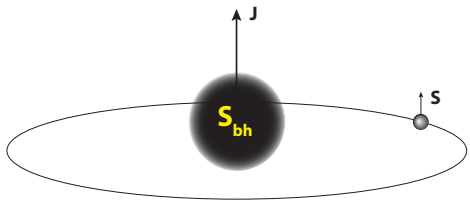

Figure 6.4. Een spinnend zwart gat of neutronenster met stellaire massa beweegt in een circulaire baan rondom een superzwaar zwart gat.

of afneemt, afhankelijk van de oriëntatie. De binnenste stabiele circulaire baan bevindt zich dus op meer of minder dan drie maal de Schwarzschildstraal.

Niet-circulaire banen in het platte vlak en periastronverschuiving

Het draaiende object beweegt zich niet op goed gedefinieerde banen zoals de circulaire banen. Wanneer de baan een klein beetje verstoord wordt, is het nog steeds mogelijk om een baan in een plat vlak te beschrijven. Maar doordat de spin niet constant is, heeft het object twee periodes. Hierdoor gedragen het punt met de kleinste afstand (periastron) en het punt met de grootste afstand (apastron) zich op een ingewikkelde manier, doordat het object steeds een ander maximum en minimum bereikt in variërende intervallen (zie Fig. 6.5).

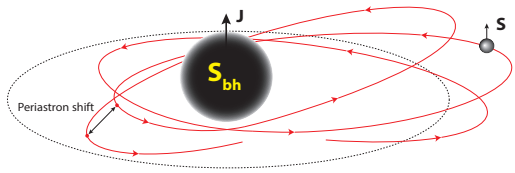

Figure 6.5. De verstoorde baan vertoont periastronverschuiving in het platte vlak. Het spinnende object bereikt verschillende periastra en apastra na variërende intervallen.

Bovendien eindigt het object na elke baan vóór het beginpunt. Deze verschuiving in de hoek van de baan door gekromde ruimtetijd staat bekend als periastron-

verschuiving. Dit is een bekend effect in de Algemene Relativiteit, zoals de door Einstein beschreven perihelionverschuiving van Mercurius. Maar het onregelmatige gedrag van het object met twee periodes is iets nieuws dat in onze theorie naar voren komt!

Geodetische precessie/de Sitter precessie

Voor een verstoord spinnend object met precessie moet de precessie van de spin gecompenseerd worden door het baanimpulsmoment. Het totale impulsmoment **J** blijft dus constant. Het object raakt dan in een periodieke beweging boven en onder het vlak om het massieve object. In andere woorden, de gehele baan precesseert om het vlak. Hier- door beweegt het baanimpulsmoment **L** langs een kegel. Dit effect wordt Geodetische precessie of de Sitterprecessie genoemd, naar Willem de Sitter.

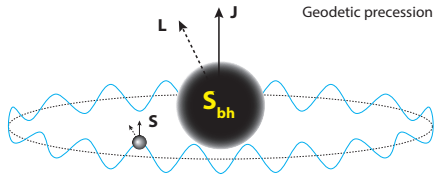

Figure 6.6. De spinprecessie wordt gecompenseerd door de precessie van het baanimpulsmoment **L**. Het baanimpulsmoment **L** beweegt langs een kegel.

Het geodetische effect werd als eerste voorspeld door de Sitter in 1916. Hij vond relativistische correcties voor de beweging in het systeem van de Aarde en de Maan. Dit effect is later ook gevonden in veel andere systemen. Wij hebben dit effect gevonden in onze dubbelsystemen met een extreme massaverhouding.

Conclusie

We hebben de dynamica van spinnende compacte objecten beschreven in een geheel nieuw formalisme en we hebben drie soorten banen en hun eigenschappen vastgesteld. Het draaiende lichaam kan zich op nog ingewikkeldere manieren gedragen, dit blijft over voor toekomstig onderzoek. Een object dat beweegt met relativistische snelheid zendt bijvoorbeeld zwaartekrachtsgolven uit: rimpelingen in de ruimtetijd.

De Europese Ruimtevaartorganisatie (ESA) werkt aan een zwaartekrachtsdetector, eLISA, die samen met de aarde rond de zon zal draaien en ondertussen rimpelingen in de ruimtetijd zal meten. Het bestuderen van de informatie van eLISA kan de geometrie van het centrale zwarte gat en de massa's en spins van de

daaromheen bewegende sterren onthullen. Bijna alle heldere sterrenstelsels bevatten één of meer centrale zware zwarte gaten. Wanneer sterrenstelsels samensmelten, gaan deze superzware zwarte gaten uiteindelijk ook samen; tijdens dit proces komt een enorme hoeveelheid zwaartekrachtsstraling vrij. Het detecteren van deze signalen zal dus niet alleen de theorieën over zwaartekracht en zwarte gaten testen, maar ook informatie verschaffen over de evolutie en de geschiedenis van het versmelten van sterrenstelsels.

Het is interessant dat Einstein, die de zwaartekrachtsgolven ontdekte in zijn relativiteitstheorie, dacht dat het nooit mogelijk zou zijn om deze ooit te detecteren. Door de recente ontdekking van zwaartekrachtsgolven door LIGO, de meting GW150914, kunnen we met trots zeggen dat we in een tijd leven waarin deze twijfel onjuist is gebleken.

Publications

- G. d'Ambrosi, S. Satish Kumar, J. van de Vis, and J. W. van Holten
  Spinning bodies in curved space-time, *Phys. Rev.* **D93**, 044051 (2016); arXiv:1511.05454v1.

- S. Satish Kumar
  Motion of a spinning particle in curved space-time, *Submitted to the proceedings of the Fourteenth Marcel Grossmann Meeting - MG14, 2015 (World Scientific);* arXiv:1512.07152v1.

- G. d'Ambrosi, S. Satish Kumar and J. W. van Holten
  Covariant hamiltonian spin dynamics in curved space-time, *Phys. Lett.* **B743** (2015), 478; arXiv:1501.04879v2.

Curriculum Vitae

I was born in Salem, Tamilnadu, India, on July 13, 1987. I completed my schooling at Sri Vidhya Mandir Senior Sec. School, Ayothiyapattanam (2002) and Sri Jothi Higher Sec. School, Tharamangalam (2004), in my home town. In the same year, I started my undergraduate in Physics at St. Joseph's College, Trichy (India). During the three years I achieved many merits. In my first and second year, I was awarded first prize in Mathematics and Chemistry – ancillary subjects, for having secured highest marks in the University examinations. At the end of my second year, I was awarded a special prize "City Emporium Jeganathan Cash Award" for being the best all - rounder among science students, which is awarded only once in two years in the science departments. In 2007, I finished my undergraduate with distinction and four medals, for outstanding performance in the Physics examinations.

Then I did my Master's in Physics at University of Delhi (enrolled in St. Stephen's college) from 2008 to 2010. On the second year of the Master program, I specialised in General Relativity and Quantum Field Theory. In the summer 2009, I was selected as a summer research fellow by the Indian Academy of Sciences, Bangalore and worked on a project entitled "String like behaviour in quantum chromodynamics" in collaboration with Prof. N. D. Hari Dass at Indian Institute of Science, Bangalore. In these two years, I was honoured with Kesar Devi Memorial Scholarship (2009), Max India Scholarship (2009 and 2010) and more notably Mukarji Memorial Prize (2010) for regular work and qualities of perseverance, industry and plain living, awarded to one, among all departmental postgraduates.

In 2010 I was chosen for Erasmus Mundus Scholarship and worked as a research scholar at Free University of Berlin for two years along with Prof. Hagen Kleinert. During my time in Berlin, November 2012, I was fortunate to be invited by Prof. Jan Willem van Holten at NIKHEF, Amsterdam and worked on a collaborative project "Worldline deviations". In July 2013, I moved to Amsterdam to develop my research work as a PhD thesis at Lorentz Institute, and till May 2016 the research was funded by Leiden Institute of Physics. During this period, I was also associated with NIKHEF as a long term guest researcher. During my PhD I

was teaching assistant for the course on Black Holes and Gravitational Waves, and published three research articles: a letter, a paper, and a conference proceeding. In these three years of PhD research I have served DRSTP as a PhD student council member. In November 2015, I was nominated for the Committee on International Freedom of Scientists, APS. In March 2016, I received the "Best Poster Prize" for presenting my PhD research work at 609^{th} WE-Heraeus-Seminar – Relativistic Geodesy: Foundations and Applications, Physikzentrum, Bad Honnef, Germany.

Acknowledgements

First and foremost I express my sincere thanks to my PhD advisor and research collaborator Prof. dr. Jan Willem van Holten. He has been tremendously encouraging me with his immense knowledge and infinite patience, in all the best and worst moments. I have enjoyed all the uncountable blackboard discussions with him. His guidance has helped me to grow as a research scientist, teacher and in writing this thesis. I am greatly inspired and wish to continue collaborating with him in future.

Secondly, I would like to thank the scientific director of Leiden Institute of Physics (LION), Prof. dr. Eric R. Eliel, for offering me this research position with funding. Without this, I would not have finished my PhD.

Besides my advisor, I would like to thank the rest of my thesis committee: Prof. em. dr. H. van Leeuwen, Prof. dr. R. Kerner, Prof. dr. S. Vandoren, Prof. A. Achucarro, Dr. M. Postma, Dr. T. Prokopec, and Prof. em. dr. H. Bloete for their insightful comments and encouragement.

I am grateful to my other collaborators Giuseppe and Jorinde, with whom I have enjoyed all the research calculations and discussions. My special thanks to Kees and Robbert for helping me with the illustrations used in my presentations and thesis. Thanks to Bruno and Jenny for sharing knowledge on Science communication.

I sincerely thank Prof. dr. Eric Laenen, for accommodating and providing me with all the facilities at NIKHEF during my short visit in 2012 and for the whole duration of my PhD. I also thank all the other senior and junior colleagues and friends at Leiden University and NIKHEF for extending their positive influence and motivations. I also extend my gratitude to the administrative colleagues at Leiden University and NIKHEF – Barry, Ed, Fran, Marianne, Margareth, Marije, Pieter and Rowena.

I thank my former supervisor Prof. Hagen Kleinert at Free University of Berlin for accommodating and supervising me for my time in Berlin and for encouraging me for this PhD. My sincere and special thanks to Prof. N. D. Hari Dass, with whom I did my first research project and who has been supporting me throughout my research carrier.

Finally, I must express my very profound gratitude to my family and relatives for providing me with unfailing support and continuous encouragement throughout my years of life and through the process of education. This accomplishment would not have been possible without them.

$$\left(1-\frac{2M}{R}\right)^2 R u^\varphi \left[\frac{2M^2\eta}{R^3} - M u^\varphi + M\eta u^{\varphi 2} + (R^2 - 6MR + 6M^2) R u^{\varphi 3}\right]$$

$$= \kappa m \left\{ \frac{M(\eta - R^2 u^\varphi)}{R^2} \left\{ \frac{6M^2\eta}{R^3}\left(1-\frac{2M}{R}\right)\left(2-\frac{m}{M}\right) \right.\right.$$

$$-4Mu^\varphi\left[3\left(1-\frac{2M}{R}\right)\left(1-\frac{M}{R}-\frac{m}{2R}\right)+\frac{M\eta^2}{R^3}\left(1-\frac{3M}{R}\right)\right]$$

$$+\eta R u^{\varphi 2}\left[\frac{2M}{R}\left(7-\frac{16M}{R}\right)-\frac{3m}{M}\left(1-\frac{2M}{R}\right)\left(1-\frac{4M}{R}+\frac{6M^2}{R^2}\right)\right]$$

$$\left.\left.+12R^3 u^{\varphi 3}\left[1-\frac{49M}{6R}+\frac{19M^2}{R^2}-\frac{13M^3}{R^3}+\frac{m}{4M}\left(1-\frac{6M}{R}+\frac{14M^2}{R^2}-\frac{12M^3}{R^3}\right)\right]\right\}\right\}$$

$$+\kappa^2 m^2 \left\{ \frac{12M(\eta - R^2 u^\varphi)^2}{R^3}\left\{ \frac{3M^2}{R^2}\left(1-\frac{2M}{R}\right)+\frac{2M^3\eta^2}{R^5} \right.\right.$$

$$-\frac{M\eta}{R}u^\varphi\left[\frac{M}{R}\left(5-\frac{6M}{R}\right)-\frac{3m}{M}\left(1-\frac{2M}{R}\right)^2\right]$$

$$\left.\left.-MRu^{\varphi 2}\left[3-\frac{20M}{R}+\frac{26M^2}{R^2}+\frac{3m}{M}\left(1-\frac{2M}{R}\right)^2\right]\right\}\right\}$$

$$+\kappa^3 m^3 \left\{ \frac{72M^3(\eta - R^2 u^\varphi)^4}{R^7}\left[\frac{M}{R}-\frac{3m}{2M}\left(1-\frac{2M}{R}\right)\right]\right\}$$

Casimir PhD series 2016-20
ISBN 978-90-8593-264-2

Stellingen

Behorend bij het proefschrift
Spin Dynamics in General Relativity

1. Comparing with the conventional analysis of spinning particle dynamics it is seen that the constraint on the mass dipole (Pirani condition) has been replaced by a proper equation of motion. As a result in our formalism of classical relativistic mechanics the mass-dipole Z cannot vanish permanently, except in the flat field-free Minkowski space-time. However, it is easily established that the two approaches can be made to agree to linear order in the spin tensor.

   Chapter 4

2. The planar motion of a spinning particle in curved space-time requires alignment of the spin with the orbital angular momentum and vice versa.

   Chapter 4

3. The radial deviation from circular orbit in Schwarzschild space-time have double periods. Hence the periastron and apastron will behave in a complicated way, as the body reaches different minimal or maximal radial distances at non-constant intervals.

   Chapter 5

4. The presence of spin alters the stability condition and therefore the location of the ISCO. When the magnitude of the spin increases, the radius of the ISCO increases or decreases, depending on the orientation. Therefore, for a spinning particle the ISCO can be found at more or less than three times the Schwarzschild radius. Over the range of predominant physical interest, $-0.5 < \sigma/M < 0.5$, the ISCO curve coincides with the curve derived by minimising the orbital angular momentum.

   Chapter 5

5. The description of Extreme Mass Ratio mergers using the plunge starting from a circular orbit can be improved beyond the treatment by G. d'Ambrosi and co-workers by including non-circular starting orbits and spin.

   G. d'Ambrosi et al., Class. Quant. Grav. **32** (2015)

6. The analysis of the gravitational wave events detected by the LIGO and VIRGO collaborations can be improved by allowing arbitrary orientations of the spins of the initial black holes.

   B. P. Abbott et al., PRL **116**, 061102 (2016)

7. The radiation dynamics of stellar objects orbiting around supermassive black holes must be studied in the bumpy black hole space-times proposed by S. Vigeland and S. Hughes, to explore possible deviations from General Relativity.

   S. Vigeland et al., PRD **81**, 024030 (2010)

8. The shape of a flame is affected by gravity as theoretically modelled by S.S. Krishnan and his collaborators. This model can be tested in an environment of microgravity in free fall experiments with airplanes flying parabolic paths.

   S.S. Krishnan et al., Combustion Theory and Modelling,
   Vol. **12**, No. 4, (2008)

9. Do it yourself!

Satish Kumar, Saravanan,
Leiden, 07-07-2016